SURFACE MODIFIED POLY(AMIDOAMINE) (PAMAM) DENDRIMER FOR DRUG DELIVERY APPLICATIONS

LIU YUANJIE

(B.SC. in Pharmaceutical Science), Fudan University

A THESIS SUBMITTED

FOR THE DEGREE OF DOCTOR OF PHILOSOPHY

DEPARTMENT OF PHARMACY

NATIONAL UNIVERSITY OF SINGAPORE

2014

Declaration

I hereby declare that this thesis is my original work and it has been written by me in its entirety.

I have duly acknowledged all the sources of information which have been used in the thesis.

This thesis has also not been submitted for any degree in any university previously.

Liu Yuanjie

1 August 2014

Acknowledgements

I would like to express my sincerest gratitude to my supervisor, Dr. Chiu Ngar Chee, Gigi for her patience, guidance and support in my PhD journey. There are invaluable wisdoms that I learnt from you both inside and outside the lab.

I would like to thanks Ms Tan Bee Jen, whom I learnt lab skills from. Also thank her for helping as lab technician with the lab management and support.

I am really grateful to have a group of wonderful lab mates, Dr Ling Leong Uung, Dr Anumita Chaudhury, Dr Shaikh Mohammed Ishaque, Dr Tan Kuan Boone, Mr Sun Longwei, and Mr Sudipto Bari. Thank you for your help, suggestions, and companion.

I would also like to thank A/Prof Chan Sui Yung and A/Prof Go Mei Lin for their suggestions in my research projects as well as their guidance in AAPS-NUS Student Chapter and Pharmacy Graduate Committee. Thanks to all my executive committee members, Ms Mahnaz Darvish Damavandi, Mr Chang Kai Lun, Ms Bahety Priti Baldeodas, Ms Aparna Saigal, Dr Pan Jing, Ms Zhang Luqi, Dr Jaspreet Singh, and Dr Tan Kheng Lin for the great work achieved by us.

I also want to thank the staffs and students in Department of Pharmacy, NUS, especially A/Prof Koh Hwee Ling, Ms Chew Ying Ying, Ms Ng Sek Eng and Ms Ng Swee Eng for their help in different aspects of my PhD journey.

Last but not least, thanks to my family and friends. Especially thanks to my parents for everything.

Table of Content

LIST OF TABLES

LIST OF FIGURES

LIST OF ABBREVIATIONS

5-FU	5-Fluorouracil
8-MPO	8-methoxypsoralene
α-CDE	α-cyclodextrin
ACV	acyclovir
AFM	atomic force microscopy
ANOVA	analysis of variance
aPTT	activated partial thromboplastin time
AUC	area under the curve
AUMC	area under the moment curve
BCS	Biopharmaceutics Classification System
BSA	bovine serum albumin
Cl/F	total body clearance for extravascular administration
CHCA	α-cyano-4-hydroxycinnamic acid
CNDPs	critical nanoscale design parameters
CSi-PEO	poly(ethylene oxide) grafted carbosilane
CT	computer tomography
CYS	cysteamine
DAB	diaminobutane
DAE	diaminoethane
DIC	disseminated intravascular coagulation
DMEM	Dulbecco's Modified Eagle Medium
DPPC	1,2-dipalmitoyl-*sn*-glycero-3-phosphocholine
ED_{50}	median effective dose
EDA	ethylenediamine
EGF	epidermal growth factor
EMEM	Eagle’s minimal essential medium
EN	1,2-diaminoethane
EPR	enhanced permeation and retention
ESI	electrospray ionization
FA	folic acid
FBS	fetal bovine serum
FITC	fluorescein
FT-IR	fourier transform infrared
GCV	ganciclovir
Gd	gadolinium
GI	gastrointestinal
GPC	gel permeation chromatography
GSH	glutathione

HBSS	Hank's balanced salt solution
HER2	human growth facter receptor-2
HPG	hyperhranched polyglycerol
HSA	human serum albumin
HUVEC	human umbilical vein endothelial cells
IC_{50}	half maximal inhibitory concentration
IL-6	interleukin-6
LLDs	Liposomal Locked-in dendrimer
LTS	long term survivors
LY	lucifer yellow
MA	methylacrylate
MALDI-TOF	matrix-assisted laser desorption ionization time-of-flight
Man- α-CDE	mannose- α-cyclodextrin
MIP-2	macrophage inflammatory protein-2
mPEG-SCM	methoxy poly(ethylene glycol) succinimidyl carboxymethyl
MTD	maximum tolerated dose
MTT	3-(4,5-dimethylthiazolyl-2)-2,5-diphenyltetrazolium bromide
MRI	magnetic resonance imaging
MRT	mean residence time
MTX	methotrexate
MW	molecular weight
NAC	N-Acetyl-L-Cysteine
NASAIDs	non-steroidal anti-inflammatory drugs
PAMAM	poly(amidoamine)
PEI	poly(ethyleneimine)
PEO	poly(ethylene oxide)
PEG	poly(ethylene glycol)
P-gp	P-glycoprotein
PHA	polyhydroxyalkanoate
PM	PAMAM dendrimer
PPI	poly(propyleneimine)
PSMA	prostate-specific membrane antigen
Pt	cisplatin
PT	Prothrombin time
PTX	paclitaxel
QDs	quantum dots
R-110	rhodamine-110
R-123	rhodamine-123
RBC	red blood cell

RGD	arginine-glycine-aspartate
ROS	reactive oxygen species
SEM	scanning electron microscope
SEM	standard error of the mean
TBA	2-Iminothiolane hydrochloride, Traut's Reagent
TCPS	tissue culture polystyrene
TEER	transepithelial electrical resistance
THF	tetrahydrofuran
TIMP	tissue inhibitor of metalloproteinase
TNF-α	tumor necrosis factor –α
Vz/F	volume of distribution based on the terminal phase
ZO-1	occludin

LIST OF PUBLICATIONS

Journal Publications

1. Liu, Y., & Chiu, G. N. (2013). Dual-functionalized PAMAM dendrimers with improved P-glycoprotein inhibition and tight junction modulating effect. Biomacromolecules, 14(12), 4226-4235.

2. Shaikh, I. M., Tan, K. B., Chaudhury, A., Liu, Y., Tan, B. J., Tan, B. M., & Chiu, G. N. (2013). Liposome co-encapsulation of synergistic combination of irinotecan and doxorubicin for the treatment of intraperitoneally grown ovarian tumor xenograft. Journal of Controlled Release, 172(3), 852-861.

3. Tan, B. J., Liu, Y., Chang, K. L., Lim, B. K., & Chiu, G. N. (2012). Perorally active nanomicellar formulation of quercetin in the treatment of lung cancer. International Journal of Nanomedicine, 7, 651-661.

4. Coyuco, J. C., Liu, Y., Tan, B. J., & Chiu, G. N. (2011). Functionalized carbon nanomaterials: exploring the interactions with Caco-2 cells for potential oral drug delivery. International Journal of Nanomedicine, 6, 2253-2263.

5. Liu, Y., Pang Y.Z.,Toh M., Chiu, G.N. (2014). Surface functionalization of PAMAM dendrimers via PEGylation and thiolation improved blood compatibility. *(In preparation)*

6. Liu, Y., Ng, Y., Toh M., Chiu, G.N. (2014). Dendrimer-Lipid hybrid nanosystem as a novel delivery vehicle for paclitaxel. *(In preparation)*

Podium presentation

1. Liu Y,Toh M.R., Chiu GNC. Dendrimer-lipid hybrid nanosystem as a delivery vehicle of paclitaxel. AAPS-NUS 9th PharmSci@Asia Symposium, Fudan University, Shanghai, China, 05-06 June 2014.

2. Liu Y, Chiu GNC. Blood compatibility of Poly(amidoamine) (PAMAM) dendrimers. ITB-NUS Pharmacy Scientific Symposium 2013, National University of Singapore, Singapore, 12 Nov 2013.

3. Liu Y, Chiu GNC. Double-derivatized dendrimer as P-glycoprotein inhibitor and tight junction modulator for oral drug delivery. Annual Pharmacy

Research Symposium 2013, National University of Singapore, Singapore, April 2013

4. Liu Y, Ng Y, Chiu GNC. Dendrimer-lipid hybrid nanosystem as a delivery vehicle of paclitaxel. AAPS-NUS 7th PharmSci@Asia Symposium, National University of Singapore, Singapore, June 2012.

Poster presentations

1. Liu Y, Chiu GNC. Double-derivatized dendrimer as P-glycoprotein inhibitor and tight junction modulator for oral drug delivery. 3rd International Symposium - Frontiers in Polymer Science 2013, Sitges, Spain, 21-23 May 2013.

2. Liu Y, Ng Y, Chiu GNC. Dendrimer-lipid Hybrid Nanosystem as a Novel Delivery Vehicle for Paclitaxel. AAPS Annual Meeting & Exposition 2012, Chicago, IL, USA, 14-18 Oct 2012.

Awards

1. Travelship, AAPS-NUS 9th PharmSci@Asia Symposium, Fudan University, Shanghai, China, June 2014

2. Podium presentation award, Annual Pharmacy Research Symposium 2013, National University of Singapore, April 2013

3. Podium presentation award, 7th AAPS-NUS PharmSci@Asia Symposium, National University of Singapore, Singapore, June 2012

4. Travel award, Formulation Design and Development Section, AAPS Annual Meeting & Exposition 2012, Chicago, IL, USA, 14-18 Oct 2012.

SUMMARY

Dendrimers are synthetic, hyperbranched polymers with repeating units emanating from a core to form a three-dimensional structure. With attractive structural properties, dendrimers emerge as a promising nanoscale material for biomedical applications. However, a major challenge is how to decrease the inherent toxicity of dendrimers while leveraging on the beneficial properties for the intended applications. The large number of functional groups available for surface modification provides opportunities to address the challenge. Thus, this thesis aims to study the effect of dendrimer surface modification on toxicity reduction and improvement of functionality in drug delivery applications.

In chapter 3, the Poly (ethylene glycol)-conjugated (PEGylated) and thiolated dendrimers were successfully prepared and characterized. PEGylation and thiolation could reduce toxicity of polymers to biological components. However, a combination of both has not been attempted on Poly(amidoamine) PAMAM dendrimers before. Amine-terminated PAMAM Dendrimers generation 4.0 with two different PEGylation ratios, 1.8:1 and 4.0:1, were synthesized. Thiolation ratio for all the PEGylated dendrimers and original dendrimer in average was 7:1. The physicochemical properties of all the prepared dendrimer derivatives were characterized including ^{1}H-NMR spectra, Fourier transform infrared spectroscopy (FT-IR), yield, size, zeta potential, thiol group concentration and molecular weight.

In chapter 4, different types of PAMAM dendrimers were tested for their compatibility with major blood components, including cells, serum albumin, complements, clotting factors and platelets. The unmodified amine-terminated dendrimer displayed generation- and concentration-dependent toxic effects on blood components and functions. PEGylation was shown to be an effective way to improve blood compatibility of cationic dendrimers in our study. Further modifying PEGylated dendrimers with thiolation reduced their effect on haemolysis, complement activation, prothrombin time (PT) and activated partial thromboplastin time (aPTT). Such improved blood compatibility warrant further exploration of these surface modified PAMAM dendrimer for drug delivery applications.

Dual functionalized PAMAM dendrimers were evaluated for their potential use in oral drug delivery as tight junction modulator and P-gylcoprotein (P-gp) inhibitor in chapter 5. PEG(1.8)-PM-TBA(7.0) displayed low cytotoxicity in Caco-2 and MDCK/MDR1 cells, while significantly increased cellular accumulation and permeation of the P-gp substrate Rhodamine-123 (R-123) as well as reversibly disrupted tight junction integrity shown via transepithelial electrical resistance (TEER) measurement over time. This dendrimer derivative also improved oral bioavailability of model drug ganciclovir (GCV) in vivo pharmacokinetic study.

Besides surface conjugation, complexation is another way to modify dendrimers. Chapter 6 explored the potential application of modifying dendrimers via physical complexation with lipids into dendrimer-lipid hybrid nanosystems for the delivery of paclitaxel (PTX). Such system was evaluated for the therapeutic effect in the

treatment of ovarian cancer. The hybrid nanosystem of PTX significantly improved inhibitory effect on IGROV-1 cells. PTX in the hybrid nanosystem could significantly improve the survival of tumor-bearing animals, with 50% increase in the median survival time, despite a 10-fold dose reduction. Thus, this dendrimer-hybrid nanosystem demonstrated great advantages to deliver PTX for ovarian cancer treatment.

Taken together, the findings in this thesis demonstrate that surface modification with multiple groups or complexation could improve dendrimer functionality in drug delivery applications as well as reducing its toxicity.

CHAPTER 1. INTRODUCTION

1.1 Overview of Dendrimers

Dendrimers are synthetic, hyperbranched polymers with repeating units emanating from a core to form a three-dimensional structure. They represent a new class of polymeric compounds which are distinguished from traditional linear polymers by their unusual fractal-like architecture[1]. Dendrimer is first discovered in the early 1980's by *Donald Tomalia* and co-workers [2]. The term dendrimer is derived from the Greek language 'dendron' and now refers to polymers with tree-like structure. Its structure includes three parts: a core, repeating branches and outer shells. By regulating the synthesis condition of the dendrimer, precise control of molecular weight, chemical structure, number of surface groups and low polydispersity could be achieved. Dendrimer generation is defined as the number of repeating branch cycles that is added upon the core. Dendrimers with higher generations have larger sizes, molecular weighs, more branches and surface groups. The unique structure and properties make dendrimers highly attractive as emerging novel materials in various applications, such as drug delivery [3-5], gene therapy[6], diagnostics[7], electronics and photonics[8]. Some examples of commercially available dendrimers are Poly(propyleneimine) (PPI), Poly(ethyleneimine) (PEI) and Poly(amidoamine) (PAMAM). Among them, PAMAM dendrimers are the first dendrimer family to be synthesized, characterized and commercialized[9]. Figure 1.1 shows the structure of PAMAM dendrimer and PPI dendrimer.

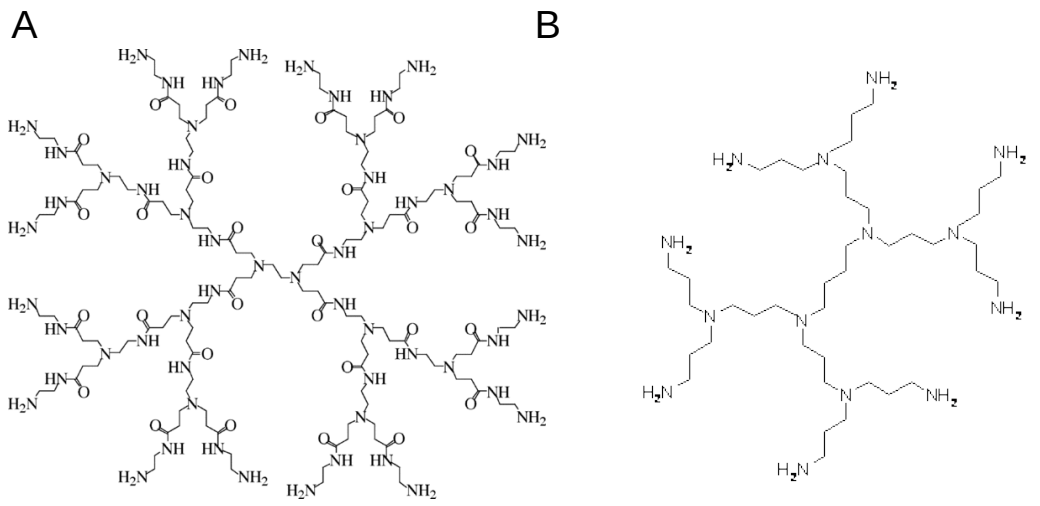

Figure 1.1 Chemical structures of dendrimers. (A) PAMAM dendrimer G2.0. (B) PPI dendrimer G2.0.

1.2 Dendrimer Synthesis

There are mainly two methods to synthesize dendrimers. Two conventional ways are the divergent and convergent methods. These two methods are fundamentally different in the construction concepts. Each method has its own benefits as well as disadvantages.

1.2.1 The divergent synthesis method

The divergent method was developed by *Fritz Vögtle*[10]. It starts with an initiator core and then the monomeric modules are assembled branch upon branch to form dendrimers [11]. As shown in Figure 1.2 (A), the initial core reacts with monomer molecules, which has one reactive group and a few dormant groups. This step leads to the first generation dendrimer. Subsequently, the molecule surface groups are activated to react with more monomers to form the second generation dendrimer. This process is repeated until the expected generation is

reached. The divergent approach is good for mass production of dendrimers [12]. However, a major disadvantage of this method is that excess monomers are required and this will lead to extensive purification process.

1.2.2 The convergent synthesis method

The convergent method was introduced by Hawker and Frechet to solve the drawback of the divergent methods [13]. This method firstly prepares the peripheral dendritic fragment followed by progressing inward to produce dendrimer [13]. When the dendritic arms meet required generations, then they are attached to the core molecules (Figure 1.2 (B)). The convergent methods need less purification process and have more precise control over the structure [12]. Yet, the limitation with convergent synthesis method is that only low generation of dendrimers could be generated with this method [14].

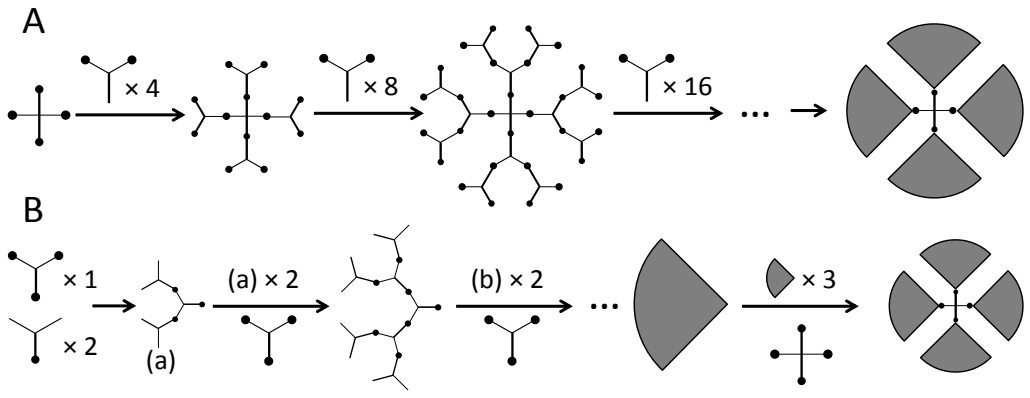

Figure 1.2. Dendrimer synthesis methods. (A) The divergent synthesis method. (B) The convergent synthesis method.

1.2.3 Poly(amidoamine) PAMAM dendrimer synthesis

PAMAM dendrimer, also known as starburst dendrimer, is the first synthesized and reported dendrimer. The synthesis method is divergent method, including two steps: (a) alkylation with methylacrylate and (b) amidation with ethylenediamine (EDA) [15]. Firstly, 1,2-diaminoethane (EN), the initial core, in methanol was added dropwise to methanol solution of methylacrylate (MA) under stirring and nitrogen environment over 2 h. Feed ratio of EN to MA is 1:5. Then the mixture was stirred at 0 ℃ for 30 min and allowed to warm to room temperature. After 24 h stirring in room temperature, the solvent was evaporated by rotary evaporator and vacuum. The synthesized precursor in methanol is carefully added to excess amount of EN in methanol at 0 ℃ under vigorous stirring. The rate of addition is controlled so that the temperature won't rise above 40 ℃. After complete addition, the mixture is stirred for at least 96 h at room temperature until no ester group could be detected by NMR. The solvent is removed under reduced pressure with temperature below 40 ℃. The excess EN is removed by an azeotropic mixture of toluene and methanol (9:1). The remaining toluene was removed by azeotropic distillation using methanol. The final product is amine-terminated generation 0 PAMAM dendrimer. Then the alkylation and amidation steps are repeated alternatively to build up the generation. After alkylation step, the ester terminal groups could be further turned into carboxyl groups by saponification and this type of dendrimer is generally referred to as 'half generation'. After amidation step, the amine terminated dendrimer is referred to as 'full generation' dendrimer.

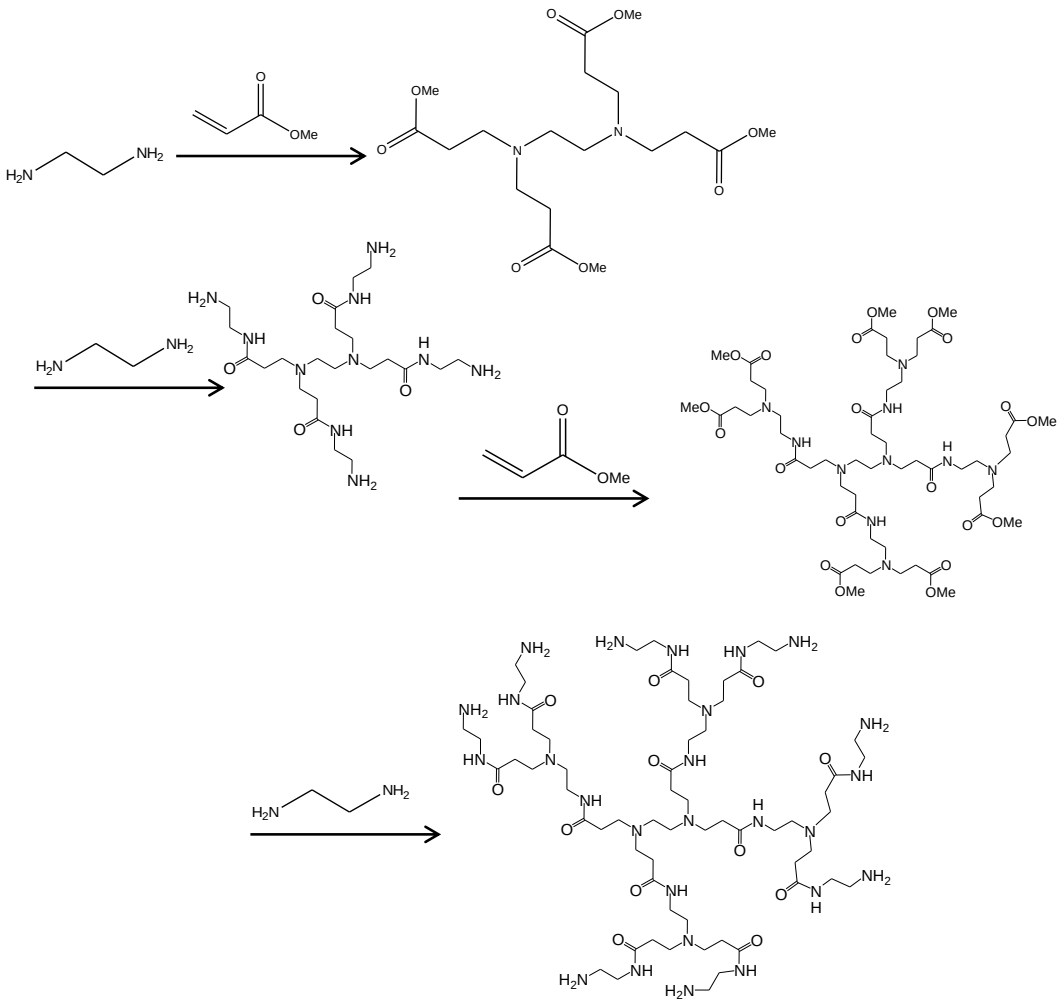

Scheme 1.1. PAMAM dendrimer synthesis scheme from core to PAMAM generatio 1.0

1.3 Physicochemical properties of Dendrimer

The physicochemical properties of dendrimers are largely related to their unique structure, generation, surface groups, molecular weight and diameter. The theoretical molecular weight (MW) of dendrimer could be calculated by the following equation:

$$MW = MW_c + N_c \left[MW_b \left(\frac{N_b^G - 1}{N_b - 1} \right) + MW_t N_b^G \right]^*$$

*MW_c: molecular weight of core

MW_b: molecular weight of branch cells

MW_t : molecular weight of terminal groups

N_c: multiplicities of core

N_b: multiplicities of branch cells

G: generation

The number of surface groups can be calculated by the equation below:

$$Z = N_c \times N_b^G$$

where Z is the number of surface groups.

Table 1.1 shows the relationship between dendrimer generation and some other parameters. In general, as dendrimer generation increases, it has larger sizes, molecular weighs, more branches and surface groups. The core affects the 3D morphology of the dendrimer. The type and number of interior repeating branches influence overall size of the macromolecule and the number of surface groups [16]. Lower generation dendrimers (G < 3) are highly asymmetric. While as generation increases, the dendrimer shows a globular structure [17]. When the dendrimer grow to a critical branched state, the generation cannot increase furthermore because the periphery are densely packed, which leaves no space for growth. This is called the 'starburst effect' [18].

Table 1.1 Relationship between PAMAM dendrimer generation and parameters [19]

G	0	1	2	3	4	5	6	7
M.W.	517	1,430	3,256	6,909	14,215	28,826	58,048	116,493
$N_{surface}$	4	8	16	32	64	128	256	512
D (nm)	N.A.	N.A.	2.2	3.1	4.0	5.3	6.7	8.0

G: generation. M.W.: molecular weight. $N_{surface}$: number of surface groups. D: diameter

The surface groups of dendrimer largely affect dendrimer's properties and applications (Figure 1.3). The nature and density of dendrimer surface groups strongly influence dendrimer solubility. Dendrimers with hydrophilic terminal groups are more soluble in polar solvent, while hydrophobic groups terminated dendrimers are soluble in nonpolar solvent. Dendrimer toxicity is also closely related to the surface groups. Dendrimers with cationic surface groups are relatively more toxic than the dendrimers with anionic surface groups or bearing neutral groups [20]. The large number of dendrimer terminal groups can also be utilized for surface modification to achieve desired properties in biomedical applications, for example, targeted drug delivery.

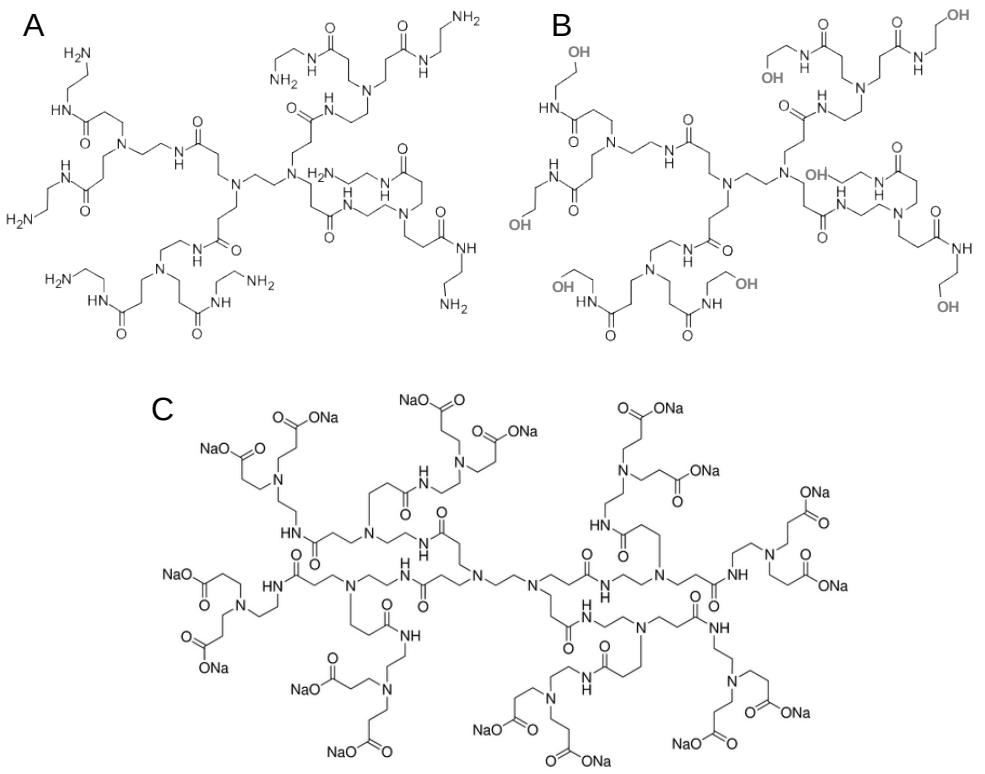

Figure 1.3. PAMAM dendrimers with different surface groups. (A) PAMAM G1-NH_2, (B) PAMAM G1-OH, (C) PAMAM G1.5-COOH

Dendrimer structure shows many improved physicochemical properties compared to traditional linear polymers. The synthesis method of dendrimer could specifically control dendrimer size, generation and structure. Thus, dendrimers are monodisperse macromolecules. However, the linear polymers are random in nature and have different sizes due to the traditional polymerization process [12]. In solution, the high density of surface groups improved solubility of dendrimer. In a solubility test, the solubility of dendritic polyester was remarkably higher than that of analogous linear polyester in tetrahydrofuran (THF) [12]. The morphology of dendrimer in solution is spherical shape; in contrast, linear chains exist as flexible coils. Dendrimer solutions have significantly lower viscosity than

linear polymers [21]. As molecular weight of dendrimers increase, the intrinsic viscosity goes to a maximum at the fourth generation and then begins to decline [22]. However, for linear polymers, the intrinsic viscosity increases as molecular weight increases. All these unique properties of dendrimer make it as an attractive material for biomedical applications.

1.4 Biomedical applications of Dendrimer

1.4.1 Dendrimer in gene delivery

Many different types of gene delivery vectors have been developed to carry gene into host cells. The earliest gene delivery vector is virus, which has high transfection efficiency. Alipogene tiparvovec (trade name Glybera) was the first approved gene therapy product based on viral vector. However, immune responses, safety and cost are the major concerns for application of virus viral vector in gene delivery. Cationic liposomes and oligopeptides are developed later on as non-viral vector. However, these materials are relatively more toxic and the transfection efficiency is not high. Thus, poly-cationic polymers are developed as novel alternatives for gene delivery. The electrostatic interaction between the negative phosphate backbones of DNA/RNA strand and the high density cationic surface groups of dendrimer is the main principle for dendrimer based gene delivery vector [23]. Scanning force microscopy data also confirmed the structure that DNA wraps around the dendronized polymers [24]. The gene/dendrimer complex is endosomally uptaken by the cells, and after lysosomal fusion and

subsequent endosomal escape, the genetic materials are released from the complex in the vicinity of nucleus [25].

Dendrimers have been demonstrated as efficient in vitro gene transfection agents in many studies. Early studies demonstrated that Starburst^{TM} PAMAM dendrimers showed maximal transfection of luciferase at dendrimer to DNA at charge ratio 6:1 [26]. It is suggested by the author that the high pKa of amine groups could buffer pH changes in the endosome. Such property contributes to the high transfection efficiency of the dendrimer [26]. Later, *Bielinska et al.* studied twenty different types of polyamidoamine dendrimers for gene transfection in mammalian cells. It is shown that dendrimers could deliver plasmid DNA as well as antisense oligonucleotides [27]. The transfection efficiency was related to the intrinsic properties of dendrimers, including generation, size, shape, and the number of surface primary amine groups. Overall, the higher generation dendrimers (G > 5.0) were found to be of superior efficiency in variety of cell types[27]. Interestingly, *Tang et al.* reported a dramatic enhancement (> 50-fold) of transfection activity by heating PAMAM dendrimers in solvolytic solvents [28]. Heating treatment caused dendrimer degradation, resulting in heterodisperse and fractured dendrimers. The enhanced transfection efficiency of such fractured dendrimers was considered mainly due to the increase in flexibility of complexation and release of DNA [28]. This PAMAM dendrimer based transfection agent is commercialized as Superfect^{TM} and demonstrated superior transfection activity among different polymeric transfection materials. However,

longer incubation time was required for Superfect™ and the transfection activity varied depending on the specific cell line [29].

Some of dendrimer based gene delivery studies proceeded to in vivo experiment and showed promising results. *Kukowska et al.* used PAMAM G9 to form complex with pCF1CAT plasmid and evaluated gene expression on female BALB/c mice after i.v. administration [30]. pCF1CAT plasmid showed high level of transgene expression in the lung at 12 and 24 h after injection. Then the second peak of expression appeared 3 to 5 days after administration. In comparison, a minimal level of CAT protein was expressed in the lung for naked plasmid DNA. It is also important to note that protein expression was not observed in organs other than the lung, which is the expected site for gene expression in this study. These results indicate that i.v. administered PAMAM G9 dendrimer could be an effective vector for pulmonary gene transfer. In another study, PAMAM G3 conjugated with α-cyclodextrin (α-CDE) formed complexes with pDNA [31]. Conjugates with three different α-CDE/PAMAM ratios of 1.1, 2.4, and 5.4 were prepared and evaluated in this study. After intravenous administration of dendrimer/pDNA complexes in mice, dendrimer conjugates with α-CDE/PAMAM ratio of 2.4 showed the highest gene transfer efficiency in spleen, liver, and kidney after 12 h. The diameter of the pDNA/ α-CDE conjugated PAMAM particles have average size of ~ 500 nm, which might be the reason for enhanced accumulation in spleen and liver. Similarly, *Wada et al.* surface modified PAMAM G2 with α-cyclodextrin bearing mannose (Man- α-CDE) for gene delivery [32]. This PAMAM conjugated with Man- α-CDE

showed significantly higher transfer activity than dendrimer and α-CDE in kidney 12 h after i.v. injection in mice. In other major organs, including heart, lung, spleen, and liver, the transfer activities were similar for all the vectors. Taken together from these results, the delivery vehicle may play an important role in the gene transfer location. It might be highly related to the dendrimer generation and surface modification groups.

Delivery of anticancer gene for cancer therapy is one of the most studied applications of dendrimers. Such approach aims to inactivate or destroy mutated gene in the cancer cells [33]. *Dufes et al.* reported PPI dendrimer based systemic delivery of tumor necrosis factor alpha (TNF alpha) gene. Such TNF alpha/dendrimer complex significantly improved animal survival compared to TNF alpha alone [34]. *Nakanishi et al.* demonstrated that pGEH.FasL/PAMAM dendrimer complex significantly reduced the viability of prostate cancer cells as well as improved therapeutic effect of cisplatin in systemic co-administration for the treatment of xenograft tumor [35]. The same group reported dendrimer deliver of suicide gene that pSES.Tk/dendrimer significantly prolonged the survival of mice implanted with A573 cells [36]. *Vincent et al.* used 36-mer anionic oligomers associated dendrimer for delivery of angiostatin and tissue inhibitor of metalloproteinase (TIMP)-2 genes. In vivo intratumoral angiostatin/dendrimer or TIMP-2/dendrimer gene delivery system effectively inhibited tumor growth by 71% and 84%, respectively. Moreover, the combined gene transfer approach inhibited 96% of tumor growth [37]. All of these studies demonstrated that dendrimer could be potent non-viral gene delivery vector for cancer therapy. Besides cancer

treatment, dendrimers were also reported for the treatment of other diseases, such as neurodegenerative diseases [38, 39], anti-HIV therapy [40, 41], ischaemic heart diseases [42], diabetes [43], and stroke [40].

1.4.2 Dendrimer as drug delivery system

Dendrimers are studied extensively for drug delivery applications due to the unique structure properties. The hydrophilic nature of dendrimer is helpful to deliver hydrophobic drugs with poor water solubility. Drugs can be encapsulated into dendrimer by three different manners: (1) covalent conjugation on peripheral groups of dendrimers, (2) non-covalent encapsulation in the internal cavity of dendrimer and (3) complexation by electrostatic interaction. Moreover, high density of surface groups allows for functional modification to achieve extra desirable properties, such as targeting, controlled release, reduced toxicity, prolonged circulation time. Due to these properties, dendrimers are most commonly studied for systemic delivery of therapeutic molecules. Besides, dendrimers have also been explored for various administration routes, such as oral delivery, ocular delivery, pulmonary delivery, and transdermal delivery.

1.4.2.1 Dendrimer in intravenous drug delivery

Intravenous injection provides the most rapid and highest bioavailability for systemic delivery of medications. With nano-scale and water soluble properties, dendrimers have been studied as a drug carrier to deliver drug in systemic circulation. Cancer therapy and DNA delivery are two main focuses of using dendrimers as carriers for intravenous administration in recent years. *Bhadra et*

al. studied the pharmacokinetic profile of 5-Fluorouracil (5-FU) encapsulated in PEG5000 modified PAMAM G4 dendrimer [44]. The 5-FU in PEGylated PAMAM formulation showed steady and sustained release up to 12 h. In comparison, 5-FU in unmodified PAMAM or free drug showed much faster drug release profile and could be detected up to 6 h and 1.5 h, respectively. It is concluded by the author that such PEGylated system can act as long circulatory and sustained release system to deliver anti-cancer drug. *Malik et al.* i.v. injected cisplatin (Pt) conjugated PAMAM G3.5-COOH to treat a palpable s.c. B16F10 melanoma [45]. The dendrimer-Pt showed 50-fold higher drug accumulation in solid tumor tissue compared to Pt by the enhanced permeation and retention effect. The dendrimer-Pt conjugate showed antitumor activity whereas cisplatin alone was inactive. This study indicates that dendrimer-drug conjugation could help to increase drug retention in tumor so that the therapeutic efficiency could be enhanced. In another study done by *Kukowska et al*., PAMAM G5 dendrimer was surface modified with acetyl groups, folic acid, methotrexate (MTX), and fluorescein (FITC) to achieve targeted delivery of MTX into immunodeficient mice bearing human KB tumors that over express the folic acid receptor [46]. 4 days post i.v. injection, 9% of the folic acid conjugated dendrimer selectively accumulated in tumor tissue, meanwhile about 15% were accumulated in liver. The MTX conjugated with dendrimer formulation effectively delayed tumor growth at dose 4-fold lower than the free drug, indicating the improved therapeutic effect of MTX conjugated with surface modified PAMAM dendrimer.

1.4.2.2 Dendrimer in oral drug delivery

Oral drug delivery is the most common route of administration of medicinal agents. It is convenient, relatively safe and has high patient compliance. However, different types of drugs often encounter variable bioavailability due to the complex biological barriers and chemical/physical environment in gastrointestinal (GI) tract. Drug molecules will experience harsh pH changes from acidic environment in stomach to nearly alkaline intestine. Enzymes and bacteria in the intestinal epithelium also cause degradation or metabolism of drugs. Moreover, drug is limited by various biological barriers such as tight junction proteins and drug efflux pumps. One major physical barrier for oral drug delivery is tight junctions expressed in intestinal epithelium. The physiological function of tight junctions is to regulate the passage of ions, water and small molecules as well as block the free diffusion of large molecules between the apical and basolateral domains of the intestinal membrane [47]. However, the presence of tight junction in intestinal epithelium largely limits the paracellular pathway for drugs to diffuse into blood circulation.

Sakthivel et al. was the first to report rapid absorption of dendrimer after oral administration in Sprague−Dawley rats [48]. Subsequently, poly (amido amine) or PAMAM dendrimers were studied for transepithelial transport. Supporting lines of evidence demonstrated that PAMAM dendrimers can pass through GI epithelial barriers in a generation- and surface charge-dependent manner [49, 50]. Charged PAMAM dendrimers are transported across Caco-2 monolayers by a combination of paracellular and endocytotic pathways [51]. Paracellular transport

is reflected by an opening of the tight junction of the epithelium, which could be characterized by a decrease in transepithelial electrical resistance (TEER), increased permeability of model compounds, and disrupted expression of tight junction markers such as occludin (ZO-1). PAMAM dendrimers of cationic or anionic surface charge have been shown to decrease TEER and increase ^{14}C-mannitol permeability [52, 53], suggesting that the ability of PAMAM dendrimers to modulate integrity of tight junction and promote paracellular transport. Expression of occludin and actin filaments in Caco-2 cell monolayers was also shown to be disrupted upon incubation with cationic or anionic PAMAM dendrimers [54]. Endocytosis inhibitors such as brefeldin A, colchicine, filipin, and sucrose could reduce Caco-2 uptake of amine-terminated PAMAM G4.0 dendrimer [55]. Both clathrin- and caveolin-mediated pathways have been shown to be involved in the cellular uptake of PAMAM G3.5 dendrimer [56]. Studies have shown that PAMAM dendrimers could increase oral bioavailability of poorly soluble compound silybin [57] and P-gp substrate doxorubicin [58] by forming drug-PAMAM complexes. In addition, drugs are conjugated covalently with dendrimer to form a prodrug-dendrimer conjugate for oral delivery. P-gp substrate drug propranolol was conjugated with PAMAM dendrimer and was shown to be less affected by P-glycoprotein efflux effect in cellular transport study across Caco-2 cell monolayers [59]. In another study, anticancer drug SN-38 was conjugated to PAMAM G3.5 and tested its potential in oral delivery. The conjugate showed increased transepithelial transport of SN-38 compared to the free drug with reduced toxicity [60]. *Najlah et al.* utilized PAMAM G0 to

enhance transepithelial permeability of hydrophobic drug naproxen [61]. Two different linkers lactic ester and diethylene glycol were used to conjugate drug with dendrimers. Both conjugates showed significant increase of naproxen transport. However, conjugate with lactic ester showed much slower hydrolysis in both plasma and liver homogenate compared to conjugate with diethylene glycol ester linker [61].

1.4.2.3 Dendrimer in transdermal drug delivery

Dendrimers were firstly reported as penetration enhancer for transdermal drug delivery in a polyhydroxyalkanoate (PHA)-based system [62]. Such dendrimer-containing PHA matrix enhanced tamsulosin permeation to clinically required amount demonstrated in skin model. Subsequently, dendrimers have been explored in various studies as transport vehicles for drugs with poor water solubility or low permeability. PAMAM G2, G2.5, G3, G3.5 and G4 were tested as solubility enhancer of riboflavin (vitamin B2). The PAMAM-riboflavin complex was firstly prepared in methanol and then formed an o/w emulsion after methanol evaporation. It was shown that PAMAM G2 was the best as solubility enhancer as well as permeation enhancer for riboflavin in vitro transdermal model [63]. In another study, PAMAM G2.5, G3, G3.5, G4 were evaluated as transdermal delivery carrier of 8-methoxypsoralene (8-MOP), photosensitizer for PUVA therapy [64]. PAMAM G3 and G4 enhanced the solubility of 8-MOP as well as providing controlled drug release profiles indicating that the dendrimer might improve delivery property of 8-MOP in PUVA therapy. Dendrimers were also studied with non-steroidal anti-inflammatory drugs (NSAIDs) for

transdermal delivery. PAMAM G4-NH_2, G4-OH, and G4.5 were applied to deliver indomethacin [65]. G4-NH_2 showed the best effect to increase steady-state flux of the drug both in vitro and in vivo. Therapeutic effect of indomethacin was improved by 1.6- and 1.5-fold for G4-NH_2 and G4-OH formulations, respectively, compared to pure drug suspension. Later, *Cheng Y. et al*. used PAMAM G5 to deliver ketoprofen and diflunisal [66]. Both in vitro and in vivo studies showed improved permeation of model drugs in dendrimer complex formulation. Moreover, the bioavailability of ketoprofen-PAMAM and diflunisal-PAMAM were 2.73-fold and 2.48-fold, respectively, higher than the pure drug suspensions.

1.4.2.4 Dendrimer in ocular delivery

The eye is an organ readily accessible for drug delivery purposes, yet the complex structure and physiological properties cause great challenges in clinical application. Topical applications are most commonly used for treating anterior segment-related diseases [67]. Steroids, anti-inflammatory drugs, anti-fungal, antibiotics, and miotics are typically used in liquid forms via topical route [67-69]. However, these drugs have low ocular bioavailability mainly due to the low permeability across an intact corneal epithelium or easily washed out by tears [70, 71].

Vandamme and Brobeck explored PAMAM as ophthalmic vehicle for ocular delivery [72]. Various PAMAM dendrimers with different surface groups (-OH, -COOH, --NH_2) and generations (from 1.5 to 4) were tested in this study to understand generation and surface charge dependent effect. PAMAM G1.5-

COOH and PAMAM G4-OH were identified as the best ones to increase ocular residence time among all tested. The residence time was not concentration dependent at dendrimer concentration ranging from 0.25-2%. All of these dendrimers at concentration 2.0% or lower were classified as weakly irritant without causing any ocular irritation. Thus, dendrimers could be further explored to bring benefits to ocular drug delivery.

Yao et al. studied dendrimer-puerarin complexes in ocular drug delivery system. The puerarin in complexes showed slower in vitro release and prolonged ocular residence times in rabbits compared with puerarin eye drops [73]. The permeation study was performed on excised cornea of rabbits by a Valia-Chien diffusion apparatus. The permeability coefficient of puerarin in the dendrimer-puerarin complexese was enhanced by 2.48 (PAMAM G3), 1.99 (PAMAM G4), and 1.36 (PAMAM G5) times, respectively, indicating that PAMAM dendrimer could increase the corneal permeation of puerarin mainly by altering the corneal barrier [74]. In the pharmacokinetic studies, the puerarin samples were collected from rabbit's aqueous humor by in vivo microdialysis and quantified by mass spectroscopy. The AUC of puerarin complexed with dendrimer was increased by 2.3 (PAMAM G3), 3.5 (PAMAM G4), and 2.1 (PAMAM G5) times compared to puerarin alone, respectively [75]. These studies showed the promise of applying PAMAM dendrimers in ocular drug delivery.

1.4.2.5 Dendrimer in pulmonary delivery

Pulmonary delivery has several advantages in drug delivery applications, such as avoidance of first-pass metabolism, large surface areas for drug absorption, noninvasive administration, and local delivery for the treatment of respiratory or pulmonary diseases. Pulmonary route has been explored to deliver small molecules, proteins, peptides, and genes for the treatment of diseases such as asthma, pulmonary hypertension, cystic fibrosis, lung cancer, and various infections [76-80].

Bai et al. reported dendrimers as carrier for pulmonary delivery of enoxaparin, a low-molecular weight heparin [81]. PAMAM G2 and G3 could form complex with enoxaparin via electrostatic interactions and improved relative bioavailability of enoxaparin by 40%, meanwhile negatively charge PAMAM G2.5 had no effect. Importantly, the dendrimer-enoxaparin complex did not adversely affect the mucociliary transport rate or produce extensive damage to the lungs, which warrants further evaluation of positively charged dendrimers as promising vehicle for pulmonary drug delivery. In another study of the same group, PEGylated dendrimer (PEG2000-PAMAM G3) was evaluated as carrier of low molecular weight heparin (LMWH) for pulmonary delivery [82]. The half-life of LMWH in PEG-dendrimer formulation was increased by 2.4-fold compared to LMWH in saline control formulation. In a rodent model to demonstrate whether such formulation could reduce thrombus weight, the LMWH in PEG-dendrimer formulation administered at 48 h intervals showed similar efficacy to LMWH administered via subcutaneous route at 24 h intervals. The results suggest that

PEG-dendrimer loaded with LMWH could potentially be used as noninvasive pulmonary delivery system to treat thromboembolic disorder.

1.4.2.6 Dendrimer in targeted drug delivery

Targeted drug delivery is desirable to increase therapeutic efficiency as well as to reduce adverse effects of the treatment, for example, in cancer therapy. Dendrimer could provide such benefits either by passive targeting or active targeting, depends on the formulation design. In passive targeting, the nano-scale size of dendrimer itself could prolong the circulation time of the formulation and increase accumulation in tumor tissues due to enhanced permeation and retention effect (EPR). In active targeting, the targeting ligands could be conjugated to the external surface groups of dendrimer to achieve targeted delivery of bioactives. Various targeting ligands have been conjugated to dendrimer to demonstrate targeting effect of such delivery system. *Thomas et al.* conjugated CD14 and prostate-specific membrane antigen (PSMA) antibodies to PAMAM G5 and showed a specific binding and internalization to the antigen-expressing cells [83]. *Shukla et al.* reported anti-HER2 mAb (monoclonal antibody) conjugated PAMAM G5 to target human growth facter receptor-2 (HER2), a promising target overexpressed in various tumors [84]. Both in vitro and in vivo models demonstrated targeting effect of the conjugates to HER2-epxressing tumors. Such results indicate the potential of dendrimer based targeting delivery. Folic acid is commonly applied as targeting ligand to cancer cells. *Quintana et al.* conjugated folic acid, fluorescein, and methotrexate to the surface of dendrimers to achieve targeting, imaging and intracellular drug delivery capabilities [85]. The result

showed that this system had high selectivity and improved cytotoxicity to KB cells compared to free drug (over 100-fold). In another study of Kukowska-*Latallo et al.*, folic acid conjugated PAMAM G5 was used to deliver methotrexate (G5-FA-MTX) [46]. Such system was highly concentrated in tumor and liver tissue over 4 days after administration. Prior administration of folic acid decreased accumulation of folate-conjugated dendrimers, indicating the competitive and selective binding of folate-conjugated dendrimer to folate-receptor. G5-FA-MTX system also significantly reduced tumor volume as well as improved survival in SCID mice bearing KB xenografts. Therefore, dendrimer structure provides great advantage to conjugate multiple functional groups on its surface to achieve targeted drug delivery.

1.4.3 Dendrimer in diagnosis

Dendrimers are explored as imaging tools for various applications, such as contrast agents for X-ray[86] and magnetic resonance imaging (MRI) or molecular probes [87]. Gadolinium (Gd) is the most widely used contrast agent in MRI. *Wiener et al*. developed a PAMAM dendrimer based chelator to complex with Gd(III) [88]. Such dendrimer-metal chelate conjugate increased Gd loading as well as prolonged circulation lifetime of Gd, which makes dendrimer preferable over low molecular weight MRI contract agents. In another study, *Kobayashi et al.* developed PAMAM G8-Gd based contrast agent [89]. A single dose of 15 Gy resulted in significant image enhancement of tumor tissue. Based on this concept, targeting ligands can be further attached to the dendrimer to achieve specific targeting and imaging effect. *Wiener et al.* prepared folate-

conjugated dendrimer-chelates for diagnosis of tumors cells expressing the high-affinity folate receptors [90]. The conjugates showed selectively increased signal for cells with overexpression of folate receptors and such increase was inhibited by an excess of free folic acid.

Similar to MRI, dendrimers were also studied to improve the effect of iodinated contrast agents in computer tomography (CT). *Fu et al.* synthesized an array of dendritic iodinated contrast agents with different PEG cores (3, 6, 12 kDa) and G3, G4, G5 poly (lysine) dendrimers (Figure 1.4) [91]. A representative compound, G4 poly (lysine) dendrimer with PEG12 kDa core, showed a strong and persistent intravascular enhancement with monoexponential blood half-life of ~35 min, 7-fold of typical exhaustion times for small molecule CT contrast agents. It is proposed by the authors that these large molecular constructs could be be potentially used for tumor microvascular CT imaging. Dendrimers have also been surface modified as molecular probe [92], fluorescent pH sensor [93], DNA probe [94, 95], avidin biosensor [96], and amino alcohols detector [97].

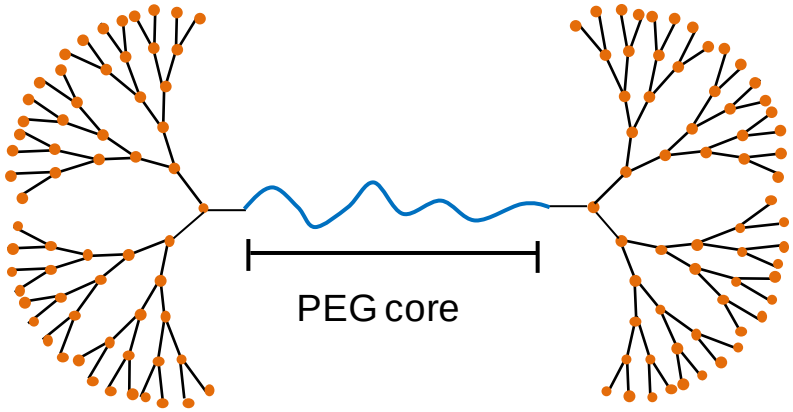

Figure 1.4. Representative structure of poly(lysine) dendrimer with PEG core.

1.5 Dendrimer Toxicity

Despite the promising findings of dendrimers for various potential biomedical applications, toxicity profile is still a major concern especially for intravenous injection, which is considered as the major route of administration for dendrimer based drug delivery system and targeted diagnostics. In general, the toxic effect of dendrimer was surface charge, concentration and generation dependent. Positively charged dendrimers interact with negatively charged blood components by electrostatic interactions. Such effect strongly affects the stability and function of the blood components [98-100]. In comparison, neutral or negatively charged dendrimers show much less effect on the blood components [98, 101]. Besides surface charge, dendrimer toxicity is increased as the generation increases, which correlate to the increase of surface groups, molecular weight, charge density and particle size.

1.5.1 In vitro cytotoxicity

In vitro cytotoxicity of dendrimer is mainly evaluated with different types of cancer cell lines. In early studies, *Malik et al.* evaluated cytotoxicity of PAMAM, PEI and poly(ethylene oxide) grafted carbosilane (CSi-PEO) dendrimers [100]. Cationic dendrimers showed generation, concentration, and cell type dependent toxicity. For anionic dendrimers, they were not haemolytic or cytotoxic below 1 mg/ml for the tested cell lines. *Javprasesphant et al.* studied cytotoxicity of different generations PAMAM on Caco-2 cells [102]. For both cationic and anionic dendrimers, toxicity increased with size, generation and concentration.

Modification of cationic dendrimers surface groups with lauroyl or PEG chains decreased toxicity. It was also reported that increased incubation time led to increased cytotoxicity of dendrimer in HepG2 and COS-7 cell lines by *Agashe et al.* [103]. Similarly, PAMAM G5 dendrimers were found to disrupt membrane of human umbilical vein endothelial cells (HUVEC) in a time-dependent manner [104]. Surface modification with PEG was shown to be an effective method to decrease dendrimer cytotoxicity.

1.5.2 Toxicity of dendrimer on blood components

1.5.2.1 Effect of dendrimer on erythrocytes

Erythrocytes deliver oxygen to body tissues through circulatory system. The morphology of normal erythrocytes is round and biconcave shape. Affected by intrinsic or extrinsic factors, erythrocytes can transform to echinocytes (crenated cells) or stomatocytes (cup-shaped cells) [105]. Echinocytosis is a reversible condition of erythrocytes that may be found in hyperlipidemia caused by liver dysfunction [106]. Stomatocytes might be seen as a non-specific observation in various conditions, such as regenerative anemias, liver disease, or lead poisoning. Interaction with dendrimer can change the shape of erythrocyte. The concentration dependent effect of PAMAM dendrimer G4.0 on erythrocyte morphology was reported by *Domanski et al.* [107]. After 1 hour incubation, 1 nM PAMAM G4.0 caused echinocytic transformation. 10 nM concentration caused elongated and spindle-shaped cells. At 100 nM, drephanocyte-like forms is observed. In another study by *Malik et al.*, echinocytic transformation and

spheroechinocytes were observed after 1 hour of incubation with PAMAM, poly(propyleneimine), and poly(ethylene oxide) (PEO) grafted carbosilane (CSi-PEO) dendrimer samples [100]. Such observations could be explained by the bilayer couple hypothesis that cationic components may interact mainly with one side of the bilayer to cause an asymmetric expansion of one monolayer [108]. Another common effect of cationic dendrimer treated erythrocytes is aggregation and cluster formation [100, 109]. For neutral PEG and stearoyl chain (C18) derivatized hyperhranched polyglycerol (HPG) dendrimer (HPG-C18-PEG polymer), spherocytosis with spicules were observed for erythrocytes after incubation for 1 hour above 5 mg/ml, much higher concentration than the cationic dendrimers [110].

Disruption of erythrocyte morphology is also accompanied by dendrimer induced haemolysis. The haemolysis effect of dendrimer is largely dependent on the surface charge, generation, concentration and incubation time. Early study done by *Malik et al*. reported generation, concentration dependent haemolysis by various dendrimers [100]. Cationic PAMAM dendrimers showed clear generation-dependent haemolysis from generation 1 to 4. However, diaminobutane (DAB) and diaminoethane (DAE) dendrimers did not show generation dependent haemolysis. This might due to the structure similarity between these two types of dendrimers. Also, the different inner structure, mainly amide and tertiary amino groups, may also contribute to the difference of haemolytic effect. Anionic PAMAM, DAB and PEO-modified CSi-PEO dendrimers were not haemolytic up to 2mg/ml. However, carboxyl terminated

PAMAM triggered haemolysis above 2 mg/ml. *Ziemba et al*. studied the incubation time dependent haemolysis caused by PPI dendrimers [109]. It was clearly shown that prolonged incubation time induced higher level of haemolysis. Such effect was remarkably reduced after surface modification with maltotriose [110].

The interaction between erythrocyte and dendrimer is mainly due to electrostatic interaction. The surface of an erythrocyte is negatively charged due to the presence of glycolipids and some glycated integral and peripheral proteins. The negatively charged surface prevents aggregation and adhesion to blood vessels and other blood components [111]. The cationic dendrimers could target the anionic lipids or proteins to disrupt the structural integrity of the cell membrane. Such membrane disruption effect of cationic dendrimer is enhanced as generation increases [101].

The effect of other blood components on dendrimer induced haemolysis is also studied previously. An interesting finding is that the haemolysis is significantly reduced if human serum albumin or human plasma is added into the system [109]. Similar result was also reported by *Klajnert et al.* that the haemolytic effect of PAMAM G5 is significantly decreased in the presence of human serum albumin [112]. Thus, dendrimer might have a higher affinity to albumin than erythrocyte. This result indicates that the blood components might help to diminish the effect of dendrimer to a single system. Thus, it is necessary to increase the complexity of experiment design to understand the effect of dendrimer on blood component in the presence of the whole blood system.

1.5.2.2 Effect of dendrimer on serum albumin

Serum albumin is the most abundant protein in circulatory system with many physiological functions. The most important function of serum albumin is transportation of various compounds, such as metabolites, endogenous toxins, hormones, drugs [113, 114]. For toxic substances, binding with albumin will reduce the toxic effect in blood circulation.

Thus, it is necessary to understand the interaction between dendrimer and serum albumin in order to further evaluate the systemic toxic effect of dendrimer in circulation system.

Human serum albumin (HSA) and bovine serum albumin (BSA) are commonly used to study the interaction with dendrimer, mainly because HSA and BSA are structurally homologous. Both HSA and BSA are composed of three domains [115, 116]. The main difference is that HSA has only one tryptophan residue Trp-214 but BSA has two tryptophan, Trp-212 and Trp-134, which are fluorophores capable of fluorescence quenching [115]. Such effect is commonly used to study the interaction between dendrimer and serum albumin. In general, as dendrimer concentration increases, the fluorescence signal will decrease, indicating more interaction with serum albumin. The relationship between fluorescent quenching and dendrimer concentration can be displayed by Stern-Volmer plot (Figure 1.5). The slope of the curve, known as Stern-Volmer constant (K_{sv}), can be obtained from the plot for comparison [117, 118].

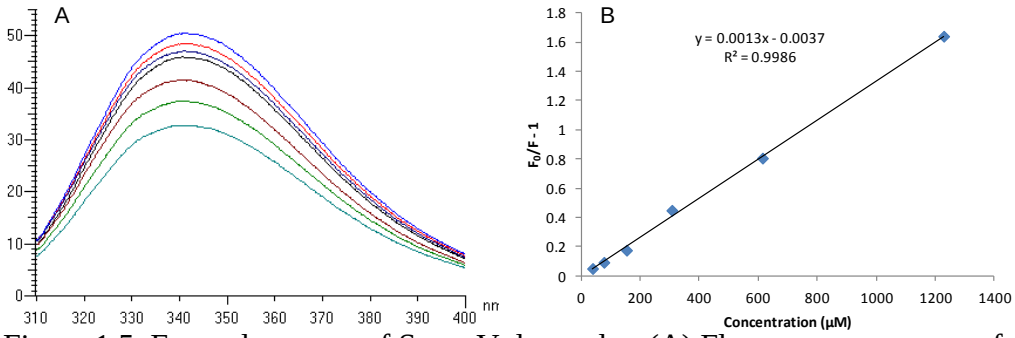

Figure 1.5. Example curves of Stern-Volmer plot. (A) Fluorescence spectra of BSA after incubation with dendrimer samples at various concentrations. (B) Stern-Volmer plot derived from the fluorescence signal at 340 nm.

Table 1.2 shows a collection of Stern-Volmer binding constant reported for different dendrimers. Although the values vary in different experiment settings, general trends can be observed. Generation dependent binding effect was studied by *Giri et al.* [119]. For amine terminated PAMAM dendrimers, the binding effect is higher as generation increases from 0 to 6. Interestingly, the binding constant of PAMAM G8 is lower than PAMAM G6. This could be explained by the size-based selective binding mechanism that dendrimer has a higher binding affinity toward a protein with comparable molecular surface area [120]. HSA has a heart-shaped 3-D structure similar to an equilateral triangular prism with side of ~8nm and height of ~3nm [121] (Figure 1.6). The length of HSA sides is similar to hydrodynamic diameter of PAMAM G6 (7.62nm) [119], which consistent with the size-based selective binding mechanism.

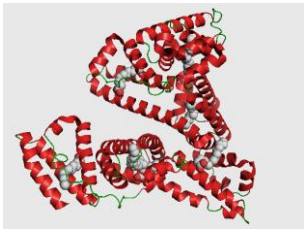

Figure 1.6. 3D structure of human serum albumin [122].

Table 1.2 Stern-Volmer binding constant of dendrimer with serum albumin

Dendrimer	K_{sv} (M^{-1}) with BSA	
mPEG-PAMAM G3	5×10^{3}	[115]
mPEG-PAMAM G4	1×10^{4}	[115]
PAMAM G4	1.1×10^{4}	[115]
PAMAM G4	8.38×10^{3}	[123]
PAMAM G3.5	3.83×10^{3}	[123]
PAMAM G4-OH	2.87×10^{3}	[123]
PAMAM G3.5	3.5×10^{3}	[123]
PAMAM G4	7.6×10^{3}	[123]
Dendrimer	K_{sv} (M^{-1}) with HSA	
mPEG-PAMAM G3	1.3×10^{3}	[124]
mPEG-PAMAM G4	2.2×10^{4}	[124]
PAMAM G4	2.6×10^{4}	[124]
PAMAM-SAH G4	1.3×10^{3}	[124]
Cd2+	2.2×10^{3}	[125]
PAMAM G3.5	1.6×10^{3}	[125]
“PAMAM G3.5-Cd2+” complex	1.4×10^{3}	[125]
G4 PAMAM-pyrrolidone	1.2×10^{5}	[126]
PAMAM G0	1.67×10^{5}	[119]
PAMAM G1	2.83×10^{5}	[119]
PAMAM G2	2.91×10^{5}	[119]
PAMAM G3	3.65×10^{5}	[119]
PAMAM G4	1.67×10^{6}	[119]
PAMAM G5	3.10×10^{6}	[119]
PAMAM G6	5.42×10^{6}	[119]
PAMAM G8	3.30×10^{6}	[119]
PAMAM G4-EDA core	1.67×10^{6}	[119]
PAMAM G4-DAB core	8.45×10^{5}	[119]
PAMAM G4-DAH core	9.59×10^{5}	[119]
PAMAM G4-DAD core	8.38×10^{5}	[119]
PAMAM G4-CYST core	1.43×10^{6}	[119]
PAMAM G4-amine	1.67×10^{6}	[119]
PAMAM G4-amidoethylethanolamine	1.47×10^{6}	[119]
PAMAM G4-succinamic acid	2.52×10^{6}	[119]
PAMAM G4-sodium carboxylate	4.62×10^{6}	[119]
PAMAM G4-pyrrolidinone	2.46×10^{5}	[119]
PAMAM G4-Tris	2.95×10^{5}	[119]
PAMAM G4-amidoethanol	1.29×10^{4}	[119]
PAMAM G4-polyethylene glycol (PEG)	1.77×10^{4}	[119]

The surface charge dependent binding effect between PAMAM dendrimer and BSA was reported by *Klajnert et al.* [123]. The binding constant for PAMAM-NH2 G4, PAMAM-COOH G3.5 and PAMAM-OH G4 is in decreasing order.

Since both PAMAM-NH_2 G4 and PAMAM-COOH G3.5 were ionized at pH 7.4 and have higher binding interaction than the neutral PAMAM-OH, the binding interaction is mainly by electrostatic interaction. At pH 7.4, overall BSA is negatively charged [123]; therefore, the amine-terminated dendrimers have the highest interaction with BSA. However, domain III of albumin is weakly positively charged in physiological pH [123], which explains the higher binding constant of anionic dendrimer compared to neutral dendrimer. In another work by *Giri et al*., similar trend is observed that PAMAM G4 dendrimers with neutral terminal groups have lower binding constants compared to charged dendrimers. The binding of neutral dendrimer is mainly by hydrogen bond between -OH terminal and protein amino acid residues [119]. However, the binding constant of anionic dendrimers is higher than the cationic dendrimers. Since HSA has five different binding sites for carboxylic acids consisting of hydrophobic pockets capped by positively charged amino residues [127], it is suggested to be the main reason for the high level of binding between carboxyl-terminated dendrimer and HSA.

Surface modification of dendrimer could affect the binding interaction with serum albumin. Previous work by *Mandeville et al.* and *Reyes et al*. studied the binding effect of mPEG-PAMAM G3, mPEG-PAMAM G4, PAMAM G4 with BSA and HSA, respectively [115, 128]. The order of binding is PAMAM G4 > mPEG-PAMAM G4 > mPEG-PAMAM G3 for both BSA and HSA. Such order of binding is explained by the formation of hydrogen bonding between mPEG and the PAMAM dendron [115], which hinders the binding interaction between

PAMAM and serum albumin. *Sekowski et al.* studied the binding interaction between PAMAM G3.5, $Cd2^{+}$, and PAMAM G3.5-$Cd2^{+}$ with HSA. After forming a complex with $Cd2^{+}$, the binding constant of PAMAM G3.5-$Cd2^{+}$ is lower than PAMAM G3.5 [125]. These results indicate that shielding the surface charge of dendrimer will help minimize the binding interaction between dendrimer and serum albumin.

Some mechanisms of interactions between PAMAM dendrimers and serum albumins have been proposed previously. Klajanert and Bryszewska reported that dendrimers bind albumins mainly by electrostatic interaction [117], which explained the stronger binding effect of cationic dendrimers compared to anionic dendrimers. Subsequent studies showed that PAMAM dendrimers decreased protein α-helix conformation and increased β-sheet conformation [115, 129], which indicated that secondary structures of albumin was also altered by dendrimer interaction. Some other proposed mechanisms included hydrogen bonding between dendrimer internal groups and protein amino acid residues and hydrophobic interactions [119]. For carboxyl-terminated dendrimer, specific interactions between dendrimer carboxylic groups and protein aliphatic acid binding sites was also considered as important [119].

1.5.2.3 Effect of dendrimer on complement system

The complement pathway is a host defence system which is activated when a foreign material comes into contact with blood. It initiates a series of chemical reactions involving several peptides and enzymes, then leads to inflammation

[130]. There are three separate pathways, the classical pathway, the lectin pathway, and the alternative pathway [131]. Among the three pathways, the alternative pathway is activated by nonspecific binding of C3 on the surface of foreign substances. Biomaterials, including dendrimers, have been shown to activate complement system by alternative pathway [131]. Polymers such as dextran, regenerated cellulose, sephadex, nylon, poly(methylmethacrylate), poly(propylene), poly(acrylamide), poly(hydroxyethylmethacrylate) and plasticized PVC are known to activate the complement system [132-134]. After the alternative pathway is activated, C3 will be cleaved by C3 convertase into C3a and C3b, which are anaphylatoxins that will further lead to activation of the immune system. The concentration of C3a in plasma is commonly used as a measurement of the extent of complement activation [130].

Only a few studies have evaluated the effect of dendrimer on complement system. *Christian et al.* studied the complement activation by PAMAM G5-DNA complex. PAMAM G5 caused obvious complement activation as concentration increased from 0.1 μM to 10 μM. Such effect is reduced as PAMAM/DNA charge ratio decreased from 16:1 to 1:1. At 1:1 ratio, no complement activation effect was observed, indicating that such effect is highly dependent on the surface charge. Since the amine groups are considered to be potent activators of the complement system via alternative pathway [135], surface modification to reduce peripheral amine groups could help reduce complement activation. *Rajesh et al.* studied the complement activation effect of PEGylated hyerbranched cationic polymers. All the tested polymers, PG-PEG-Amine, PG-PEG-Amine-18, PG-PEG-Amine-44

and PG-PEG-Amine-100, showed very minimum C3a generation, using concentration of up to 10 mg/ml concentration. With limited information available, more studies should be done to evaluate complement activation of various types of dendrimers.

1.5.2.4 Effect of dendrimer on coagulation system

Platelets are small anucleated cells of blood coagulation system derived from megakaryocytes in bone marrow [136]. The diameter of platelet is 2-3 μm [137] and the concentration under physiological conditions is $150\text{-}450\times10^{9}$ per liter circulating in the peripheral blood in 10 days [138]. The main function of platelet is hemostasis. Platelets are very sensitive to the microenvironment and can be activated by different physiological agonists such as thrombin, collagen and adenosine-diphosphate, as well as external components such as nanomaterials, drugs and microorganisms [138]. *Dobrovolskaia et al.* compared the effect of PAMAM dendrimers with different sizes and surface groups on platelets in vitro. It is shown that carboxyl-terminated and hydroxyl-terminated PAMAM dendrimers did not cause platelet aggregation, irrespective of their size and generation [139]. Similar result was observed in another study by *Jones et al.* that neutral (G7-OH) and anionic (G6.5-COOH) PAMAM dendrimer did not alter platelet function or morphology while cationic PAMAM dendrimer G7 caused significant changes of platelet functions [140]. For amine-terminated dendrimers, the effect is largely dependent on the generation and size. Higher generation PAMAM dendrimers (G4-G6) caused platelet aggregation as well as release of ATP, thrombospondin and PDGF. Although G3 did not induce platelet

aggregation, an increase of CD62P marker on platelet surface was observed in both G3 and G6 treated platelets [139]. It is also suggested that the observed platelet aggregation is mainly through rapid disruption of membrane integrity rather than signaling-mediated events [139]. In addition, PAMAM G7-NH2 is suggested to induce changes in the platelet cytoskeleton, resulting in release of α-granule contents including P-selectin, RANTES, and PF4 [140]. It is also important to note that cationic G7 dendrimer reduced platelet-dependent thrombin generation. This might be due to morphological changes of platelet membrane so that procoagulant protein binding and prothrombinase complex formation are blocked, which subsequently lead to reduction of thrombin generation [140]. However, only a few studies have reported the effect of dendrimer on platelets. It is necessary to further explore the effect and mechanism of dendrimer-platelet interaction.

Platelet activation usually leads to platelet-dependent thrombin generation, however, PAMAM G7 was reported to attenuate platelet-dependent thrombin generation [140]. Such observation was further supported by *Junes et al.* that PAMAM G7 inhibits thrombin generation rather than thrombin activity [141]. Instead of thrombin generation, PAMAM G7 directly interacts with fibrinogen to form dense, high-molecular-weight aggregates with minimal fibrin fibril formation [141]. It is proposed by the author that such effect is mainly through positively charged dendrimer surface and negatively charged D or E domains of uncleaved fibrinogen rather than classic coagulation pathway. Such mechanism might explain previous finding that intravenous injection of cationic dendrimers

caused a disseminated intravascular coagulation (DIC)-like condition accompanied by production of fibrinogen degradation products and rapid mortality [142].

1.5.2.5 Effect of dendrimer on immune system

Nanomaterials could trigger immune response through a complex process after administration. If the effect is immunostimulatory, the nanomaterials may have short circulation time due to rapid removal as foreign substances. However, if the effect is immunosuppressive, the nanomaterials may risk the whole system more susceptible to infections. In a study of *Roberts et al.* showed that amine terminated PAMAM G3, G5 and G7 did not cause immunogenicity both in vitro and in vivo [143]. *Rajananthanan et al.* studied the ability of amine terminated PAMAM G5 to amplify antigen-specific antibody responses after administration with a soluble protein antigen. PAMAM G5 weakly enhanced anti-ovalbumin immunoglobulin G and immunoglobulin M levels [144]. The inflammatory response of dendrimer treated mouse macrophage cells were evaluated by *Naha et al.* [145]. Amine-terminated PAMAM G4, G5 and G6 showed generation dependent effect. Higher generation dendrimer induced increased intracellular ROS and cytokine production, including macrophage inflammatory protein-2 (MIP-2), interleukin-6 (IL-6), and tumor necrosis factor-α (TNF- α), which may lead to oxidative stress and inflammatory response and ultimately lead to cell death [145]. Based on this result and a few more studies, the mechanism model is proposed to be endocytosis, oxidative stress, endosomal rupture, mitochondrial attach followed by apoptosis [145-147] (Figure 1.7).

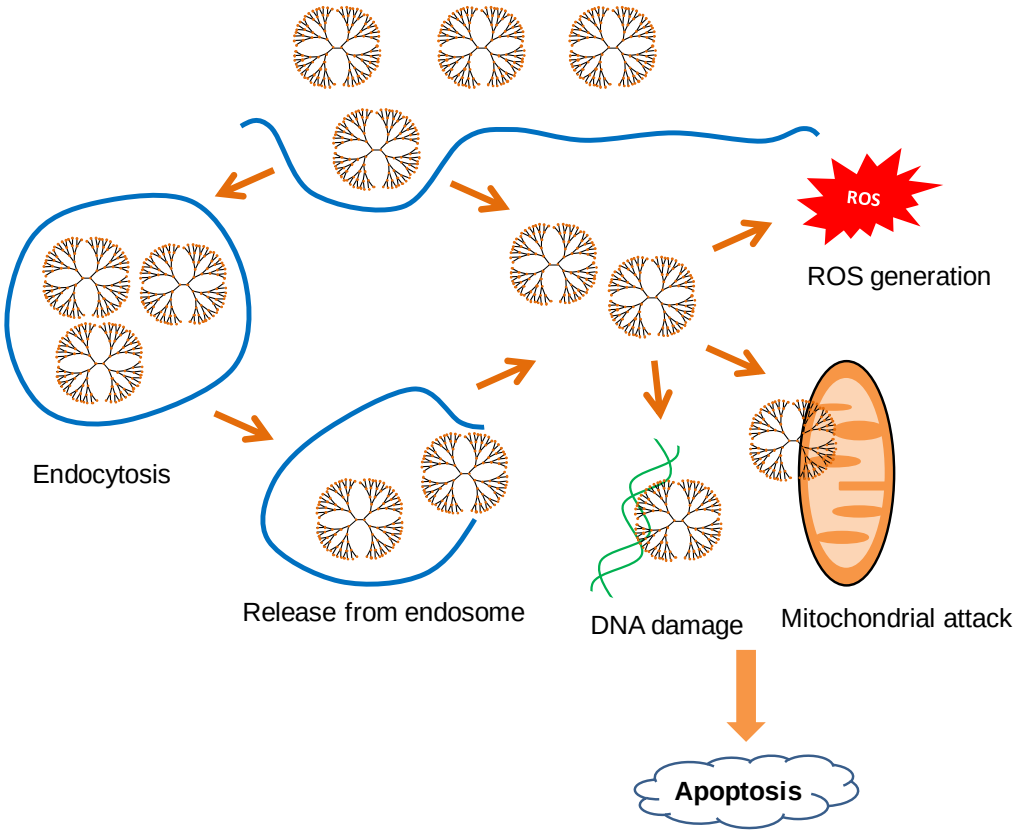

Figure 1.7. Proposed mechanism of dendrimer cytotoxicity

1.5.3 In vivo toxicity and biodistribution of dendrimers

A major focus of the in vivo toxicity of dendrimers is to establish the maximum tolerated dose. *Chauhan et al.* injected PAMAM G4-NH2 and PAMAM G4-OH intraperitoneally to Swiss albino mice for 15 consecutive days and monitored their toxicity profiles subsequently. PAMAM G4-NH2 at 10 mg/kg did not cause any toxic effect. However, at 19mg/kg, declined glucose level, increased alanine aminotransferase and aspartate aminotransferase activities were observed. Kidney and liver toxicity was also observed for PAMAM G4-NH2 at high dose level (19 mg/kg) during the recovery period (15 days after the treatment) [148]. Similar

result was reported by *Greish et al.* to evaluate acute toxicity on CD-1 mice after intravenous injection of PAMAM G4 and PAMAM G7 dendrimers. Amine-terminated dendrimers were toxic at doses higher than 10 mg/kg while carboxyl- and hydroxyl-terminated dendrimers (G3.5-COOH, G6.5-COOH, G4-OH, and G7-OH) were tolerated at doses 50-fold higher [142]. *Roberts et al.* reported animal death after administration of PAMAM G7-NH_2 at 45 mg/kg [143]. For oral administration of dendrimers, G4-NH_2 was tolerated at 100 mg/kg with no observed toxicity effect, meanwhile G7-NH_2 was found to be toxic at 50 mg/kg [142]. All the tested carboxyl- and hydroxyl-terminated dendrimers were tolerated at 300 mg/kg. A recent study by *Pryor et al.* evaluated in vivo toxicity of dendrimers by using embryonic zebrafish model for the first time [149]. Cationic PAMAM dendrimers from generation 3 to 6 caused 100% mortality at concentration above 50 ppm after 24 h post-fertilization. However, it is important to establish the correlation with other in vivo toxicity models.

Malik et al. studied biodistribution of ^{125}I-labelled PAMAM dendrimers after i.v. injection to Wistar rats [100]. Anionic dendrimers PAMAM G2.5-COOH G3.5-COOH and G5.5-COOH circulated longer (20-40% recovered dose in blood at 1 h) than cationic dendrimer PAMAM G3-NH_2 and G4-NH_2 (<2% recovered dose in blood at 1 h). For both anionic and cationic dendrimers, majority were captured in liver at 1 h after administration. Sadekar studied the biodistribution of PAMAM-OH dendrimers in orthotopic ovarian tumor-bearing mice [150]. The dendrimers showed different biodistribution profile for different generations. PAMAM G5-OH mainly accumulates in kidney over 1 week. G6-OH distributed both in liver

and kidney. G7-OH had longer plasma circulation time, resulting in non-specific distribution in major organs, including heart, lung, liver, spleen, kidney as well as tumor.

1.6 Surface engineering of dendrimers

The abundant surface groups of dendrimer make it highly flexible for various surface engineering schemes to achieve desirable properties. A major reason for surface modification is to reduce potential toxicity of cationic dendrimers. Apart from that, dendrimer functionality could also be improved for other purposes by attachment of ligands. Such benefits include improved biodistribution and pharmacokinetic properties, targeting to specific site for action, increased solubility profile, higher drug encapsulation, sustained and controlled drug release [20]. Commonly reported surface engineering strategies are summarized below in Figure 1.8.

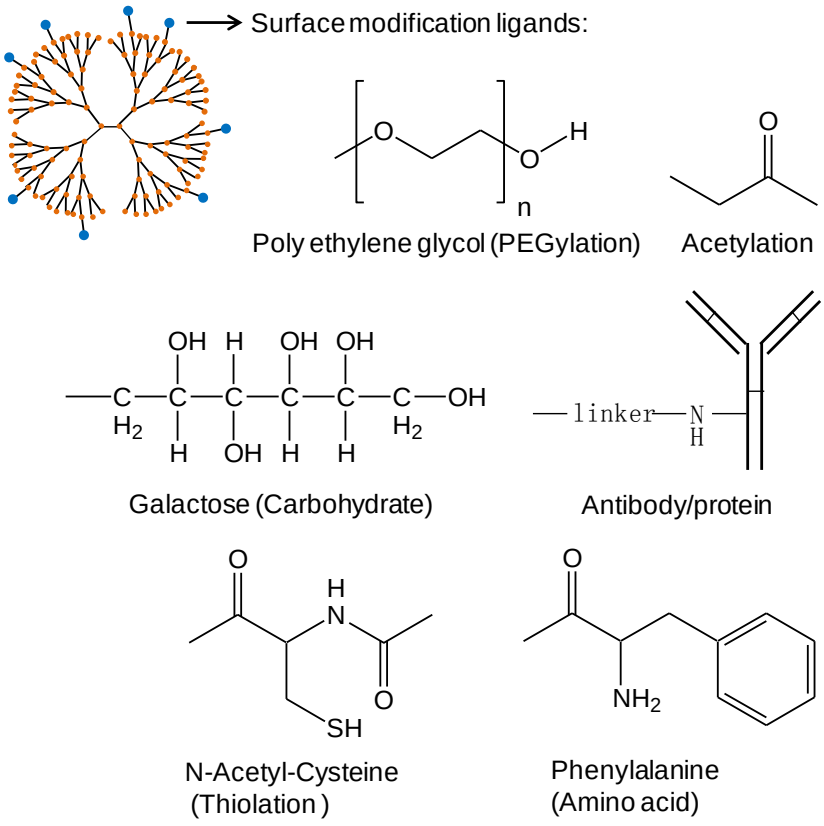

Figure 1.8. Structures of reported dendrimer surface modification ligands.

1.6.1 PEGylated dendrimers

Modifying dendrimer surface with PEG groups is the most commonly applied method to reduce toxicity as well as to improve its expected functionalities [151-154]. *Jevprasesphant et al.* studied the effect of surface modification with PEG2000 or lauroyl chains on dendrimer toxicity [102]. Decreased cellular toxicity was observed with increased number of attached lauroyl or PEG chains. Such reduction of toxicity is explained by shielding of the positive charge on the dendrimer surface. Another possible reason is the space between cell membrane and dendrimer surface group created by PEG to prevent electrostatic interactions between dendrimers with cell membrane. *Bhadra et al.* reported PEG5000

conjugated PAMAM G4 for delivery of anti-cancer drug 5-fluorouracil [44]. Haemolytic toxicity of dendrimer was reduced for PEG modified PAMAM G4. Moreover, such formulation was found to have increased drug-loading capacity and reduced drug release rate. *Kim et al.* prepared PAMAM-PEG-PAMAM triblock copolymer as gene delivery carrier [155]. The copolymer had improved water solubility, little cytotoxicity and high transfection efficiency as gene delivery system. Similarly, *Qi et al.* surface modified PAMAM G5 and G6 with PEG5000 for gene delivery [152]. PEGylated PAMAM significantly reduced the haemolysis effect and in vitro and in vivo toxicity of PAMAM. PAMAM with 8% molar ratio PEGylation showed the highest transfection efficiency both in vitro and in vivo. *Chen et al.* reported acute in vivo toxicity of PEGylated melamine dendrimer. No toxicity was observed for male C3H mice in a single dose up to 2.56 g/kg i.p. or 1.28 g/kg i.v. [156]. Thus, PEGylated dendrimers greatly reduced toxic effect of dendrimer and enables the dendrimer to be studied in a wide range of biomedical applications.

1.6.2 Carbohydrate conjugated dendrimers

Dendrimer surface modified with carbohydrate could provide benefits such as reduced haemolytic toxicity, cytotoxicity and immunogenicity as well as controlled and targeted drug delivery [157, 158]. *Agrawal et al.* prepared galactose modified poly-L-lysine dendrimers as a delivery vehicle of chloroquine phosphate [157]. The galactose modified dendrimer was less toxic than unmodified dendrimer and could be potentially used for controlled delivery of chloroquine phosphate. Similarly, *Bhadra et al.* coated PPI dendrimer surface

with galactose and studied delivery of primaquine phosphate to liver organ [158]. Surface coated PPI improved drug entrapment efficiency and prolonged drug release compared to unmodified PPI. This could be explained by the increased steric hindrance caused by coating with galactose. Thus, the increased numbers of functional groups further provide space for drug entrapment and prevent the drug release from the open structure. It also showed reduced toxicity and effective targeting to liver. *Agashe et al.* studied the toxicity of PPI G5 modified with lactose and mannose [103]. Surface modified PPI greatly reduced cytotoxicity and haemolytic toxicity compared to parent dendrimer without modification.

1.6.3 Acetylated dendrimers

Acetylation is another popular method to specifically modify the surface of amine terminated dendrimers to reduce its toxicity. *Rohit et al.* modified PAMAM G2-NH_2 and G4-NH_2 with acetyl groups and studied their effect on Caco-2 cell monolayers. For fully acetylated PAMAM G4 and G2, no toxicity on Caco-2 cells was observed at 1 mM concentration. Furthermore, the permeability and uptake profiles of acetylated dendrimers were similar to unmodified dendrimers, indicating reduced toxicity while remaining desirable properties of PAMAM dendrimers as transepithelial transport carrier [159]. *Waite et al.* studied acetylated PAMAM G5-NH_2 for delivery of siRNA to U87 malignant glioma cells. Amine acetylation of dendrimer resulted in decreased cytotoxicity to U87 cells, as well as enhanced dissociation of dendrimer/siRNA complexes [160]. However, high degree of acetylation reduced the gene silencing efficiency of the

dendrimer/siRNA complex, mainly due to reduced positive charge. Thus, it is important to find a balance in the surface modification process to maintain the functionality as well as reduce toxicity. *Zhou et al.* synthesized a series of poly(amide-amine) dendrimers with a core of 1,4,7,10-tetraazacyclododecane [161]. It was found that the water solubility of G4 and G5 dendrimers was greatly improved after acetylation. Such dendrimer was further conjugated with 1-bromoacetyl-5-fluorouracil to achieve controlled release of anti-tumor drug 5-fluorouracil.

1.6.4 Thiolated dendrimers

Dendrimers are surface modified with thiol groups for various research purposes. One main purpose is to utilize the interaction between thiol groups and metal ions. In an early study of Chehic and Crooks, PAMAM dendrimers functionalized with thiol groups were found to form stable monolayers on planar Au substrates. They also prepared water-soluble nanoparticles with diameter of 1-2 nm. Such thiolated dendrimer coated Au nanoparticles were stable up to 120 Au atoms/dendrimer [162]. This material was an attractive candidate for use in sensing devices and for catalysis. In another example, thiolated Diaminobutane-based poly(propyleneimine) (DAB) dendrimers were studied to encapsulate CdSe quantum dots (QDs) [163]. The thiolated surface helped to increase the affinity towards QDs and enabled the dendrimer surface to act as a ligand towards soft metal ions. Cd(II) and Pb(II) showed the higher enhancement and quenching effects respectively towards the fluorescence of such composition. It was

concluded by the author that this newly developed nanosensor has potential for bioanalytical soft metal detection and quantification.

Another potential application of thiolated dendrimer is to form cleavable disulfide linkage to deliver compounds at specific trigger condition. *Navath et al.* prepared thiolated PAMAM dendrimer and further conjugated with N-acetyl-L-cysteine (NAC) [164]. Such conjugate is designed for intracellular delivery of NAC where the glutathione (GSH) level is high enough to cleave the disulfide bond. The activity of both PAMAM G4-NH_2 and PAMAM G3.5-COOH conjugates were confirmed as they showed significantly better nitrite inhibition both at 24 and 72 h compared to free NAC, indicating the protective role of dendrimer conjugation as well as rapid GSH responsive release of NAC. With the same concept, PAMAM G4 dendrimer was conjugated to NAC in another study [165]. The conjugate can deliver near 60% of NAC within 1 h at intracellular GSH concentrations but no NAC release at plasma GSH levels. In reactive oxygen species (ROS) assay tested on activated microglial cells, the dendrimer NAC conjugates showed an order of magnitude increase in anti-oxidant activity compared to free drug.

Recently, thiolated dendrimer is reported as viable mucoadhesive excipient for controlled drug delivery [166]. PAMAM G3.5-COOH was conjugated with cysteamine (CYS) and used as a delivery vehicle for acyclovir. The thiolated dendrimers showed sustained release profile of acyclovir and higher mucoadhesion effect. The in vitro mucoadhesive activity was related to the PAMAM-CYS conjugation ratio. For PAMAM-CYS conjugate at 1:60 molar ratio, the mucoadhesive activity was 1.53-fold higher than the PAMAM-CYS

conjugate at 1:30 molar ratio and 2.89-fold higher than the dendrimer alone formulation. These results indicate that thiolated dendrimers could be potentially used as a mucoadhesive carrier in oral drug delivery.

1.6.5 Antibody conjugated dendrimers

Some studies have reported the conjugation of dendrimers with antibodies to achieve improved functionality, mainly targeting to specific receptor. An important aspect for antibody conjugated dendrimer is that whether such system will influence the immunoactivity of antibody. *Wangler et al.* studied the effect of dendrimer conjugation on the immunoreactivity of antibody [167]. Anti-EGFR antibody hMAb425 were conjugated with PAMAM of different sizes containing various number of chelating agents per conjugation site. The result showed that the number of derivatization sites largely influence the immunoreactivity rather than dendrimer size. *Shukla et al.* conjugated anti-HER2 receptor monoclonal antibody (anti-HER2 mAb) to PAMAM G5 [168]. The antibody conjugated dendrimer specifically targeted cell lines overexpressing HER2 due to the anti-HER2 mAb functional groups. Moreover, methotrexate loaded in the antibody modified dendrimer showed similar activity as methotrexate free drug to inhibit the dihidrofolate reductase with reduced cytotoxicity, indicating reduced non-specific toxicity to normal cells without overexpression of HER2. Such reduction of toxicity was attributed to the slowed release of methotrexate and longer retention time in lysosomal pocket. *Patri et al.* prepared J591 anti-PSMA (prostate-specific membrane antigen) monoclonal antibody conjugated PAMAM G5 to target prostate cancer cell line LNCaP [169]. The conjugate showed

selective binding to PSMA positive prostate cancer cells LNCaP over PSMA negative prostate cancer cells PC3.In another study, *Kobayashi et al.* prepared OST7 (a murine monoclonal IgG1) conjugated PAMAM G4 dendrimer [170]. Biodistribution study showed that such conjugate specifically accumulated in the KT005 tumor (16.1%) compared to control dendrimer without OST7 conjugation (5.1%) At the same time, about 30% and 15% of the OST7 conjugated PAMAM dendrimers accumulated in liver and spleen, respectively.

1.6.6 Amino acid/peptide conjugated dendrimers

Dendrimers are also conjugated with amino acid or peptide to decrease toxicity and improve functionality in applications. Phenylalanine modified PPI G5 and PAMAM G4 dendrimers were reported to be less toxic than the original versions [103, 171]. Moreover, amino acid conjugate dendrimers were also reported with higher transfection efficiency. *Kono et al.* synthesized phenylalanine conjugated dendrimers and tested transfection efficiency on CV1 cells. Dendrimer surface modified with 64 phenylalanine residues achieved high transfection efficiency [171]. Similarly, *Choi et al.* prepared L-arginine conjugated PAMAM dendrimer and tested its transfection efficiency against L-lysine-PAMAM, PAMAM and PEI on 293, HepG2, Neuro 2A and primary rat vascular smooth muscle cells [172]. Arginine-PAMAM dendrimer showed much higher transfection efficiency. Yang and Kao conjugated arginine-glycine-aspartate (RGD) peptides with PAMAM G3.5 and PAMAM G4 dendrimers. *Thomas et al.* conjugated epidermal growth factor (EGF), a peptide containing 53 amino acids, to PAMAM G5 dendrimer. Such conjugate showed binding to EGFR-expressing cell lines in a receptor-

specific fashion [173]. Thus, such EGF-dendrimer could be further conjugated with chemotherapeutic drug for targeted cancer treatment.

1.7 Chapter summary

This chapter has provided background information on dendrimer preparation, structure properties, biomedical applications, toxicity issues and surface modification methods to reduce toxicity as well as to improve functionalities. The following chapter will focus on the hypothesis and objectives of the project.

CHAPTER 2. HYPOTHESIS AND OBJECTIVES

2.1 Thesis rationale and hypothesis

Dendrimer is a unique type of polymer that possesses attractive properties for potential biomedical applications such as drug delivery, diagnostics, and gene delivery. The density and type of surface groups largely affect the physicochemical characters of dendrimer. Amine terminated dendrimers are the most widely studied because the inherent cationic charge allows for interaction with many biological components such as DNA, cell membranes and proteins. However, such interaction also poses concerns for the toxicity of dendrimer in biomedical applications. As described in chapter 1, studies have shown that surface modifications are useful strategies to reduce dendrimer toxicity. Based on these findings, the hypothesis for this project is that surface modification with various functional groups or via physical complexation will improve dendrimer functionality in drug delivery applications as well as reduce its inherent toxicity.

2.2 Objectives

1. To prepare dual functionalized dendrimers with PEGylation and thiolation. This is described in chapter 3, where the preparation of the dendrimer derivatives and physicochemical characterizations were studied.
2. To examine the compatibility of functionalized dendrimer conjugates with major blood components. This is described in chapter 4, where the toxic effect of dendrimer conjugates on various blood components was evaluated.

3. To investigate the potential application of dual functionalized dendrimers in oral drug delivery. This is described in chapter 5, where the potential application of dual functionalized dendrimers as epithelial penetration enhancer was studied in both in vitro and in vivo models. BCS class III drug ganciclovir was used as model drug for in vivo evaluation.
4. To evaluate the effect of dendrimer-lipid hybrid nanosystem on therapeutic efficacy of paclitaxel. This is described in chapter 6, where the dendrimers were physically mixed with lipids to form a hybrid nanosystem. The hybrid nanosystem was evaluated as a novel drug delivery system of paclitaxel.

CHAPTER 3. SYNTHESIS AND PHYSICOCHEMICAL CHARACTERIZATION OF PAMAM DENDRIMER DERIVATIVES

3.1 Introduction

The systemic circulation is a complex biological milieu made up of various components including blood and immune cells as well as proteins that serve important functions such as blood coagulation and host defence. Interactions of the dendrimer-based pharmaceuticals with such components could lead to rapid recognition and subsequent removal from systemic circulation which in turn dictates the in vivo fate of the dendrimer-based pharmaceuticals.

In view of the hemotoxicity of the cationic PAMAM dendrimers, manipulation of the surface properties of these dendrimers would present a viable approach in overcoming this limitation. PEGylation is a common method to surface-modify nanoscaled systems to prevent protein adsorption and cellular interactions [174, 175] and recently, thiolation of polymers has been shown to improve the hemocompatibility of polymers such as poly(D,L-lactic acid/glycolic acid) (PLGA) and poly(ethylene terephthalate) [176, 177]. Moreover, the surface thiol groups have been utilized to interact with metal ions or provide mucoadhesive properties [163, 166]. Thus, a combination of thiolation and PEGylation might further improve blood compatibility of dendrimer as well as to provide additional properties that could be applied to improve the functionalities of dendrimer in

biomedical applications. As such, in this chapter, cationic PAMAM dendrimers were functionalized with PEG or thiol or the combination of both.

The synthetic scheme of PEG-PM-SH polymer is shown in Figure 3.1. PEG groups were firstly attached to the amine group of PAMAM. Subsequently, the PEGylated dendrimer reacted with TBA to generate free thiol groups. The physicochemical properties of the dendrimer derivatives were characterized and discussed in this chapter.

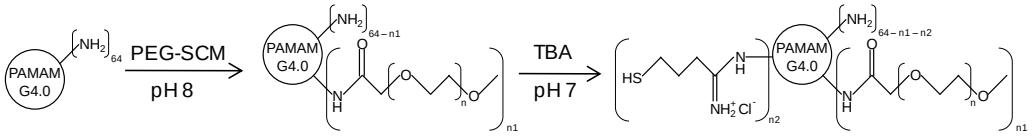

Figure 3.1. Synthetic scheme of PEG-PAMAM and PEG-PAMAM-TBA conjugates.

3.2 Materials and Methods

3.2.1 Materials

PAMAM dendrimer generation 4 with ethylenediamine core was obtained from Dendritech, Inc. (Midland, MI, U.S.A.). Methoxy poly(ethylene glycol) succinimidyl carboxymethyl (mPEG-SCM) (M.W. 2000) was purchased from Laysan Bio, Inc. (Arab, AL, U.S.). 2-Iminothiolane hydrochloride (Traut's Reagent, TBA), 5,5'-dithiobis(2-nitrobenzoic acid) (Ellman's reagent), sodium borohydride ($NaBH_4$) were obtained from Sigma-Aldrich Pte Ltd. (Singapore). All other chemicals used in the study were purchased from Sigma-Aldrich (St Louis, MO, USA) unless otherwise stated.

3.2.2 Preparation of PEG-PM Dendrimer.

PEG-PM conjugation was performed with modification from a method previously reported [178]. Briefly, 60 mg (4.2 μmol) of PAMAM-NH_2 G4 was dissolved in 5 ml of phosphate buffer (0.5 M, pH 8.0). Four (33.8 mg, 16.8 μmol) or eight (67.6 mg, 33.6 μmol) times of mPEG-SCM (M.W. 1923 determined by GPC) was added to the dendrimer solution. The reaction mixture was stirred for 24 h at room temperature in the dark and with nitrogen protection. The product was subsequently dialyzed three times against distilled water for 48 h. The dialyzed product was lyophilized and stored at 4℃ until further usage. Synthesized PEG-PM conjugates were analyzed by ^{1}H-NMR (Bruker Avance 500, Bruker AXS Pte. Ltd., Singapore) and Fourier transform infrared (FT-IR) spectroscopy (PerkinElmer Spectrum 100, PerkinElmer, Inc., MA, USA). The hydrodynamic diameter and zeta potential of synthesized polymers were analyzed by a Zetasizer Nano-ZS90 (Malvern. Instruments GmbH Herrenberg, Germany).

3.2.3 Preparation of Thiolated PEG-PM Dendrimer (PEG-PM-SH).

PEG-PM-SH was synthesized with modifications from a method previously reported [179]. Briefly, 40 mg of lyophilized PEG-PM dendrimer was dissolved in 5 ml of phosphate buffer (0.5 M, pH 7.2), and 21.1 mg (153.6 μM) of 2-iminothiolane HCl was added, with the pH of the mixture adjusted to 7.0 with NaOH (0.1 M). The reaction mixture was stirred for 24 h at room temperature in the dark and with nitrogen protection. The product was dialyzed stepwise against (1) 5 mM HCl, (2) 5 mM HCl containing 1% NaCl twice, (3) 5 mM HCl, and (4)

1 mM HCl. The dialyzed product was then lyophilized and stored at −20°C until further usage.

3.2.4 Molecular Weight Determination.

Gel permeation chromatography (GPC) was used to evaluate the relative molecular weight of PEG-PM. Polyethylene (glycol/oxide) standards (EasiVial PEG/PEO, Agilent Technologies Singapore Pte. Ltd.) with molecular weights of 106, 194, 615, 1500, 3930, 12 140, 23 520, 62 100, 116 300, 442 800, 909 500, 1 258 000 were used to construct the calibration curve. Dendrimer molecular weight was also determined by matrix-assisted laser desorption ionization time-of-flight (MALDI-TOF) mass spectrometry (4800 Proteomics Analyzer, Applied Biosystems Asia Pte Ltd.). Dendrimer samples were dissolved in methanol at a final concentration of 0.2 mg/ml. Five milligrams per milliliter of α-cyano-4-hydroxycinnamic acid (CHCA) in acetonitrile/water (75:25) with 0.1% trifluoroacetic acid was used as the matrix. Equal volumes of sample and matrix were mixed in a tube, and 1 μL was spotted on the sample plate. The instrument mode was Positive Ion mode. The operation mode was linear. Lysozyme at 100 pmol was used as the standard.

3.2.5 Determination of the Thiol Group Content.

The amount of free thiol groups attached to the PAMAM dendrimer was determined with Ellman's reagent (3 mg of 5,5'-dithiobis(2-nitrobenzoic acid) dissolved in 10 ml of 0.5 M PBS; pH 8.0). Polymer sample was dissolved in 1 ml of 0.5 M PBS (pH 8.0), and 100 μL sample was mixed with 500 μL Ellman's

reagent. The reaction was incubated in dark at 25 ℃ for 90 min. Afterwards, the absorbance was immediately measured at wavelength of 412 nm in a microtiter plate reader (Tecan, Infinite M2000). The amount of free thiol groups was calculated from a standard curve prepared using N-acetyl-cysteine. To determine the total amount of thiol groups, 1.5 mg of polymer was first dissolved in 500 μL of 0.05 M Tris buffer (pH 6.8), and 1 ml of freshly prepared 4% sodium borohydride ($NaBH_4$) solution was added. The mixture was incubated for 60 min at 37 ℃. Thereafter, 100 μL of 10 M HCl was added to inactivate the excess $NaBH_4$. The pH of the mixture was adjusted to 8.0 with 1 ml of 1 M PBS (pH 8.5). A sample of 100 μL was taken for Ellman's assay as described above.

3.3 Results

3.3.1 Structure characterization by NMR

Two PEG-PM conjugates with PEG: PAMAM feed ratios of 4:1 and 8:1 were prepared following literature method [178]. The conjugation was confirmed by NMR spectroscopic method (Figure 3.2). In PEG-PM samples, the appearance of a major peak at chemical shift at 3.4−3.6 ppm represents the protons of the repeat unit −CH2CH2O−of PEG. After conjugation with TBA, the signals at δ8.66 ppm (br, Hn) and δ1.76 ppm (br, Hq) indicate that TBA was conjugated with PAMAM dendrimers. This was further confirmed by thiol group quantification with Ellman's reagent.

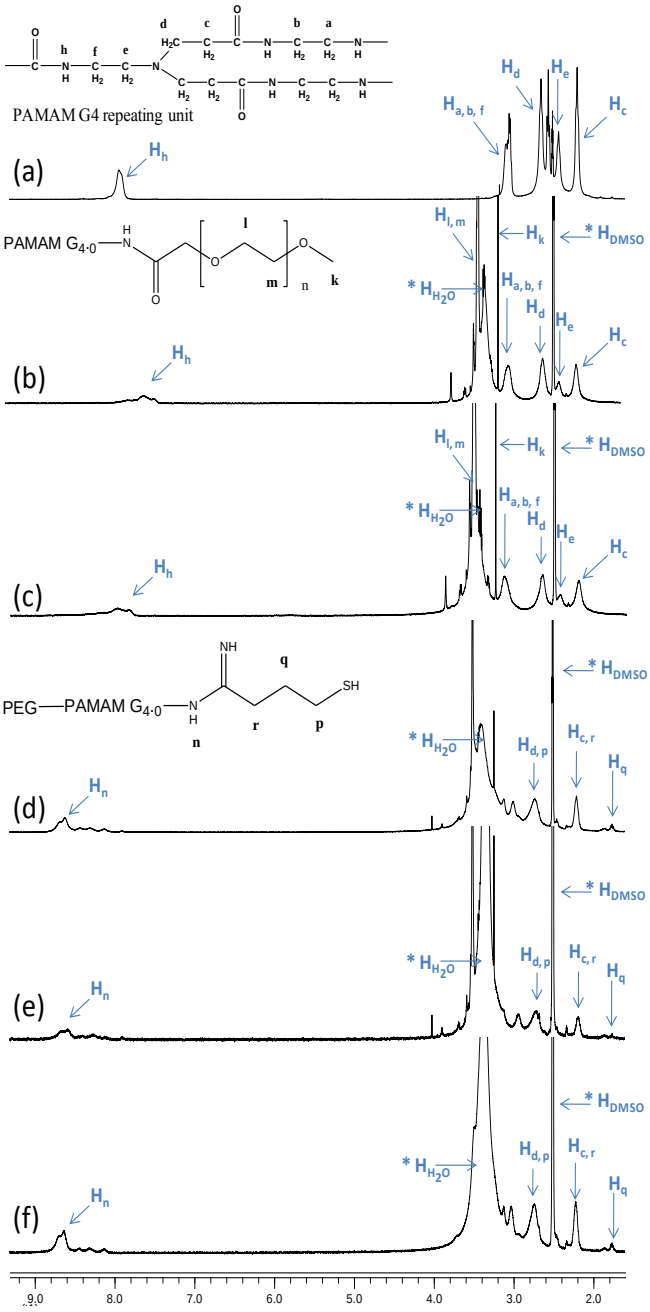

Figure 3.2. ^{1}H-NMR spectra of a) PM G4.0, b) PEG(1.8)-PM c) PEG(4.0)-PM, d) PEG(1.8)-PM-TBA(7.0), e) PEG(4.0)-PM-TBA(6.7), f) PM-TBA(7.6). The signals for PAMAM are d 7.94 ppm (s, Hh), d 2.95-3.31 ppm (m, Ha, Hb, Hf), d 2.65 ppm (br, Hd), d 2.43 ppm (br, He) and d 2.20 ppm (br, Hc). The signals for PEG-PAMAM are d 3.4-3.6 ppm (m, Hl, Hm) and d 3.24 ppm (s, Hk). The appearance of a major peak at chemical shift at 3.4-3.6 ppm represents the protons of the repeat unit -CH_2CH_2O- of PEG. After conjugation with TBA, the signals at d 8.66 ppm (br, Hn) and d 1.76 ppm (br, Hq) indicates that TBA was conjugated with PAMAM dendrimers.

3.3.2 FTIR analysis

In FTIR analysis, dendrimer samples were analyzed using KBr pellet method. The IR spectrum displayed characteristic peaks at ~3400 cm^{-1} (N-H stretch of primary amines); ~2916 cm^{-1} (aliphatic C-H stretch); ~1647 cm^{-1} (-C=O stretch of amide); ~1554 cm^{-1} (N-H bending of N substituted amide); ~1455 cm^{-1} (C-H stretch of methylene),~1063 cm^{-1} (C-O of aliphatic ether linkage) (Figure 3.3). The IR spectrum peak information is listed in Table 3.1.

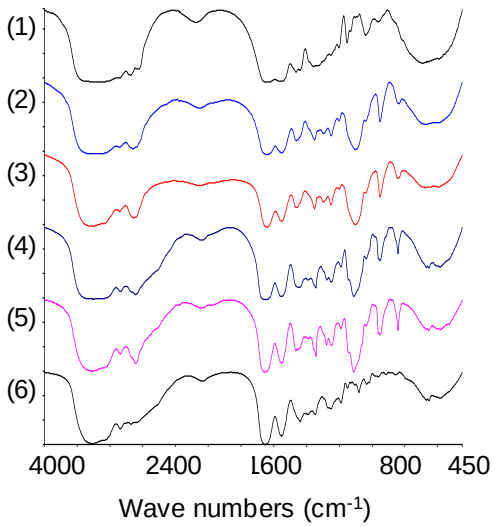

Figure 3.3. FT-IR spectra of (1) PM G4, (2) PEG(1.8)-PM, (3) PEG(4.0)-PM, (4) PEG(1.8)-PM-TBA(7.0), (5) PEG(4.0)-PM-TBA(6.7), (6) PM-TBA(7.6).

Table 3.1. IR spectrum peak information of dendrimer samples.

Dendrimer	Wave numbers (cm^{-1})
PM G4	3364.69[a], 2948.2[b], 1638.45[c], 1563.8[d], 1464.82[e], 1040.79[f]
PEG(1.8)-PM	3399.56[a], 2916.31[b], 1643.26[c], 1553.49[d], 1461.49[e], 1102.08[f]
PEG(4.0)-PM	3433.57[a], 2913.99[b], 1646.82[c], 1553.36[d], 1459.28[e], 1103.06[f]
PEG(1.8)-PM-TBA(7.0)	3399.22[a], 2885.78[b], 1654.76[c], 1554.11[d], 1441.47[e], 1037.08[f]
PEG(4.0)-PM-TBA(6.7)	3399.32[a], 2888.72[b], 1655.21[c], 1554.23[d], 1466.49[e], 1038.01[f]
PM-TBA(7.6)	3410.58[a], 2945.03[b], 1654.43[c], 1554.26[d], 1439.16[e], 1034.11[f]

[a] N-H stretch of primary amines
[b] Aliphatic C-H stretch
[c] –C=O stretch of amide
[d] N-H bending of N substituted amide
[e] C-H stretch of methylene
[f] C-O of aliphatic ether linkage

3.3.3 Yield, size, zeta potential and molecular weight determination

All the synthesized polymers were obtained with average yields of >80%, except for PM-TBA(7.6), which only had a yield of ~41% (Table 3.2). The particle size and zeta potential of these polymers were measured by Zetasizer Nano-ZS90. All the PEG or TBA conjugated dendrimers showed similar particle size and zeta potential as compared to unmodified PAMAM dendrimer because of low PEGylation ratio and introduction of imino groups to the surface while attaching TBA to the surface of PAMAM (Table 3.2). The molecular weight of dendrimers was tested by GPC and MALDI-TOF MS as listed in Figure 3.4, 3.5 and Table 3.2.

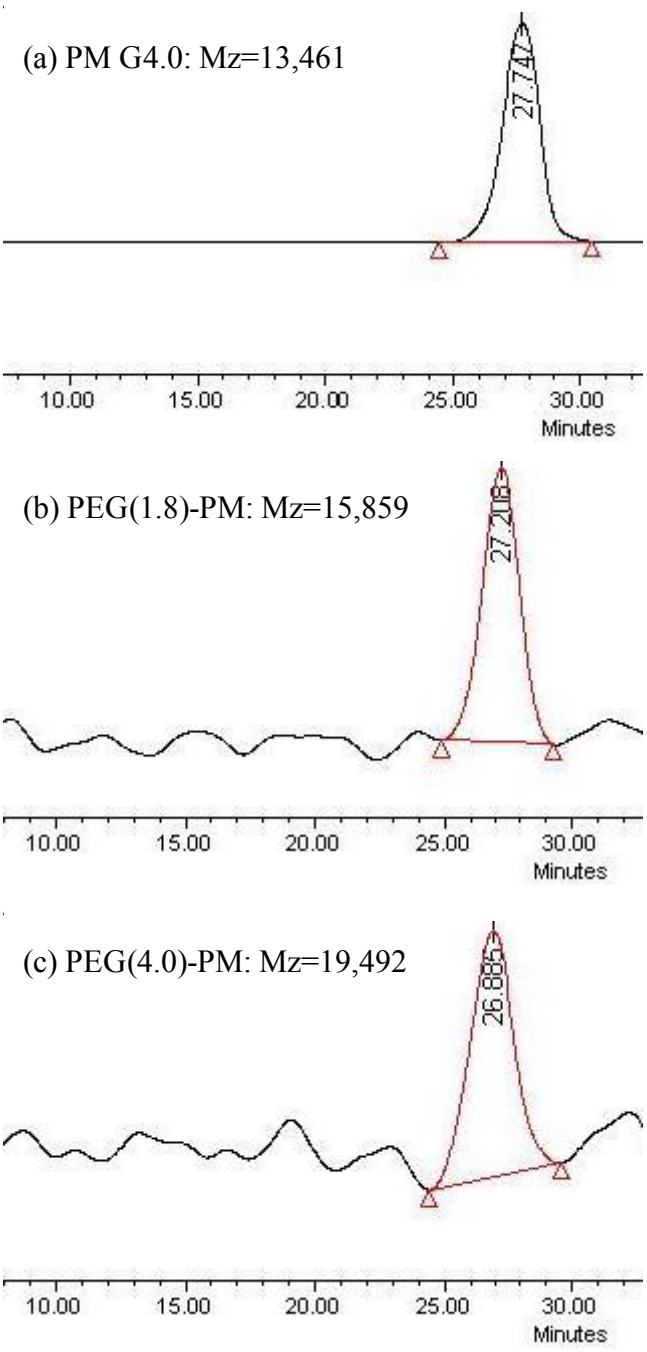

Figure 3.4. Representative GPC chromatogram of a) PM G4.0, b) PEG(1.8)-PM c) PEG(4.0)-PM sample.

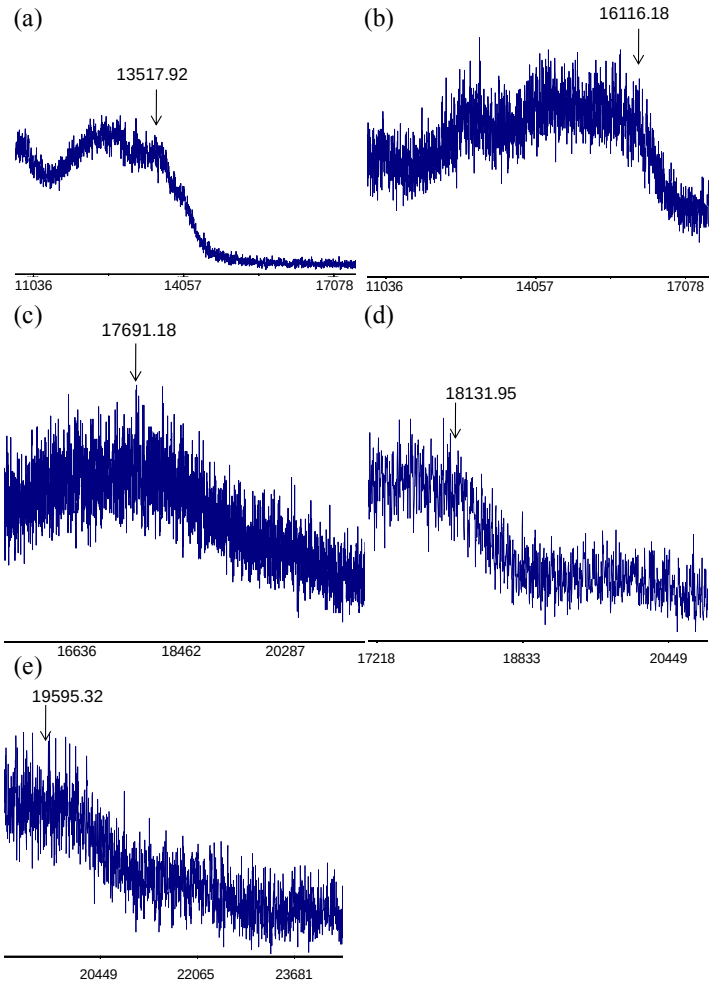

Figure 3.5. Molecular weight of a) PM G4.0, b) PEG(1.8)-PM, c) PEG(1.8)-PM-TBA(7.0), d) PEG(4.0)-PM, e) PEG(4.0)-PM-TBA(6.7) determined by MALDI-TOF mass spectrometry.

Table 3.2 Physicochemical Characterization of conjugated dendrimers

	PM G4	PEG(1.8)-PM*	PEG(4.0)-PM*	PEG(1.8)-PM-TBA(7.0)*	PEG(4.0)-PM-TBA(6.7)*	PM-TBA(7.6)*
Yield	NA	80.4% ±7.6%	93.6% ±2.4%	82.8% ±8.1%	93.9% ±3.3%	41.1% ±7.4%
Size (nm)	4.3 ±0.4	3.7 ±1.4	4.6 ±1.3	6.1 ±1.4	5.4 ±1.3	4.3 ±1.6
Zeta potential (mV)	+30.1 ±0.9	+26.9 ±5.0	+36.4 ±5.0	+28.3 ±4.6	+36.7 ±1.3	+39.2 ±1.8
$C_{free-SH}$ (μmol/g)	NA	NA	NA	172.0 ±17.5	125.2 ±20.7	332.8 ±18.4
$C_{total-SH}$ (μmol/g)	NA	NA	NA	404.7 ±42.9	313.8 ±90.9	536.3 ±71.5
M.W. (GPC)	13487	16662	20751	17372**	21430**	14259**
M.W. (MALDI-TOF)	13518	16116	18132	17691	19595	ND***
PDI	1.1 ±0.0	1.1 ±0.0	1.2 ±0.0	NA****	NA****	NA****

*The feed ratio of PEG to dendrimer for PEG(1.8)-PM, PEG(4.0)-PM was 4:1 and 8:1, respectively. The feed ratio of thiol to dendrimer for PEG(1.8)-PM-TBA(7.0), PEG(4.0)-PM-TBA(6.7), and PM-TBA(7.6) was 64:1.

**Molecular weights of (1.8)-PM-TBA(7.0), PEG(4.0)-PM-TBA(6.7), and PM-TBA(7.6) were determinate from GPC data of PM G4, PEG(1.8)-PM, PEG(4.0)-PM and thiol group quantification.

***ND: not determined.

****NA: not applicable.

3.3.4 Thiol group quantification

Traut's Reagent is very commonly used to react with primary amino groups to generate thiol groups [179-182]. The amount of free and total thiol groups conjugated on PAMAM dendrimer is shown in Table 3.2. Two feed ratios of thiol to dendrimer were used (64:1 and 128:1), and the higher feed ratio of 128:1 did not result in higher number of thiol groups per PAMAM. The lyophilized thiolated dendrimers appeared as white to yellow color powder of fibrous structure. In order to minimize oxidation during storage, the samples were purged with nitrogen gas and stored at -20℃. For PEG(1.8)-PM-TBA(7.0) and PEG(4.0)-PM-TBA(6.7) samples, 57.4% and 60.1% of the thiol groups were oxidized to disulfide bond during the preparation process. In comparison, the degree of oxidation for PM-TBA(7.6) is 38.0%, which is less extensive in comparison.

3.4 Discussion

3.4.1 Molecular weight determination

The molecular weights of various dendrimers were determined by GPC and MALDI-TOF MS. GPC is chosen as the first method as it could reflect the average absolute molar mass of the dendrimers [183] rather than the distribution of the mass fractions. Both methods showed similar results for PEGylated PAMAM and unmodified version. For PEG/dendrimer feed ratios of 4:1 and 8:1, the average conjugation ratio was 1.8:1 and 4:1, respectively. However, GPC could not provide M.W. information for thiolated dendrimers due to the presence

of aggregates. This is due to the oxidation of free thiol groups and formation of disulfide bonds among different dendrimer units. Thus, it is important to determine the degree of oxidation after preparation, as well as the stability of free thiol groups at different pH conditions.

3.4.2 Oxidation of free thiol groups after preparation

Free thiol groups are prone to oxidation to form disulfide bond during the preparation process. In order to decrease the oxidation of thiol groups, thiolation step took place after PEGylation. Nitrogen gas protection and dark environment were carefully provided during the synthesis. Moreover, the pH was adjusted to 7.0 to balance between good conjugation efficiency and minimal oxidation condition. Acidic environment was more favorable to protect free thiol groups from oxidation, yet the conjugation efficiency would be lower under acidic condition. After the synthesis, dialysis was kept in acidic conditions to minimize oxidation. When the final product was lyophilized in powder form, it was kept at acidic condition in -20℃ to minimize oxidation. Additionally, another possible method to reduce oxidation is to store the thiolated polymers together with reducing agent, for example, glutathione (GSH).

After the processes of synthesis, dialysis and lyophilization, 57.4%, 60.1% and 38.0% of the thiol groups were oxidized to disulfide bond for PEG(1.8)-PM-TBA(7.0), PEG(4.0)-PM-TBA(6.7), and PM-TBA(7.6), respectively (Table 3.1). Although PM-TBA(7.6) dendrimer had less of the free thiol groups being oxidized, the total concentration of oxidized thiol groups were in a similar range:

233 μmol/g for PEG(1.8)-PM-TBA(7.0), 189 μmol/g for PEG(4.0)-PM-TBA(6.7) and 204 μmol/g for PM-TBA(7.6). This may suggest that the preparation process oxidized a fixed amount of thiol groups.

3.5 Conclusion

In this chapter, the PEGylated and thiolated dendrimers were successfully prepared and characterized. Dendrimers with two different PEGylation ratios, 1.8:1 and 4.0:1, were synthesized. After thiolation step, the thiol groups were oxidized to disulfide bond to different extents for PEG(1.8)-PM-TBA(7.0), PEG(4.0)-PM-TBA(6.7), and PM-TBA(7.6). PEGylation showed weakly protective role against thiol groups oxidation in liquid but not in powder form. To the best of our knowledge, dual functionalized PAMAM dendrimer with TBA and PEG were not reported by other research groups so far. In the next chapter, the focus is to evaluate the compatibility of the PAMAM dendrimer conjugates with blood components.

CHAPTER 4. BLOOD COMPATIBILITY OF PAMAM DENDRIMERS AND THEIR DERIVATIVES

4.1 Introduction

Thus far, studies have demonstrated the blood toxicity of unmodified cationic PAMAM dendrimers in vivo, whereby intravenous injection of these dendrimers into mice and rats with doses >10 mg/kg produced disseminated intravascular coagulation (DIC)-like symptoms with high mortality rates [142]. Through a number of in vitro assays probing blood coagulation; haemolysis; platelet activation, aggregation and function, cationic PAMAM dendrimers have been shown to be highly hemotoxic in contrast to their anionic or neutral counterparts [100, 139, 141]. Such hemotoxicity is thought to be a result of the electrostatic interaction between the cationic PAMAM dendrimers and the negatively charged blood proteins and platelet membranes [100, 140, 141]. Furthermore, the hemotoxicity was concentration- and generation-dependent.

In the previous chapter, we have prepared dual functionalized cationic PAMAM dendrimer via PEGylation and thiolation. It is hypothesized that such dual functionalization of PAMAM dendrimers would be an effective strategy in modulating the hemotoxicity profile of these dendrimers. In this chapter, a number of in vitro assays have been performed to evaluate the effect of PAMAM dendrimers on the major blood components, including red cell morphology and lysis; viability of human monocytic cell line U-937; binding with bovine serum albumin (BSA); generation of complement C3a; blood coagulation times, and

platelet aggregation. Among these in vitro assays, hemolysis, complement activation are considered to have good predictive correlation with in vivo immunotoxicity [184]. Leukocyte proliferation and thromobogenicity are considered to be generally predictive [184].

4.2 Materials and Methods

4.2.1 PAMAM dendrimers

Amine-terminated PAMAM dendrimer generation 2.0 (PM2.0), generation 3.0 (PM3.0), generation 4.0 (PM4.0) and carboxyl-terminated PAMAM dendrimer generation 3.5 (PM3.5) with ethylenediamine core were purchased from Dendritech, Inc (Midland, MI, U.S.A.). PM4.0 were surface modified with polyethylene glycol (PEG, m.w. 2,000) and 2-Iminothiolane Hydrochloride (Traut's Reagent, TBA) as described in chapter 3. Physical properties of the dendrimers are listed in Table 3.2 and Table 4.1.

Table 4.1. Physical characterization of various PAMAM dendrimers with or without surface functionalization.

Dendrimer type	M.W.	Zeta Potential (mV)	Size (nm)	$N_{surface\ groups}$
PM2.0	3,256[a]	+22.0 ± 0.7	2.2 ± 0.2	16
PM3.0	6,909[a]	+22.5 ± 0.6	3.2 ± 0.1	32
PM4.0	13,487[b]	+30.1 ± 0.9	4.3 ± 0.4	64
PEG(1.8)-PM4.0	16,662[b]	+26.9 ± 5.0	3.7 ± 1.4	64
PEG(4.0)-PM 4.0	20,751[b]	+36.4±5.0	4.6±1.3	64
PEG(1.8)-PM4.0-TBA(7.0)	17,372[b]	+28.3 ± 4.6	6.1 ± 1.4	64
PEG(4.0)-PM4.0-TBA(6.7)	21,430[b]	+36.7±1.3	5.4±1.3	64
PM4.0-TBA(7.6)	14,259[b]	+39.2 ± 1.8	4.4 ± 1.6	64
PM3.5	13,061[c]	-26.5 ± 0.7	5.1 ± 1.1	64

[a]Theoretical molecular weight of PM2.0 and PM3.0.
[b]Molecular weight were reported in chapter 3 Table 3.2.
[c]Molecular weight of PM3.5 was determined by GPC.

4.2.2 Cell cultures

The human hematopoietic cell line U-937 was acquired from American Type Culture Collection (Manassas, USA). U-937 cells were maintained in RPMI 1640 media supplemented with 10% fetal bovine serum (FBS) and were routinely propagated in T-75 cm^2 flasks (Iwaki, Japan) in humidified atmosphere of 5% CO_2 at 37 ℃.

4.2.3 Cell viability assay

The effect of PAMAM dendrimers on U-937 cell viability was evaluated by Cell Counting Kit-8 (CCK8, Dojindo Molecular Technologies, INC., Singapore). U-937 cells were seeded in 96-well plates at a density of 2.5 $\times 10^5$ cells/well. Cells

were exposed to various dendrimers and incubated at 37℃ for 72 h. Triton-X (0.2%) was used as positive control. After incubation, 10 µl CCK8 was added to each well and kept at 37 ℃ for 4 h followed by measuring absorbance at 450 nm with Tecan SpectraFluorPlus reader. Cell viability was calculated as follows:

$$Cell\ Viability\% = (Abs_{test} - Abs_{background}) / (Abs_{vehicle} - Abs_{background}) \times 100\%$$

where Abs_{test}, $Abs_{background}$, $Abs_{vehicle}$ represent the absorbance readings from the dendrimer-treated well, the medium-only wells and the vehicle control wells, respectively. IC_{50} was estimated using the software Calcusyn version2.1 (Biosoft, Cambridge, UK).

4.2.4 Haemolysis study

Freshly collected rat blood was provided by NUS animal laboratory center with approved IACUC protocol T14/12. The whole blood sample was centrifuged at 1,500×g in 4℃ for 10 min. After removal of supernatant, the red blood cells (RBC) were washed three times with phosphate-buffered saline (PBS) and centrifuged at 1,500×g in 4℃ for 5 min. After washing steps, the RBCs were diluted in PBS to a final concentration of 4% (v/v). The RBC samples were kept in 4℃ prior to experiment and used within 24 h.

Dendrimer samples (0.25 to 4 mg/ml) or 1% Triton-X were added to the freshly prepared rat RBC samples (4% in PBS) and incubated at 37℃ for 24 h. After which, the solution was centrifuged at 1500× g for 10 min. The supernatant was collected and absorbance was measured at 550 nm for haemoglobin. Haemoglobin release was calculated as follows:

$$Haemoglobin\ release\ (\%) = (Abs_{test} - Abs_{vehicle}) / (Abs_{Triton\text{-}X} - Abs_{vehicle}) \times 100\%$$

where Abs_{test},, $Abs_{vehicle}$, $Abs_{Triton\text{-}X}$ represent the absorbance readings from the dendrimer, PBS only and Triton-X treated RBC, respectively.

4.2.5 Scanning electron microscopy (SEM) of red blood cells

4% v/v RBC were incubated with 2 mg/ml dendrimer samples at 37 ℃ for 4 h. After incubation, the cells were harvested and washed twice with ice cold PBS. After which the cells were fixed with 2.5% SEM grade glutaraldehyde at 4 ℃ for 24 h. After washing twice with PBS, cells were placed in 1% osmium tetroxide for 1 h before dehydration serially in 30%, 50%, 70%, 90% and 100% ethanol. Then the cells were resuspended in hexamethyldisilazane (HMDS). After the evaporation of HMDS, cells were coated with platinum for 5 mins. SEM images of RBC were taken with a JEOL JSM-6701F (JEOL, Tokyo, Japan) field emission scanning electron microscope.

4.2.6 Fluorescence quenching of bovine serum albumin

Dendrimer samples at various concentrations were mixed with 0.2 mg/ml BSA diluted in PBS. The samples were then incubated at 25 ℃ for 0.5 h. Fluorescence emission spectra were taken with Hitachi F-7000 fluorescence spectrophotometer. Emission spectra were measured from wavelength 310 nm to 400 nm after excitation at 295 nm. Excitation and emission slits were set at 5 nm and 2.5 nm, respectively. The fluorescent signal appeared at 340 nm wavelength and was recorded. The fluorescence quenching data were analyzed by the Stern-Volmer equation [117]:

$F_0/F - 1 = K_{sv} \times [Q]$

where F_0 and F represent the fluorescence intensity of BSA in the absence of dendrimer sample and in the presence of dendrimer samples at $[Q]$ concentration (μM), respectively. K_{sv} is the Stern-Volmer dynamic quenching constant.

4.2.7 Complement activation

C3a enzyme immunoassay kit (Quidel, San Diego, Ca) was used to assess complement component C3 activation. The formation of activation peptides, C3a and C3a des arg, was measured according to manufacturer's protocol. 95 μl human plasma (Sigma-Aldrich, with 3.8% trisodium citrate as anticoagulant) was mixed with 5 μl dendrimer sample stock solution or PBS (vehicle control) and incubated at 37 ℃ for 1 h. The samples were then diluted with the specimen diluent buffer and added to microtiter plate coated with murine monoclonal antibody specifically binding to human C3a and C3a des arg. After 1 h of incubation, the plates were washed and incubated with horseradish peroxidase (HRP)–conjugated anti-C3(C3a) polyclonal antibody for 15 min followed by washing and incubation with chromogenic substrate. Absorbance was measured at 450 nm. C3a concentration of plasma samples were calculated from a standard curve using C3a standard provided in the kit. Relative increase in C3a generation (%) was calculated as follows:

$$\textit{Relative increase in C3a generation\%} = (Abs_{test} - Abs_{vehicle}) / Abs_{vehicle} \times 100\%$$

where Abs_{test} and $Abs_{vehicle}$ represent the absorbance readings from the dendrimer samples or PBS treated RBC, respectively.

4.2.8 Determination of prothrombin time and activated partial thromboplastin time

Prothrombin time (PT) and activated partial thromboplastin time (aPTT) were measured with Sysmex CA-500 Blood Coagulation Analyzer (Sysmex Asia Pacific Pte Ltd, Singapore). 50 µl dendrimer solution was mixed with 100 µl citrated human plasma (Ci-Trol level 1, Dade Behring Marburg GmbH, Marburg, Germany). For the PT determination, the extrinsic and common coagulation pathways were activated by incubating the sample with human thromboplastin containing calcium chloride (Thromborel S, Dade Behring Marburg GmbH) and the clotting time was measured. For the aPTT determination, the intrinsic and common coagulation pathways were activated by adding an activated partial thromboplastin reagent (Actin FSL, Dade Behring Marburg GmbH) and calcium chloride (25 mM) to the sample and the clotting time was measured. PBS and 0.01% w/v heparin in PBS were used as negative and positive control, respectively.

4.2.9 Platelet aggregation measurement

Whole blood aggregation assay was tested by measuring impedance using a whole blood aggregometer (Chronolog Corporation, Havertown, PA) as described before [185]. Freshly prepared rat blood was purchased from Invivos Pte Ltd (Singapore) and kept at 37 ℃ before use. 450 µl of the blood was mixed with 450 µl saline and allowed to equilibrate for 2 min. Subsequently, 50 µl of dendrimer stock solution (4 mg/ml in saline) was added to the mixture and allowed to

equilibrate for 2 min. In order to initiate platelet aggregation, 5 µl of collagen (Chrono-Log Corporation, Havertown, PA, USA) was added to the test mixture. Saline without dendrimer was used as control. The test was allowed to run for 10 min. Change in collagen induced platelet aggregation was calculated as follows:

$$Platelet\ aggregation\% = Impedance_{test} / Impedance_{Saline} \times 100\%$$

where $Impedance_{test}$ is the impedance value for the dendrimer treated blood sample and $Impedance_{Saline}$ is the impedance value of saline treated blood samples.

4.2.10 Statistical analysis

Where appropriate, results were expressed as mean ± SEM of at least three independent experiments. Statistical significance was determined using the Student t-test or one-way analysis of variance (ANOVA) Kruskal-Wallis test followed by Dunn's test used for post-hoc multiple comparisons. P values of < 0.05 were considered to be statistically significant. Statistical analyses were carried out using SPSS software (v 19.0; IBM, Armonk, NY).

4.3 Results

4.3.1 Cytotoxicity of PAMAM dendrimers on human monocytic cell line U937

The cytotoxicity of PAMAM dendrimers was determined in U-937 cells which were exposed to a range of concentrations of the various dendrimers for 72 h (Figure 4.1). U-937 cells were selected as a model human cell line to study the toxic effect of dendrimer on monocytes. The half maximal inhibitory

concentration (IC_{50}) was calculated by CalcuSyn (Table 4.2). In general, the higher the dendrimer generation and concentration, the higher was the observed cytotoxicity. The IC_{50} values of unmodified cationic PAMAM dendrimers were in the order of PM4.0<PM3.0<PM2.0, with nearly a log-fold increase in IC_{50} value as the dendrimer decreased its generation by one. This observation is in line with the literature that cationic PAMAM cytotoxicity is generation dependent. Another observation is that surface properties of the cationic PAMAM dendrimer could modulate its cytotoxicity. Surface modification of PM4.0 with PEG alone decreased the IC_{50} by more than 5-fold (PM4.0 vs PEG(1.8)-PM4.0 and PEG(4.0)-PM4.0). On the contrary, introduction of thiol groups onto PM4.0 did not offer any benefit in reducing PM4.0 cytotoxicity. Similarly, PEGylation of PM4.0-TBA(7.6) did reduce the cytotoxicity of the thiolated dendrimer; however, such benefit could only be observed when the level of PEG engraftment was higher. Modifying the PAMAM cationic surface to an anionic surface with carboxylic acid groups could dramatically reduce the cytotoxicity, whereby a 50-fold higher in IC50 values could be observed when comparing PM3.5 with PM4.0 even though these two dendrimers had the same theoretical number of surface groups.

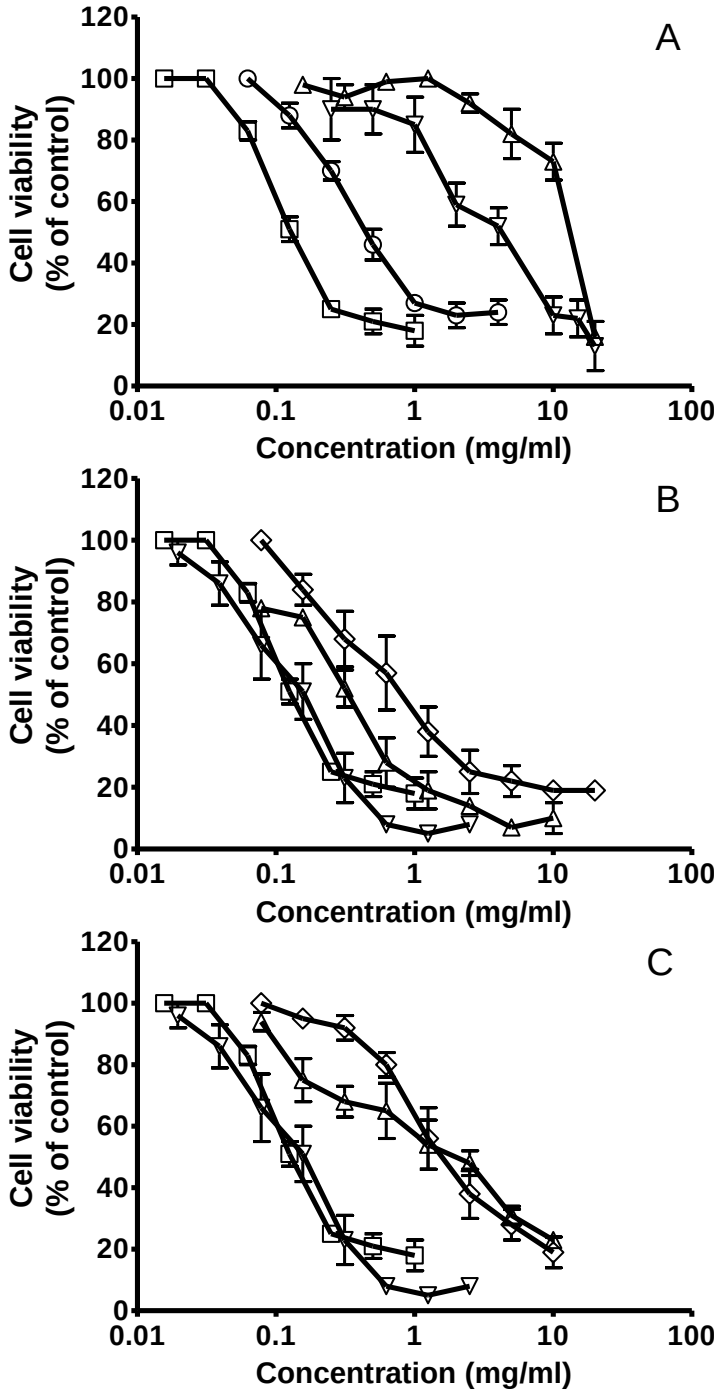

Figure 4.1. Cell viability study measured by Cell Counting Kit-8 after 72 h treatment with (A) PM2.0 (▽), PM3.0 (○), PM4.0 (□), PM3.5 (△) , (B) PM4.0 (□), PEG(1.8)-PM4.0 (◇), PEG(1.8)-PM4.0-TBA(7.0) (△), PM4.0-TBA(7.6) (▽), (C) PM4.0 (□), PEG(4.0)-PM 4.0 (◇), PEG(4.0)-PM4.0-TBA(6.7) (△), PM4.0-TBA(7.6) (▽). Data represent mean ± SEM of 3 independent experiments.

Table 4.2. IC50 values of various dendrimers in U-937 cells.

	IC50	
Dendrimer type	μM	mg/ml
PM2.0	1317 ± 550*	4.29 ± 1.79
PM3.0	129 ± 6	0.89 ± 0.04
PM4.0	19 ± 2	0.26 ± 0.02
PEG(1.8)-PM4.0	108 ± 21	1.79 ± 0.35
PEG(4.0)-PM 4.0	107 ± 15	2.21 ± 0.32
PEG(1.8)-PM4.0-TBA(7.0)	19 ± 4	0.34 ± 0.06
PEG(4.0)-PM4.0-TBA(6.7)	76 ± 13	1.63 ± 0.29
PM4.0-TBA(7.6)	13 ± 4	0.19 ± 0.06
PM3.5	1123 ± 167*	14.52 ± 2.16

Data represent mean ± SEM of 3 independent experiments. ** $p < 0.05$ compared to IC50 of PM4.0*

4.3.2 Haemolysis and RBC morphological changes induced by PAMAM dendrimers

The next set of experiments involved the examination of the effects of various PAMAM dendrimers on RBC. Hemoglobin release, which is indicative of RBC lysis, was measured 24 h after the incubation of RBC with the dendrimers (Figure 4.2). Similar to previous finding [186], PAMAM dendrimers with surface amine groups triggered hemoglobin release in a generation- and concentration-dependent manner. In contrast, anionic PM3.5 induced minimum haemolysis, even when tested at the highest concentration of 4 mg/ml. Thiolation of PM4.0 alone provided modest protection against haemolysis; yet, at the highest concentration of 4 mg/ml, ~30% of haemolysis was induced by PM4.0-TBA(7.6). Modifying

the PAMAM dendrimers with PEG alone or a combination of PEG and thiol groups could effectively reduce the extent of haemolysis to < 10% even at the highest concentration tested.

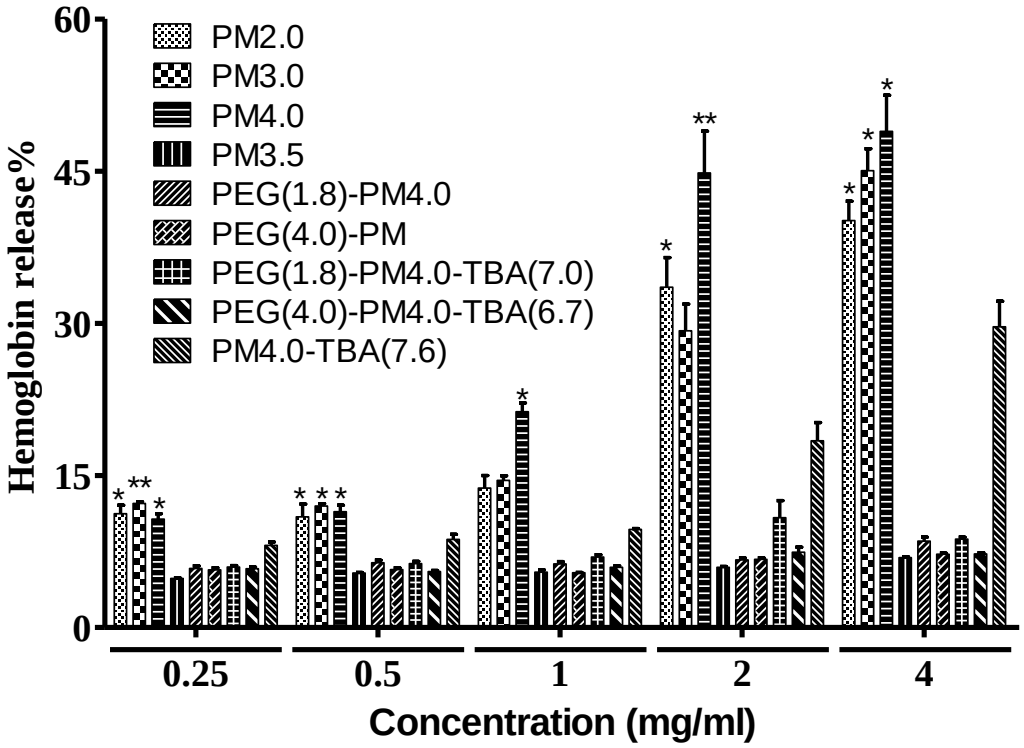

Figure 4.2. In vitro haemolysis studies of PAMAM dendrimers PM2.0 , PM3.0, PM4.0, PEG(1.8)-PM4.0, PEG(4.0)-PM 4.0, PEG(1.8)-PM4.0-TBA(7.0), PEG(4.0)-PM4.0-TBA(6.7), PM4.0-TBA(7.6), PM3.5. Data represent mean ± SEM of at least 3 independent experiments. Data represent mean ± SEM of 3 independent experiments. ** $p < 0.05$, ** $p < 0.01$ compared to PM 3.5.*

Change in RBC morphology is another important parameter for examination, as RBC morphology could impact on its flow properties and aggregation potential. The morphology of RBC was observed under SEM after exposure to various dendrimers at 2 mg/ml for 4 h (Figure 4.3). RBC exposed to saline displayed normal, round, disc-shaped and biconcave morphology (Figure 4.3), while morphological changes and aggregation were observed after exposure to the

various types of dendrimers. Clustering of RBC and presence of echinocytes could be seen in samples treated with unmodified cationic PAMAM dendrimers, and the effect was generation-dependent. Of note, exposure to anionic PM3.5, PM4.0 modified with PEG alone, or PM4.0 dual-modified with PEG and thiol groups also induced echinocyte formation, despite their minimal haemolytic effect. Modification of PM4.0 with thiol groups alone caused extensive aggregation of RBC that could be reduced by the introduction of sufficient PEG groups (PM4.0-TBA vs PEG(1.8)-PM4.0-TBA(7.0) and PEG(4.0)-PM4.0-TBA(6.7) respectively).

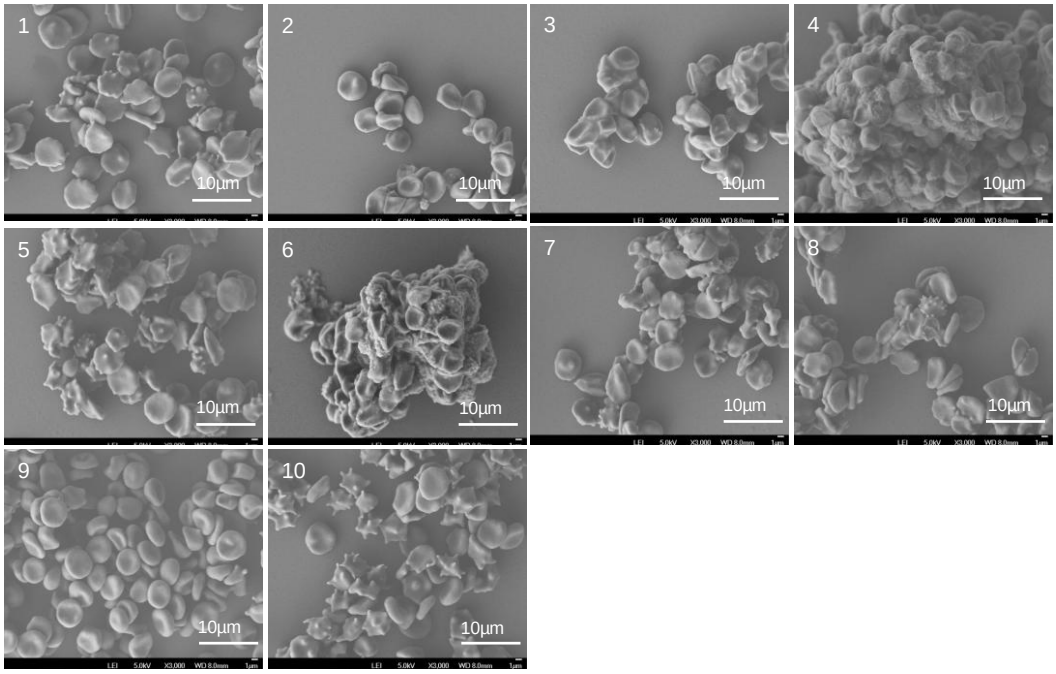

Figure 4.3. SEM images of red blood cells incubated with 2 mg/ml dendrimer samples for 4 h. (1) PM2.0, (2) PM3.0, (3) PM4.0, (4) PM3.5 (5) PM4.0-TBA(7.6), (6) PEG(1.8)-PM4.0, (7) PEG(1.8)-PM4.0-TBA(7.0), (8) PEG(4.0)-PM 4.0, (9) PEG(4.0)-PM4.0-TBA(6.7), (10) Saline. The experiments were repeated twice, each time with a minimum of three views of the same sample was captured.

4.3.3 Interaction of PAMAM dendrimers with BSA

Binding between various PAMAM dendrimers at different concentrations to BSA was studied by means of the tryptophan fluorophore of BSA at the emission wavelength of 340 nm. The relationship between fluorescence intensity and dendrimer concentration was further examined according to the classical Stern-Volmer equation which would yield the Stern-Volmer dynamic quenching constant (Ksv) that indicates the accessibility of the albumin fluorophore to the dendrimer under examination [187]. Figure 4.4 illustrate the calculation from fluorescence signal to Stern-Volmer dynamic quenching constant. The slope of the linear regression curve represents Ksv value. The Ksv values for the interaction of various PAMAM dendrimers with BSA were presented in Table 4.3. In line with previous studies [98, 117, 119], the interaction between albumin and unmodified, cationic PAMAM dendrimers increased as dendrimer generation increased from 2.0 to 4.0, whereas the anionic PM3.5 showed the lowest interaction with BSA among the dendrimers tested. PEGylation of PM4.0 alone could significantly reduce the K_{sv} values by > 2 folds. The thiolated dendrimer PM4.0-TBA(7.6) gave rise to precipitation in the test system, which prevented the inclusion of the Ksv value for comparison. The introduction of thiol groups to PEG(1.8)-PM4.0 increased the K_{sv} value, whereas thiolation of PEG(4.0)-PM4.0 did not affect the Ksv value, suggesting a higher level of PEG is required to reduce the interaction of thiolated PAMAM with BSA.

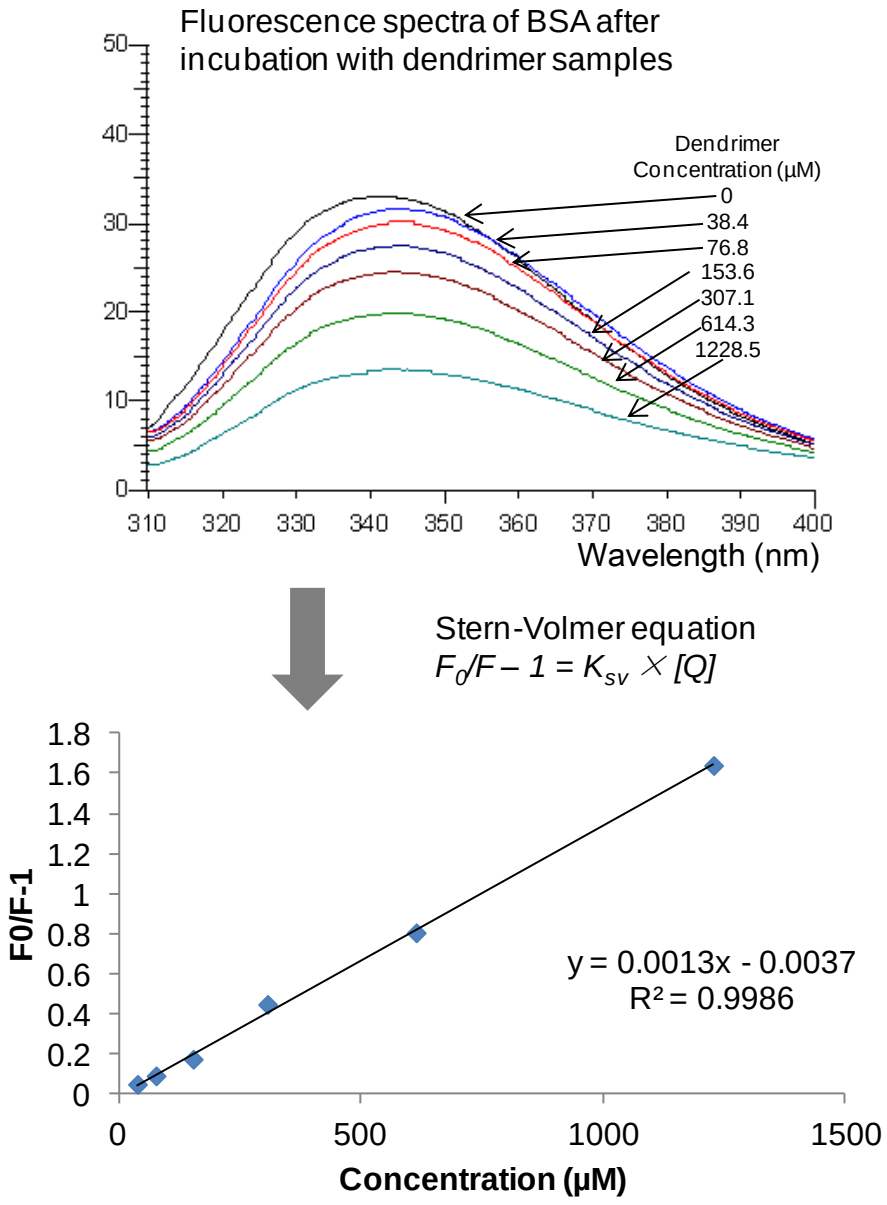

Figure 4.4 Representative figure of Stern-Volmer constant calculation. Each curve represents the fluorescent signal of BSA mixed with different concentration of dendrimer. The fluorescent signal at 330 nm and dendrimer concentrations were converted to linear regression by Stern-Volmer equation. The slope of the curve represents Ksv value.

Table 4.3. Stern-Volmer quenching constant (KSV) for the interaction of PAMAM dendrimer with BSA.

Dendrimer	K_{sv} (mM^{-1})	r^2 [a]
PM2.0	$1.33 \pm 0.88^{***}$	0.98 ± 0.01
PM3.0	2.54 ± 0.23	0.99 ± 0.01
PM4.0	3.59 ± 0.22	0.99 ± 0.01
PM G3.5	$1.00 \pm 0.10^{***}$	0.96 ± 0.02
PEG(1.8)-PM4.0	$1.45 \pm 0.03^{***}$	0.99 ± 0.01
PEG(4.0)-PM 4.0	$1.53 \pm 0.20^{***}$	0.99 ± 0.01
PEG(1.8)-PM4.0-TBA(7.0)	$2.38 \pm 0.48^{**}$	0.85 ± 0.05
PEG(4.0)-PM4.0-TBA(6.7)	$1.68 \pm 0.03^{***}$	0.99 ± 0.01

[a] Coefficient of determination

*** P < 0.01, *** P < 0.005 compared to Ksv of PM4.0 (n=3)*

4.3.4 Activation of complement system by various PAMAM dendrimers

The effect of PAMAM dendrimers on complement activation was studied by measuring C3a generation after incubating human plasma with dendrimer samples at 37 ℃ for 1 h (Figure 4.5). Unmodified cationic PAMAM dendrimers, PM2.0, PM3.0 and PM4.0 at 4 mg/ml, caused higher level of C3a generation as compared to the negative control PBS. In contrast, a 2-fold reduction in C3a generation was observed when changing the cationic surface of PM4.0 to the anionic surface of PM3.5. Thiolation of PM4.0 did not reduce C3a generation in comparison to unmodified PM4.0, whereas modification of PM4.0 with PEG alone modestly decreased C3a generation in comparison to unmodified PM4.0. Of note, dual-functionalized dendrimers, PEG(1.8)-PM4.0-TBA(7.0) and PEG(4.0)-PM4.0-TBA(6.7) tested at 10 mg/ml, could significantly reduce C3a generation in comparison to PM4.0.

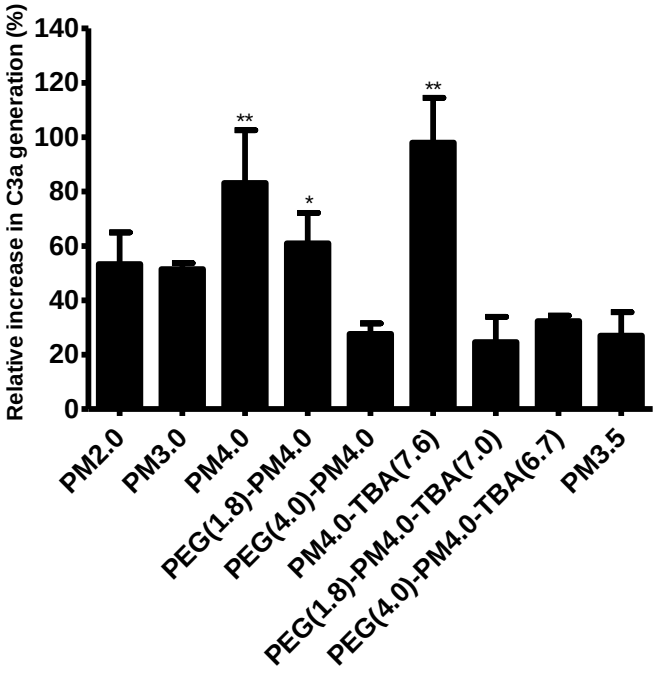

Figure 4.5. Mean relative percentage increase in C3a generation by 4 mg/ml PM2.0 , PM3.0, PM4.0, PEG(1.8)-PM4.0, PEG(4.0)-PM 4.0, PM4.0-TBA(7.6), PM3.5 or 10 mg/ml PEG(1.8)-PM4.0-TBA(7.0), PEG(4.0)-PM4.0-TBA(6.7) compared to PBS control. Data represent mean ± SEM of 3 independent experiments. Data represent mean ± SEM of 3 independent experiments. * $p < 0.05$, ** $p < 0.01$ *compared to PBS control.*

4.4 Effect of various PAMAM dendrimers on the coagulation pathways and platelet aggregation

PT and aPTT were mainly used to evaluate the extrinsic and intrinsic coagulation pathway, respectively. PT values reflect the time in fibrin clot formation after the addition of tissue thromboplastin, and aPTT values reflect the time in fibrin clot formation after the addition of partial thromboplastin reagent (actin) and calcium chloride. Heparin and PBS were included as controls for comparison. The PT results of citrated human plasma treated with various dendrimers were shown in

Figure 4.6 A and B. The mean PT values for the unmodified cationic PAMAM dendrimers (PM2.0, 3.0 and 4.0) and PM4.0 modified with PEG were summarized in Figure 4.6 A, and the concentrations tested were 0.0125 and 0.25 mg/ml. For higher concentrations (>0.25 mg/ml), these dendrimers showed prolonged or no coagulation (that is, no PT value could be registered by the equipment). At 0.25 mg/ml, PM2.0, PM3.0, PM4.0, and the PEGylated PM4.0 dendrimers yielded higher PT values as compared to PBS; furthermore, the PT values for PM4.0 and the PEGylated PM4.0 dendrimers were significantly higher than that of PBS control, indicating the anti-coagulant potential of these three dendrimers. PM4.0 modified with PEG alone showed shorter PT as compared to original PM4.0, and the effect was more obvious as PEG ratio increased. In contrast, the dual-functionalized PM4.0 dendrimers and PM3.5 did not modulate the extrinsic coagulation pathway, as their PT values were not statistically different from that of PBS even when tested at 4 mg/ml. Similar to PT determination, citrated human plasma treated with various dendrimers showed prolonged aPTT or no coagulation at concentrations that were higher than those reported in Figure 4.6 C. Among the unmodified cationic PAMAM dendrimers, PM2.0 was the most potent in causing no coagulation of the citrated plasma. Modification with PEG alone did not alter the anti-coagulant potential of PM4.0. On the contrary, PEG(1.8)-PM4.0-TBA(7.0) and PM3.5 did not modulate the intrinsic coagulation pathway, as their aPTT values were not statistically different from that of PBS even when tested at 4 mg/ml. In addition to PT and aPTT values, collagen-induced platelet aggregation was also determined, and the results

are summarized in Figure 4.7. PM4.0, PM4.0 modified with TBA and PM3.5 did not significantly alter collagen-induced platelet aggregation; however, PEGylation alone or dual functionalization of PM4.0 could significantly reduce collagen-induced platelet aggregation.

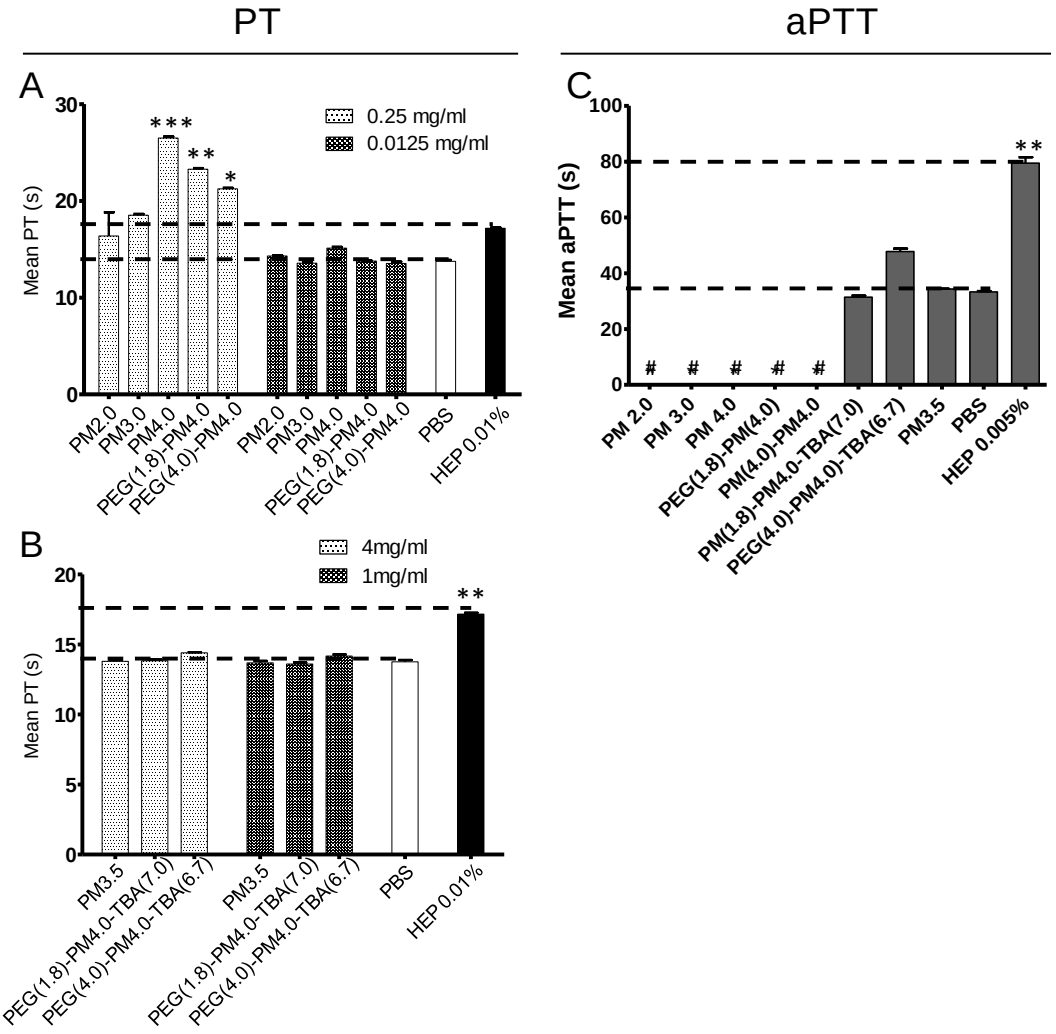

Figure 4.6. Mean PT and aPTT values for different PAMAM dendrimers. (a) PT of PM2.0, PM3.0, PM4.0, PEG(1.8)-PM4.0 and PEG(4.0)-PM4.0 at 0.25 mg/ml and 0.0125 mg/ml, respectively. (b) PT of PM3.5, PEG(1.8)-PM4.0-TBA(7.0) and PEG(4.0)-PM4.0-TBA(6.7) at 4mg/ml and 1mg/ml, respectively. (c) aPTT of PEG(1.8)-PM4.0-TBA(7.0) (4 mg/ml), PEG(1.8)-PM4.0-TBA(7.0) (1 mg/ml), PM3.5 (4 mg/ml). Data represent mean ± SEM of 3 independent experiments. * *p < 0.05, ** p < 0.01, *** p<0.001 compared to PBS control.*
# indicates that the aPTT was above the detection range when dendrimer concentration was above 0.125 mg/ml.

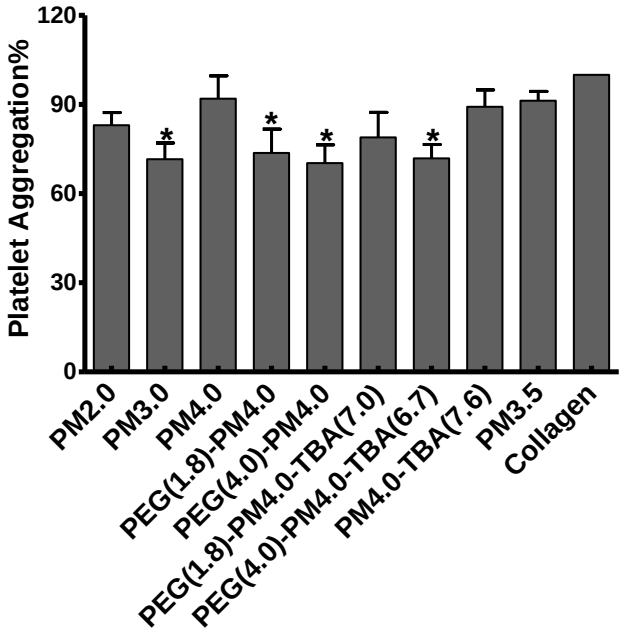

Figure 4.7. Effect of dendrimers (at 2 mg/ml) on collagen induced platelet aggregation. Data represent mean ± SEM of 5 independent experiments. * $p < 0.05$, *to collagen control.*

4.5 Discussion

The term "dendritic effect" is used to describe intrinsic physico-chemical and application property patterns exhibited by dendrons and dendrimers [188]. Dendritic effect is closely related to several critical nanoscale design parameters (CNDPs), including: (a) size, (b) shape, (c) surface chemistry, (d) flexibility/rigidity, (e) architecture and (f) elemental composition. This chapter mainly focused on surface chemistry dependent toxic effect of dendrimer on blood components [188]. Cationic PAMAM dendrimers demonstrated DIC-like hemotoxicity in vivo, and such hemotoxic effects would hamper the potential of cationic PAMAM based nanopharmaceuticals to be further translated into clinical applications. While modifying PAMAM dendrimer into one bearing an anionic surface could substantially reduce its hemotoxicity as shown by our results here as

well as others previously reported [186, 189], the cationic charge plays an important role in the electrostatic complexation with nucleic acid materials and drug molecules. As such, it is the intentions of our current study to surface modify the cationic PAMAM dendrimers with PEG or thiol or a combination of both functional groups so as to improve their hemo-compatibility. The surface modified PM4.0 dendrimers in the current study displayed positive zeta potentials, ranging from +27 to +39 mV, which were similar to that of the unmodified PM4.0, and the maintenance of such cationic surface would be useful for complexation with the negatively charged nucleic acid materials. The ability of the various modified PAMAM dendrimers to interact with blood cells and platelets as well as important proteins of the blood coagulation system and complement system will be discussed in light of the type of surface modifications in the following sections.

4.5.1 Interactions with RBC and monocytes

Interactions between nanopharmaceuticals and RBC could give rise to potentially severe acute toxicities such as haemolysis, anemia and other life-threatening conditions, and interactions with monocytes would give an indication to the immunosuppressive potential of the nanopharmaceuticals [184]. Under normal conditions, erythrocytes have biconcave disc shape, which can be transformed to echinocytes (crenated cells) or stomatocytes (cup-shaped cells) under intrinsic or extrinsic conditions [190] As shown in Figure 4.3, the RBCs showed irregular contour after incubation with dendrimers. PM3.5 induced obvious echinocytic transformation. In PM3.0 and PM4.0 treated samples, spheroechinocytes were more profound. Although PM 3.5 did not cause obvious haemolysis, the RBCs

showed symptom of acanthocyte with spiked cell membrane. Similar symptoms were reported previously when the RBCs were treated with hyperbranched polyglycerol-polyethylene glycol polymers and peroxynitrite [191, 192]. The aggregation observed for PM4.0 treated RBCs were mainly due to the electrostatic interactions between positive charge of dendrimers and the negatively charged glycolipids and glycoproteins of RBC membranes [107]. For the thiolated dendrimer PM4.0-TBA(7.6) and PEG(1.8)-PM4.0-TBA(7.0), however, severe aggregation and clusters were formed. This might be due to the cross-linking of the covalent disulfide bonds among thiolated dendrimers. Such phenomenon raised caution to apply thiolated polymers directly into blood circulation as they might cause aggregation of blood component and clot. Surface modification of PM4.0 with PEG alone could effectively reduce RBC lysis, and such results are in line with previous studies [193]. The result of dendrimer toxicity study on U-937 cells showed that dendrimer toxicity was concentration, generation and surface group dependent (Figure 4.1 and Table 4.2), agrees with previously reported in both mammalian and ecotoxicological studies [20, 194]. PEGylation effectively decreased toxicity of positively charged dendrimers on U-937 cells.

4.5.2 Interactions with BSA

Serum albumins are the most abundant soluble proteins in the blood circulation. They play crucial roles to transport various fatty acids, amino acids, hemin, bilirubin and drug molecules [195, 196]. It is important to evaluate the interaction between drug delivery vehicles and serum albumins because such interaction

might affect biological functions of albumin and pharmacokinetic profile of the nanopharmaeutical. Some mechanisms of interactions between PAMAM dendrimers and serum albumins have been proposed previously. Klajanert and Bryszewska reported that dendrimers bind albumins mainly by electrostatic interaction [117], which explained the stronger binding effect of cationic dendrimers compared to anionic dendrimers. As shown in Table 4.3, surface modified dendrimers showed fewer albumins binding effect compared to unmodified PM4.0. Similar observations were reported by *Tajmir-Riahi et al.* that dendrimer interaction with human serum albumin were in the order of PM4.0 > mPEG-PM4.0 > mPEG-PM3.0 [124]. It is also suggested that intramolecular hydrogen bonding between PEG and PAMAM dendrimer should result in weaker interaction in dendrimer/albumin complexes [124].

4.5.3 Interaction with the complement pathway

The complement pathway is a host defense system which is activated when a foreign material comes into contact with blood. It initiates a series of biochemical reactions involving several peptides and enzymes, that could be potent promoters of inflammatory response [130], and such agents are known as anaphylatoxins (such as C3a, C4a and C5a). Complement activation related pseudoallergy (CARPA) syndrome is a dose-limiting toxicity of certain liposomal and polymeric nanopharmaceuticals [197, 198]. Moreover, nanoparticle initiated complement activation can lead to rapid removal of the nanoparticles from systemic circulation by mononuclear cells via receptor-mediated phagocytosis of complement [199]. In this study, amine-terminated PAMAM dendrimers initiated much higher level

of complement activation as compared to PBS control group. Similar effect of positive charged PAMAM dendrimer was previously reported that PAMAM generation 5.0-DNA complex activated the complement system after 1h incubation at 37℃ [200]. Thiolation alone did not offer any benefit and exhibited similar level of C3a activation as compared to unmodified PAMAM. On the contrary, as PEGylation ratio increased, complement activation was reduced as compared to unmodified PM4.0. Dual functionalization of PM4.0 improved complement compatibility, whereby PEG(1.8)-PM4.0-TBA(7.0), and PEG(4.0)-PM4.0-TBA(6.7) showed equivalent level of complement activation as PM3.5 and PEG(4.0)-PM4.0.

4.5.4 Interaction with coagulation pathways and platelets

The thrombogenic potential of nanopharmaceuticals is an important criterion for assessment in view of the growing concern of the possibility of vascular thrombosis and DIC-like toxicities [184]. Assessing thrombogenicity is a complex process that involves multiple end-points such as platelets and coagulation pathways, and furthermore, careful evaluation on the hemo-compatibility of nanomaterials is needed when they show positive reactivity even for one single in vitro coagulation test. In this study, surface modification could help diminish the effect of dendrimer on clotting formation time. For dual functionalized dendrimers, both of PEG(1.8)-PM4.0-TBA(7.0), and PEG(4.0)-PM4.0-TBA(6.7) were tested at much higher concentrations than the unmodified dendrimers, and yet, PT and aPTT remained unaffected. Thiolation has been employed as a strategy to reduce platelet activation of polymers and thereby

improving hemo-compatibility [176, 201]; however, thiolation by TBA in our hands is only modestly effective in reducing the toxicity of cationic PAMAM. This implies that the TBA functional group may not be as effective as PEG in providing steric hindrance or shielding the positive charge.

4.6 Conclusion

In this chapter, different types of PAMAM dendrimers were tested for their compatibility with major blood components, including cells, serum albumin, complements, clotting factors and platelets. The unmodified amine-terminated dendrimer displayed generation- and concentration-dependent toxic effects on blood components and functions. Modifying cationic PAMAM dendrimers via PEGylation and thiolation improved the compatibility with blood components, as reflected collectively by in vitro assays. Such improved blood compatibility warrant further exploration of these surface modified PAMAM dendrimer for biomedical applications. In the next chapter, these PAMAM dendrimer derivatives are evaluated for their potential to improve oral bioavailability of drug compounds through overcoming the barriers of oral drug absorption.

CHAPTER 5. EXPLORATION OF PAMAM DENDRIMER AND THEIR DERIVATIVES IN ORAL DRUG DELIVERY

5.1 Introduction

In the previous chapter, the toxic effect of dendrimer derivatives on major blood components is evaluated. PEGylation and thiolation decreased the dendrimer toxicity to a lower extent and improved blood compatibility. In this chapter, the potential use of dendrimer derivatives as intestinal penetration enhancers in oral drug delivery is explored.

In oral drug delivery, a big challenge is to overcome various biological barriers so that drug can achieve adequate concentration in blood circulation. P-glycoprotein (P-gp), an important biological barrier, is a major drug efflux transporter expressed in intestinal epithelium as well as other tissues in human body, including blood-brain barrier, kidney, liver colon and stomach [202, 203]. A large number of drugs are P-gp substrates including calcium channel blockers [204], steroid hormones [205], anti-cancer drugs [206] and immunosuppressants [207]. Although small molecules have been developed as P-gp inhibitors, undesirable side effects and drug-drug interactions are major concerns that limit the usage of this class of P-gp inhibitors. Another potential class of P-gp inhibitors is polymer. Thiomers are polymers with surface modification of thiol groups. Thiolated polymers are reported to exhibit inhibitory effect on P-gp efflux pump in many studies [179, 180, 208]. It is also reported that the combination of chitosan-4-thiobutylamidine (Ch-TBA) and glutathione (GSH) shows more

pronounced P-gp inhibitory effect than Pluronic®85 and Myrj®52 [209]. Moreover, thiomers also exhibit mucoadhesive and enzyme inhibitory properties [210]. Therefore, thiomers as excipients to increase oral bioavailability of P-gp substrates is of great potential and application values.

Another major physical barrier for oral drug delivery is tight junctions expressed in intestinal epithelium. It has been reported that PAMAM dendrimer of certain surface groups and generations can pass through epithelial barriers in GIT, suggesting the possibility to apply PAMAM dendrimer as oral drug delivery carrier [211, 212]. The transportation of PAMAM across epithelial membrane is due to both paracellular and transcellular pathways [213]. *El-Sayed et al.* reported that PAMAM dendrimers from G0 to G4 with amine surface groups decreased the transepithelial electrical resistance (TEER) values when tested in Caco-2 cell monolayer. Meanwhile the permeability of mannitol, which is a known marker for paracellular permeation, was increased [211]. These findings suggest that cationic PAMAM dendrimer could modulate the tight junction and provide opportunities for drug molecules to cross epithelial barrier through paracellular pathway.

However, thiolated PAMAM dendrimer has not been evaluated for its potential application in oral drug delivery. Therefore, in this chapter, PAMAM dendrimer modified with either PEG or thiol alone or the combination of both will be evaluated for their abilities to modulate epithelial tight junction and inhibit P-gp efflux.

5.2 Materials and Methods

5.2.1 Materials

PAMAM dendrimer generation 4 was obtained from Dendritech, Inc (Midland, MI, U.S.A.). Methoxy poly(ethylene glycol) succinimidyl carboxymethyl (mPEG-SCM) (M.W. 2,000) was purchased from Laysan Bio, Inc (Arab, AL, U.S.). Pluronic® 85 was a gift from BASF Ltd (Singapore). Lucifer yellow was purchased from Invitrogen Corporation (Carlsbad, CA, U.S.). 2-Iminothiolane Hydrochloride (Traut's Reagent, TBA), 5,5'-dithiobis(2-nitrobenzoic acid) (Ellman's reagent), sodium borohydride (NaBH4), Rhodamine-123 (R-123), Rhodamine-110 (R-110) and fluorescein isothiocyanate (FITC) were obtained from Sigma-Aldrich Pte Ltd (Singapore).

5.2.2 Thiol Group Stability Study at various pH conditions.

Thiolated dendrimers were dissolved in PBS at different pH conditions (pH 7.4, 6.5, 4.0 and 1.5) and incubated at 37°C. At 0, 1, 2, 4, and 6 h, a 100 μL sample was withdrawn and free thiol groups were quantified as described above. The results were expressed as percentages of free thiol groups compared to the sample at t = 0 h.

5.2.3 Cell Culture

The human colon adenocarcinoma cell line (Caco-2) was purchased from the American Type Culture Collection (Manassas, VA, USA). Madin-Darby canine kidney (MDCK)-multidrug resistance-1 (MDR1) cell line was a gift from Dr. Go

Mei Lin (National University of Singapore, Singapore). Cells were grown in T-75 cm^2 flasks (Iwaki, Japan) in humidified atmosphere of 5% CO_2 at 37°C. Caco-2 cell was maintained in Eagle's minimal essential medium (EMEM) supplemented with 15% fetal bovine serum (FBS), 1% L-glutamine, 100 units/ml penicillin and 100 μg/ml streptomycin. MDCK/MDR1 cell was maintained in Dulbecco's Modified Eagle Medium (DMEM) supplemented with 10% FBS, 100 units/ml penicillin and 100 μg/ml streptomycin. Upon 80-90% confluence, Caco-2 cells (between passage number 60-80) and MDCK-MDR1 cells (between passage number 10-20) were spilt using 1.0% trypsin containing 1.0 mM EDTA. Media were changed every 3 days.

5.2.4 Lactose dehydrogenase (LDH) release assay

Caco-2 cells and MDCK/MDR1 cells were seeded in 96-well plates at a density of 1.33×10^4 cells/well for 21 days and of 1×10^5 cells/well for 3 days, respectively, before experimentation. Triton-X (0.2%) was used to induce maximum LDH release. Cells with media only were used as the negative control. Cells were exposed to various dendrimers and incubated at 37°C for 24, 48 or 72 h after which the culture media was collected for LDH detection using Cytotox-One Homogenous Membrane Integrity Assay Kit (Promega Corporation, Winsicon, USA) following the manufacturer's instructions. LDH released into the culture medium was measured with an enzymatic assay that results in the conversion of resazurin into a fluorescent resorufin product, and the amount of fluorescence produced is proportional to the number of lysed cells. Fluorescence was

measured using the Tecan SpectraFluorPlus reader ($\lambda_{ex}/\lambda_{em}$: 560/590 nm). Cytotoxicity was calculated as follows:

$$Percent\ cytotoxicity\ (\%) = \frac{(F_{treated} - F_{untreated})}{(F_{triton-X} - F_{untreated})} \times 100\%$$

where $F_{treated}$, $F_{untreated}$, and $F_{triton\text{-}X}$ represent the fluorescence reading from cells treated with the polymer sample, the vehicle control, and 0.2% triton-X, respectively.

5.2.5 R-123 and R-110 Accumulation Study in Caco-2 and MDCK/MDR1 Cells

Caco-2 cells were seeded in 24-well culture slides at a density of 8×10^4 cells/well and incubated for 21 days before experimentation. MDCK/MDR1 cells were seeded in 24-well culture slides at a density of 2.5×10^5 cells/well and incubated for 3 days before experimentation. Cells were exposed to 2 mg/ml of dendrimers, Pluronic P85 (P85), or HBSS buffer mixed either with 5 μM R-123 or 5 μM R-110. After incubation for 90 min at 37 ℃, cells were washed three times with PBS and lysed with 1% Triton-X to release intracellular R-123 or R-110. After centrifuge at 13,000 rpm for 5 min to remove cell debris, fluorescence intensity of R-123 ($\lambda_{ex}/\lambda_{em}$: 485/530 nm) or R110 ($\lambda_{ex}/\lambda_{em}$: 496/520 nm) in cell lysates was measured using Tecan SpectraFluorPlus reader. The amount of R-123 or R-110 accumulated was normalized to the protein content of the cells determined by the Bio-Rad protein assay kit (Bio-Rad, Hercules, CA) according to manufacturer's manual.

5.2.6 R-123 Permeability Study in Caco-2 and MDCK/MDR1 Cell Monolayers

As shown in Figure 5.1, Caco-2 cells were seeded at a density of 1.2 $\times 10^4$ cells/well on a 24-well collagen coated polycarbonate filter membrane transwell inserts obtained from BD Biocoat (Erembodegem, Belgium, UK) and incubated at 37°C for 21 days. MDCK/MDR1 cells were seeded at a density of 5×10^4 cells/well on the 24-well transwell inserts for 3 days. The volumes of media were 0.2 ml and 0.5 ml on the apical and basolateral compartments, respectively. Donor solutions, composed of either 2 mg/ml synthesized dendrimers or 0.1 mg/ml P85 mixed with 5 μM R-123 dissolved in HBSS buffer, were added to either apical or basolateral chamber. In parallel, HBSS buffer with R-123 was investigated as control. The transwells were then incubated at 37°C. The permeability of R-123 was determined by sampling the receiving chamber at regular time intervals (every 20 min) for 3 h. The sampled volumes were replaced with fresh HBSS buffer in order to maintain sink conditions. All the collected samples were quantified using Tecan fluorescent plate reader at $\lambda_{ex}/\lambda_{em}$ of 485/530 nm. The apparent permeability coefficient (Papp, cm/s) was calculated according to the following equation:

$$P_{app} = \frac{dQ}{dt} \times \frac{1}{A \times C_0}$$

where dQ/dt is the steady-state flux, A is the surface area of the filter (0.3 cm^2) and C_0 is the initial concentration in the donor chamber.

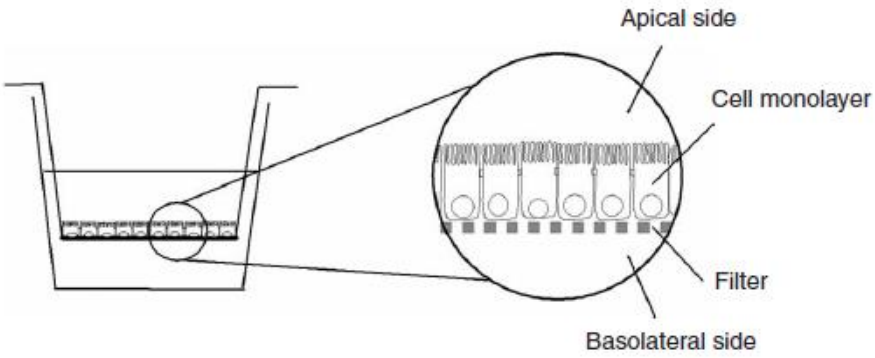

Figure 5.1 Diagram of a Caco-2 monolayer grown on a permeable filter [214]

5.2.7 Tight junction staining with anti-ZO-1 antibody

Caco-2 cells were seeded in 4-well Lab-tek chamber glass slides from Nalge Nunc Inc (Naperville, IL) at a density of 7.2 $\times 10^4$ cells/well and cultured for 21 days before experiment. Cells were exposed to either PAMAM dendrimer samples, HBSS (vehicle control) or 0.05% Triton-X for 24 h at 37°C. After incubation, cells were washed three times with ice-cold PBS, and fixed with ice-cold methanol for 10 min. Subsequently, cells were rinsed with ice-cold PBS and blocked with 1% BSA for 30 min. Cells were then incubated with 2 µg/ml primary antibody (purified mouse anti-human ZO-1, BD Transduction Laboratories, San Jose, CA) for 1 h. The cells were washed three times with PBS and incubated with 4 µg/ml secondary antibody (Alexa Fluor® 568 Goat Anti-Mouse IgG) for 1 h. Finally, cells were washed three times with PBS and viewed under a Carl Zeiss fluorescence confocal microscope using 40× objective (Carl Zeiss, Jena, Germany). During the acquisition of the images, the following settings were used: scan mode, stack; scaling of 0.22 µm × 0.22 µm × 0.95 µm; pixel time of 1.26 µs; wavelength of 543 nm at 30%; filters of BP 565-615 IR;

Pinhole of Cha 152 μm; Beam Splitters of MBS: HFT 488/543, DBS1, Mirror, DBS2, NFT 545, NDD MBS, none. The experiments were repeated twice, each time with a minimum of three views of the same sample was captured.

5.2.8 Transepithelial Electrical Resistance (TEER) Measurement in Caco-2 Cells

Caco-2 cells were seeded on 24-well, collagen-coated polycarbonate filter membrane transwell inserts. On day 21, the baseline TEER values were measured using Millicell ERS-2 Epithelial Volt-Ohm Meter to record cell monolayer integrity. Only inserts with values >600 $\Omega \cdot cm^2$, which indicated good monolayer integrity, were subjected to experimentation. Media in both sides of the chambers were aspirated, and the chamber was washed twice with HBSS buffer. The Caco-2 cells in the inserts were exposed to either 2 mg/ml dendrimer samples or HBSS buffer for 24 h at 37°C. After taking TEER measurement, fresh media was added after washing cells twice with HBSS buffer. Further TEER measurements were recorded every 24 h for 120 h. Percentage change in TEER was calculated as follows:

$$TEER\ (\%) = \frac{R_{test,t} - R_{background,t}}{R_{test,0} - R_{background,0}} \div \frac{R_{vehicle,t} - R_{background,t}}{R_{vehicle,0} - R_{background,0}} \times 100\%$$

where $R_{test,t}$, $R_{background,t}$, $R_{vehicle,t}$ represent the TEER readings from the polymer sample treated wells, the no-cell control wells, and the vehicle control wells at time t, respectively. $(R_{test,t} - R_{background,t})/(R_{test,0} - R_{background,0})$ *and* $(R_{vehicle,t} - R_{background,t})/(R_{vehicle,0} - R_{background,0})$ represents percentage change of TEER reading

at time t compared to time 0 of Caco-2 monolayer treated with test sample or HBSS, respectively.

5.2.9 Transport of Lucifer Yellow (LY) across Caco-2 monolayer

Similar to the conditions for TEER measurement, Caco-2 cells were grown in the transwell inserts for 21 days before experimentation. The cells were treated with HBSS buffer, 2 mg/ml dendrimers or Triton-X mixed with 60 μM LY dissolved in HBSS. After incubation for 2, 4 and 24 h, 200 μl of HBSS was sampled from the basolateral chamber and same volume of fresh HBSS was added to maintain sink condition. The HBSS samples were subsequently measured for LY fluorescence using SpectraFluorPlus reader at $\lambda_{ex}/\lambda_{em}$ of 430/540 nm. LY represents a model compound that is not able to cross the normal, untreated Caco-2 monolayer, and the percentage of LY transported to the basolateral side was calculated as follows:

$$LY\ transported\ (\%) = \frac{F_t}{F_{initial}} \times 100\%$$

where F_t, $F_{initial}$ represent the cumulative fluorescence signal of LY at time t in the basolateral side and the fluorescence signal of LY initially added to apical side, respectively.

5.2.10 Permeability of FITC-labeled dual-functionalized PAMAM dendrimer

The PEG-PM dendrimer was conjugated with FITC according to a protocol reported in the literature [215]. Briefly, PEG-PM polymer was dissolved into

DMSO. FITC in DMSO solution (5 mg/ml) was added dropwise to the dendrimer solution at a molar ratio of 1:3 under stirring at room temperature. The mixture was stirred in dark for 24 h. The reaction mixture was dialyzed against Milli-Q water three times for 24 h followed by lyophilization. The lyophilized product was then conjugated with TBA as described above. Similar to the conditions for TEER measurement, Caco-2 cells were grown in the transwell inserts for 21 days before experimentation. The cells were treated with 2 mg/ml FITC-labeled dual-functionalized dendrimers in HBSS with or without 2.4% Triton-X. At 2, 4 and 24 h, 200 µl of HBSS was sampled from the basolateral compartment and same volume of fresh HBSS was added for replenishment. Samples were then measured for FITC fluorescence SpectraFluorPlus reader at $\lambda_{ex}/\lambda_{em}$ of 492/518 nm. At 24 h, supernatant samples in the transwell inserts were collected, and the transwell inserts were washed three times with HBSS, with the washings pooled with the supernatant samples. Cells were subsequently harvested from the transwell inserts and lysed with Triton-X for FITC fluorescence determination using SpectraFluorPlus reader at $\lambda_{ex}/\lambda_{em}$ of 492/518 nm. Percentage of FITC-labeled dual-functionalized dendrimers transported to the basolateral side was calculated as follows:

$$Dendrimer\ transported\ (\%) = \frac{F_t}{F_{initial}} \times 100\%$$

where F_t, $F_{initial}$ represent the cumulative fluorescence signal of FITC labelled dendrimers at time t in basolateral side and the FITC labelled dendrimer initially added to apical side, respectively.

Percentage of FITC-labeled dual-functionalized dendrimers accumulated intracellularly was calculated as follows:

$$Dendrimer\ accumulation\ (\%) = \frac{F_{24}}{F_{initial}} \times 100\%$$

where F_{24} represent the fluorescence signal of FITC labelled dendrimer samples accumulated in cells at 24 h.

5.2.11 Pharmacokinetic study of ganciclovir in mice

All animal studies were completed using protocols approved by the Institutional Animal Care and Use Committee (IACUC) of National University of Singapore. BALB/C mice were divided into two groups. The mice had no access to food 12 h prior to the experiment. Drug samples were freshly prepared before the experiment. Ganciclovir (GCV) and PAMAM were dissolved in saline at 1 mg/ml and 4 mg/ml, respectively. Then GCV and PAMAM solution were mixed at 1:1 ratio for administration. Control group was orally administered with GCV free drug (0.5 mg/ml in saline) at dose of 10 mg/kg. The other group was administered with a mixture of GCV (0.5 mg/ml in saline, 10 mg/kg) and PEG(1.8)-PM-TBA(7.0) (2 mg/ml in saline, 40 mg/kg) (GCV/ PEG(1.8)-PM-TBA(7.0)). At each time points (10 min,30 min, 2 h, 4 h, 6 h and 24 h), the mice were euthanized with CO_2 gas. Blood were collected from animals by heart puncture. Subsequently, the blood samples were centrifuged at 13,000 rpm at 4°C for 15 min. The plasma samples were collected and kept at – 80°C until analysis by LC-MS/MS described below.

5.2.12 LC-MS/MS analysis of GCV

200 µl plasma samples were mixed with 10 µl internal standard (acyclovir, 10 µg/ml) and 600 µl methanol for protein precipitation. After vortex mixing for 30 s, the mixture was centrifuged at 13,000 rpm at 4°C for 15 min. 600 µl of supernatant was collected after centrifuge and the solvent was evaporated with Savant SpeedVac SC100 Centrifugal Evaporator (Savant Instruments, Inc., NY, USA). Subsequently, the sample was reconstituted with 150 µl mobile phase. The liquid chromatography separation was carried out on Agilent 1290 Infinity LC System (Agilent, USA). Sample was separated on an Acquity UPLC HSS T3 Column (1.8 µm, 2.1 × 150 mm, Waters, MA, USA). The mobile phase consisted of ACN (2%) and 10 mM Ammonium Formate in water (pH 3, 98%). The flow rate was set at 0.2 ml/min. The injection volume was 10 µl and run time was 10 min.

Mass spectrometric measurements were performed on Agilent 6430 Triple Quad LC/MS system with an electrospray ionization (ESI) source operating in positive ion mode. The instrument was operated with the following parameters: gas temperature of 350°C, gas flow of 10 l/min, nebulizer of 25 psi, capillary of +6000 V, Dwell of 0.2 s, fragmentor of 70 V (GCV) and 80 V (ACV), Collision Energy of 7 eV (GCV) and 8 eV (ACV). The detection ions were set as m/z 256.2 → 152.5 for ganciclovir and m/z 226.4 → 152.5 for acyclovir (ACV). The chromatogram data was analyzed with Agilent MassHunter Workstation Quantitative Anlysis Software (version B.03.02). The analysis method was linear in the range of 31.25 -1000 ng/ml.

5.2.13 Statistical analysis

Where appropriate, results were expressed as mean ± SEM of at least three independent experiments. Statistical significance was determined using the Student t-test or one-way analysis of variance (ANOVA) Kruskal-Wallis test followed by Dunn's test used for post-hoc multiple comparisons. P values of < 0.05 were considered to be statistically significant. Statistical analyses were carried out using SPSS software (v 19.0; IBM, Armonk, NY).

5.3 Results

5.3.1 Thiol Group Stability Study at various pH conditions

Stability of the free thiol groups on the PAMAM dendrimers was evaluated under different pH conditions similar to those found in GI tract [216], which could affect the oxidation of free thiol groups (Figure 5.2). It appears that PEGylation of the thiol-dendrimers helped protect the thiol groups from oxidation when the dendrimers were subjected to low pH value (pH 1.5). For PEG(4.0)-PM-TBA(6.7), >80% of free thiol groups were retained at all the tested pH values. PEG(1.8)-PM-TBA(7.0) retained >79% of free thiol groups at pH 6.5, 4 and 1.5 after 6 h, while 64% of free thiol groups remained at pH 7.4. For PM-TBA(7.6), 70% and 57% of free thiol groups were retained in pH 7.4 and 1.5, respectively.

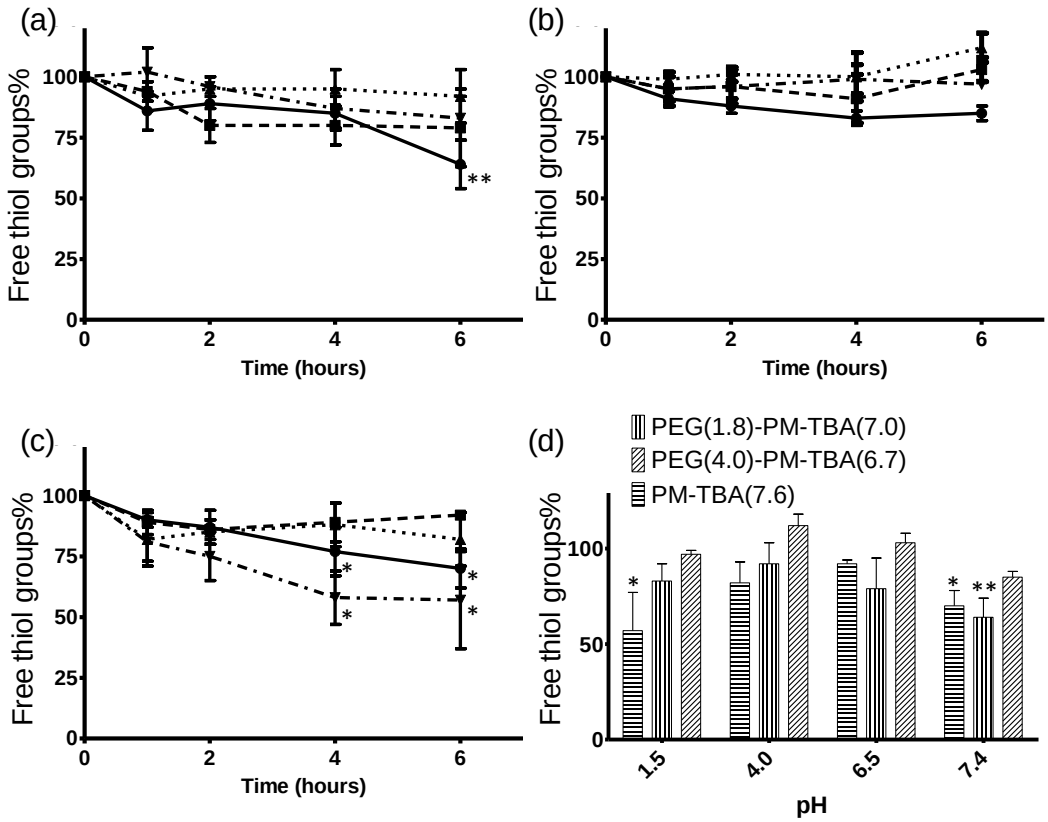

Figure 5.2. Effect of pH on the oxidation of free thiol groups of (a) PEG(1.8)-PM-TBA(7.0), (b) PEG(4.0)-PM-TBA(6.7), (c) PM-TBA(7.6) at pH 1.5 (▼), 4.0 (▲), 6.5 (■), and 7.4 (●). (d) Free thiol groups% of PEG(1.8)-PM-TBA(7.0), PEG(4.0)-PM-TBA(6.7) and PM-TBA(7.6) after 6h incubation at pH 1.5, 4.0, 6.5 and 7.4. Data represent mean ± SEM of 4 independent experiments. ** $p < 0.05$, ** $p < 0.01$, compared to free thiol groups% at time 0 h.*

5.3.2 Cytotoxicity of functionalized PAMAM dendrimers

The cytotoxicity of the functionalized PAMAM dendrimers was determined by the LDH release assay in Caco-2 and MDCK/MDR1 cells tested with various concentrations of the dendrimers for 24 h (Figure 5.3 top panels). In general, the higher the dendrimer concentration, the higher was the observed cytotoxicity. Secondly, surface-modified PAMAM dendrimers were less cytotoxic as compared to unmodified PAMAM G4, with the dual-functionalized dendrimers,

PEG(1.8)-PM-TBA(7.0) and PEG(4.0)-PM-TBA(6.7), showing the least cytotoxicity in both cell lines, with <20% LDH release at a concentration of 4 mg/ml after 24 h exposure. Further studies with longer exposure time of 48 and 72 h were conducted, and the results are shown in Figure 5.3 lower panels. Consistent with 24 h exposure data, the dual-functionalized dendrimers showed significantly less cytotoxicity in both cell lines after 48 and 72 h of exposure.

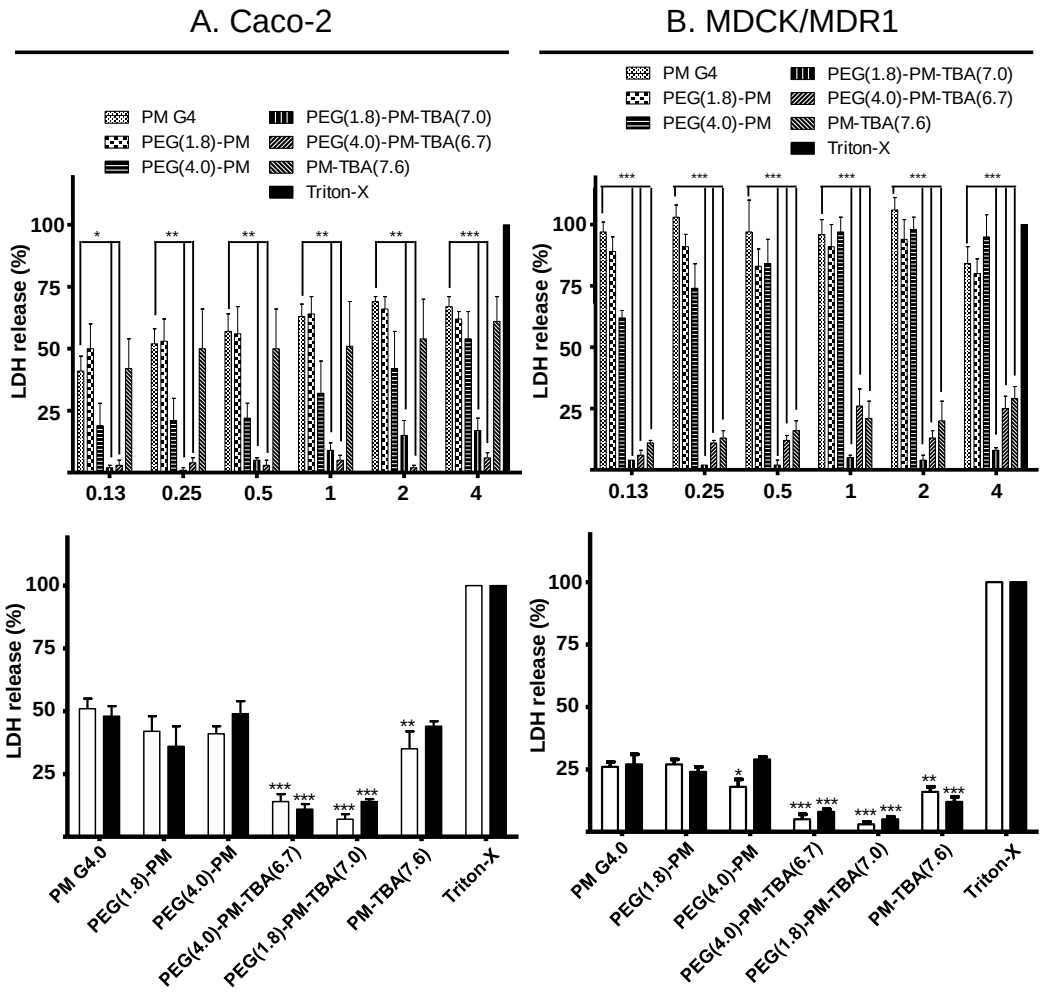

Figure 5.3. LDH released from (A) Caco-2 and (B) MDCK/MDR1 cell monolayers treated with PM G4.0, PEG(1.8)-PM, PEG(4.0)-PM, PEG(1.8)-PM-TBA(7.0), PEG(4.0)-PM-TBA(6.7), PM-TBA(7.6) for 24 h at various concentrations (top panels). Longer exposure times of 48 h (lower panels, open

bar) and 72 h (lower panels, solid bars) were also tested with dendrimer concentrations of 2 mg/ml. Data are expressed as mean ± SEM of 3 independent experiments. *$p<0.05$, **$p< 0.01$, ***$p<0.001$ compared to PM G4.*

5.3.3 Modulation of P-gp efflux by the dual-functionalized PAMAM dendrimers

In order to further explore whether the surface-modified dendrimers could specifically modulate P-gp function, cellular accumulation and epithelial permeability of the P-gp substrate R-123 was studied with results summarized in Figure 5.4. Cellular accumulation of R-123 and the non-P-gp substrate R-110 was studied in the presence and absence of the various PAMAM dendrimers. Pluronic P85, a well-accepted polymeric P-gp inhibitor [217, 218], was included for comparison. Figure 5.4 (A), (B) show that R-123/R-110 accumulation ratio was significantly increased when both cell lines were treated with PEG(1.8)-PM-TBA(7.0) and PM-TBA(7.6). In particular, the fold increase in R-123/R-110 accumulation ratio for PEG(1.8)-PM-TBA(7.0) and PM-TBA(7.6) in MDCK/MDR1 cells was higher than P85. As for PEG(4.0)-PM-TBA(6.7), the fold increase in R-123/R-110 accumulation ratio was not as high as the cells treated with PEG(1.8)-PM)-TBA(7.0).

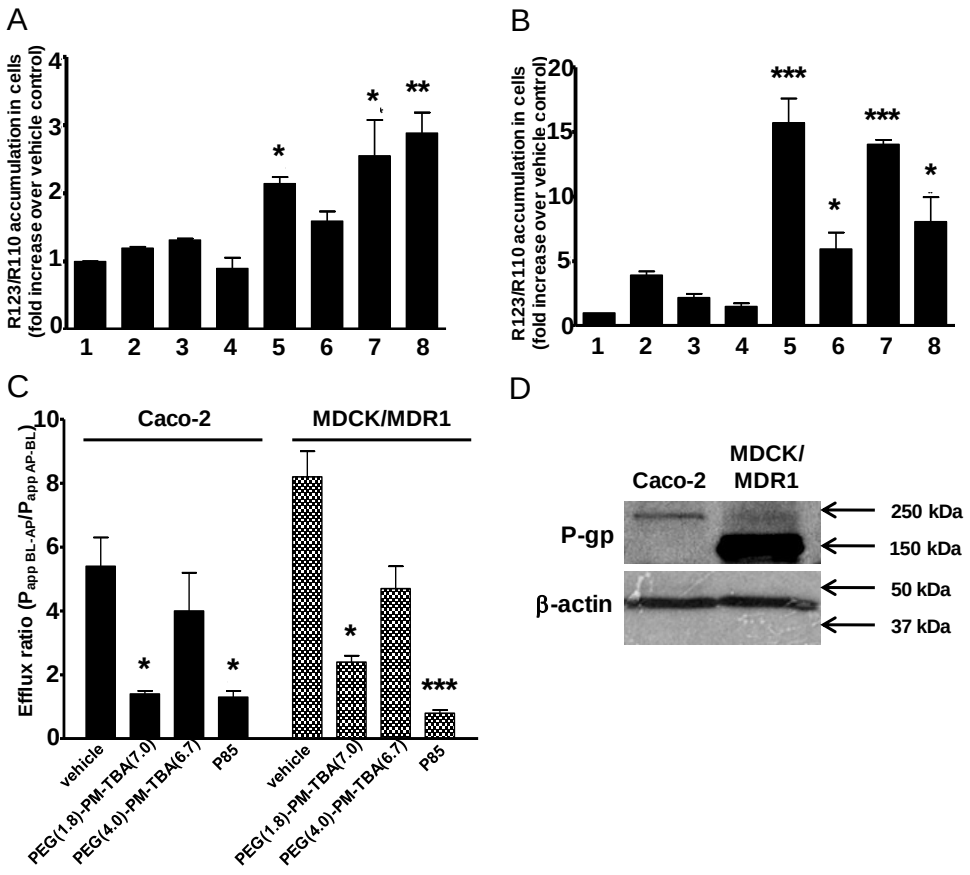

Figure 5.4. Modulation of P-gp efflux by dual-functionalized PAMAM dendrimers. R-123/R-110 cellular accumulation was studied in (A) Caco-2 and (B) MDCK/MDR1 cells. Cells were treated with 2 mg/ml of 1) vehicle control, 2) PM G4.0, 3) PEG(1.8)-PM, 4) PEG(4.0)-PM, 5) PEG(1.8)-PM-TBA(7.0), 6) PEG(4.0)-PM-TBA(6.7), 7) PM-TBA(7.6), and 8) P85. (C) Epithelial permeability of R-123 was studied in Caco-2 and MDCK/MDR1 monolayers, whereby the efflux ratio represents the ratio of the secretory apparent permeability coefficient ($P_{app\ BL-AP}$) to the absorptive apparent permeability coefficient ($P_{app\ AP-BL}$). (D) Expression of P-gp in Caco-2 and MDCK/MDR1 cells, with a representative western blot shown out of three independent studies. *Data represent mean ± SEM of 3 independent experiments, with *p<0.05, **p<0.01, ***p<0.001compared to untreated control.*

Based on the results from cytotoxicity study and cellular accumulation study, PEG(1.8)-PM-TBA(7.0) and PEG(4.0)-PM-TBA(6.7) are selected for further evaluation of absorptive (apical to basolateral, AP-BL) and secretory (basolateral to apical, BL-AP) transport of R-123 across Caco-2 and MDCK/MDR1 cell monolayer. The absorptive and secretory apparent permeability coefficients (P_{app}) and efflux ratio of R-123 across Caco-2 and MDCK/MDR1 cell monolayers are shown in Table 5.1 and Figure 5.4 (C), respectively. Of the two dual-functionalized PAMAM dendrimers, PEG(1.8)-PM-TBA(7.0) was more effective in achieving an efflux ratio of close to 1, which was mainly due to its ability to increase the absorptive transport of R-123. Furthermore, the ability of PEG(1.8)-PM-TBA(7.0) to modulate epithelial permeability of R-123 was comparable to P85 in Caco-2 cells. Of note, the difference in P-gp expression in the two cell lines (Figure 5.3 (D)) may account for the difference in the ability of PEG(1.8)-PM-TBA(7.0) in modulating the cellular accumulation and epithelial permeability of R-123.

Table 5.1 Comparison of the absorptive and secretory apparent permeability coefficients (Papp) and efflux ratio of R-123 in the presence of tested compounds on Caco-2 and MDCK/MDR1 cell monolayers.

Dendrimer	**Permeability (cm/sec) × 10^{-7}**				**Efflux ratio ($P_{app\ BL-AP}/P_{app\ AP-BL}$)**	
	Absorptive (AP to BL)		**Secretory (BL to AP)**			
	Caco-2	MDCK/MDR1	Caco-2	MDCK/MDR1	Caco-2	MDCK/MDR1
VEH	3.6 ±2.9	6.4 ±1.2	15.1 ±11.4	47.2 ±2.0	5.4 ±0.9	8.2 ±0.8
PEG(1.8)-PM-TBA(7.0)	18.4 ±8.5	15.7 ±2.6	24.1 ±10.1	35.8 ±2.0	1.4 ±0.1*	2.4 ±0.2*
PEG(4.0)-PM-TBA(6.7)	14.0 ±7.9	9.5 ±2.0	20.4 ±7.9	38.2 ±2.5	4.0 ±1.2	4.7 ±0.7
P85	24.4 ±7.7	56.5 ±7.7	29.2 ±6.7	43.9 ±3.0	1.3 ±0.2*	0.8 ±0.1***

Data represent mean ± SEM of 3 independent experiments, **p<0.05, ***p<0.001compared to vehicle control*

5.3.4 Tight junction disruption of Caco-2 cell monolayer after exposure to dendrimer derivatives

Tight junction disruption in the intestinal epithelium will open up paracellular route for drug transport. Therefore, ZO-1 staining, LY permeation and TEER measurement were conducted to examine tight junction integrity of Caco-2 cell monolayer after treatment with dendrimer derivatives. ZO-1 is a major protein expressed in the cytoplasmic plaque of the tight junction [219] and represents a marker of tight junction formation. After incubating Caco-2 cell monolayer with 2mg/ml of PM G4, PEG(1.8)-PM, PEG(4.0)-PM, PEG(1.8)-PM-TBA(7.0), PEG(4.0)-PM-TBA(6.7), PM-TBA(7.6) for 24 h, the immunofluorescence of ZO-1 was visualized with confocal microscopy. As seen in Figure 5.5, cells treated with vehicle control showed strong, uniform and integral distribution of ZO-1. In comparison, the Triton-X treated, positive control cells showed disrupted and abnormal localization of ZO-1. Of the six dendrimers evaluated, PM G4 showed a decreased and disrupted distribution of ZO-1. For PEG(1.8)-PM and PEG(4.0)-PM, the ZO-1 modulating effect was much less as compared to PM G4. After thiolation, PEG(1.8)-PM-TBA(7.0), PEG(4.0)-PM-TBA(6.7) and PM-TBA(7.6) showed stronger ZO-1 modulating effect as compared to PEGylated PAMAM dendrimers.

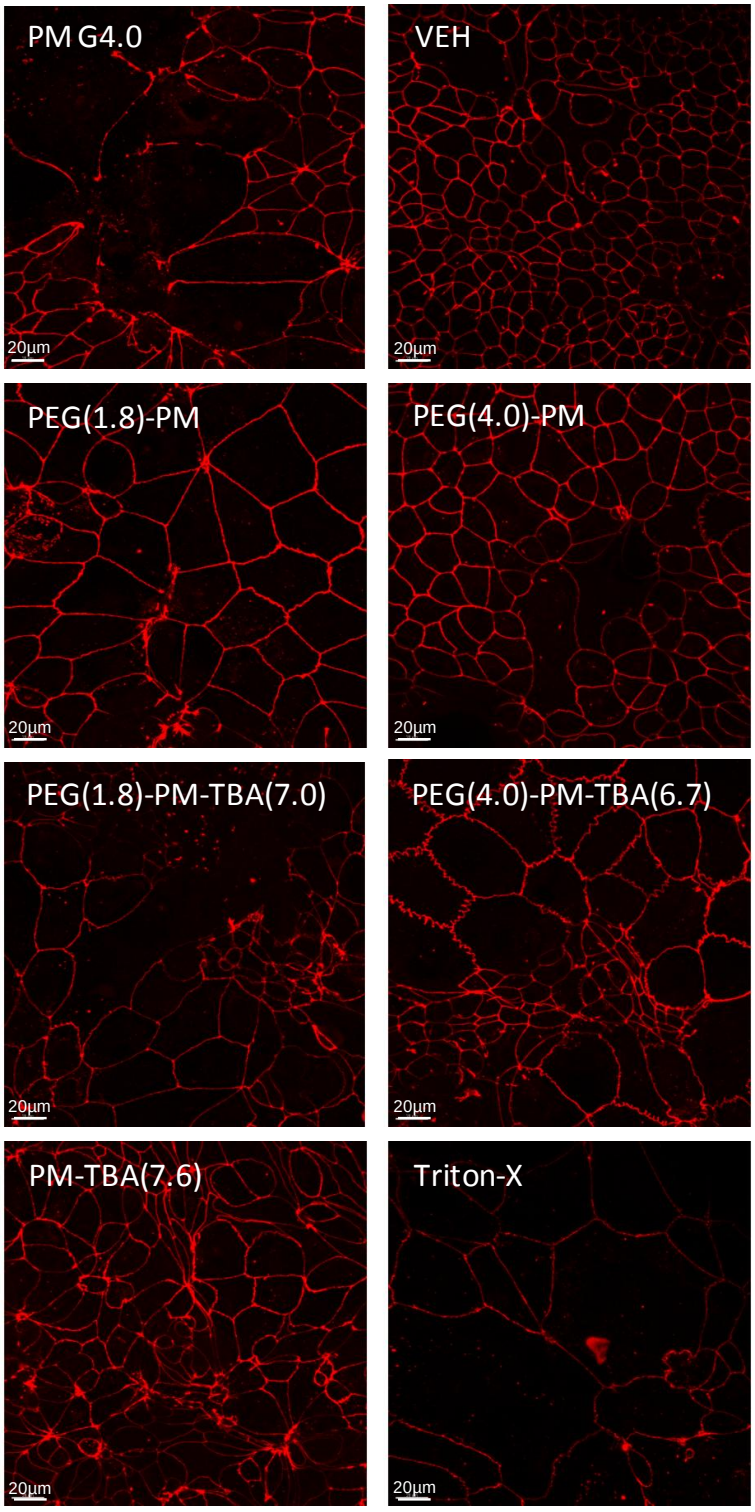

Figure 5.5. Tight junction modulating effect of dual-functionalized PAMAM dendrimers observed by ZO-1 staining under fluorescence confocal microscope. The experiments were repeated twice, each time with a minimum of three views of the same sample was captured.

In addition to ZO-1 immunofluorescence, LY which is a well-known, non-radioactive molecule impermeable to the normal, untreated epithelial monolayer for the purpose of probing monolayer integrity[220, 221] was used to evaluate the effect of the dendrimers on the tight junction integrity of Caco-2 monolayers. As seen in Figure 5.6, minimum amount of LY was detected in the basolateral side after 2 and 4 h of incubation with various dendrimers. After 24 h, the effect of dendrimers in promoting LY permeation was more apparent, whereby PEG(1.8)-PM, PEG(4.0)-PM, PEG(4.0)-PM-TBA(6.7) and PM-TBA(7.6) significantly increased LY permeation. PM G4 and PEG(1.8)-PM-TBA(7.0) also increased LY permeation by 2.0-fold and 1.9-fold as compared to control, although the increase was not statistically significant.

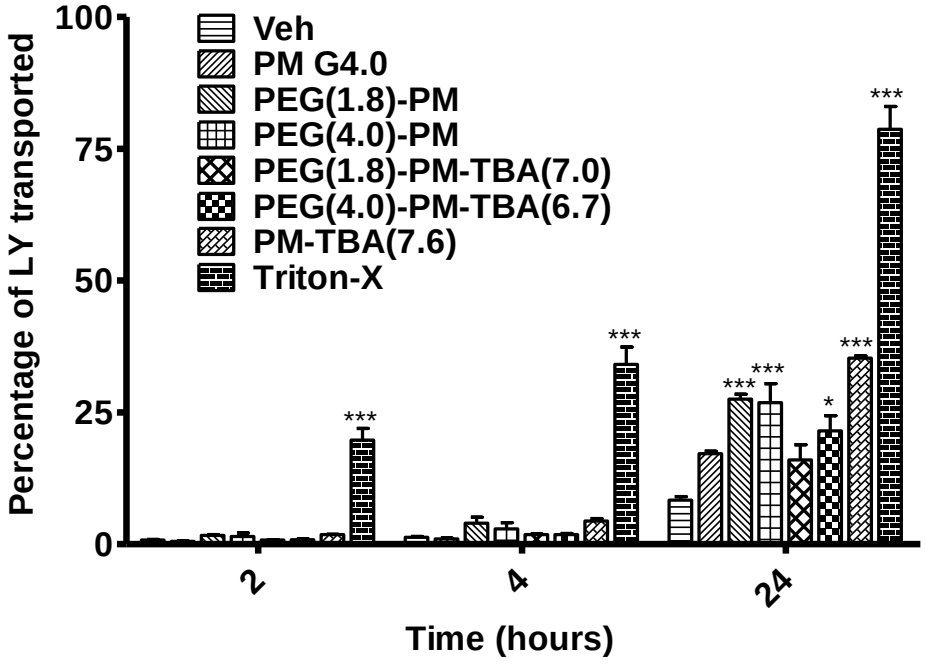

Figure 5.6. Permeation of LY across Caco-2 monolayer after treatment with 2 mg/ml of various dendrimers or 0.2% Triton-X. Data represent mean ± SEM of 3 independent experiments. **p<0.05, ***p<0.001compared to untreated control.*

While results in Figure 5.5 and Figure 5.6 demonstrated the ability of the functionalized dendrimers to modulate tight junction transport, it is important to determine if such effect is reversible, as irreversible effect would represent potential toxicity to the intestinal epithelium and the material might not be suitable for oral drug delivery. Thus, time-course TEER measurement was performed to determine the reversibility of the tight junction modulating effect by the dendrimer samples. The Caco-2 monolayer was treated with the dendrimer samples for 24 h, after which the dendrimers were removed and fresh medium was added. As shown in Figure 5.7, after 24 h treatment, the TEER values decreased >50% in all dendrimer-treated Caco-2 monolayers. Of significance, only PEG(1.8)-PM-TBA(7.0) and PEG(4.0)-PM-TBA(6.7) treated Caco-2 monolayers showed gradual increase of TEER values over time to ~100% of control. All other dendrimer and Triton-X treated Caco-2 monolayers showed irreversible decrease of TEER values, suggesting irreversible disruption of tight junctions and potential epithelial toxicity.

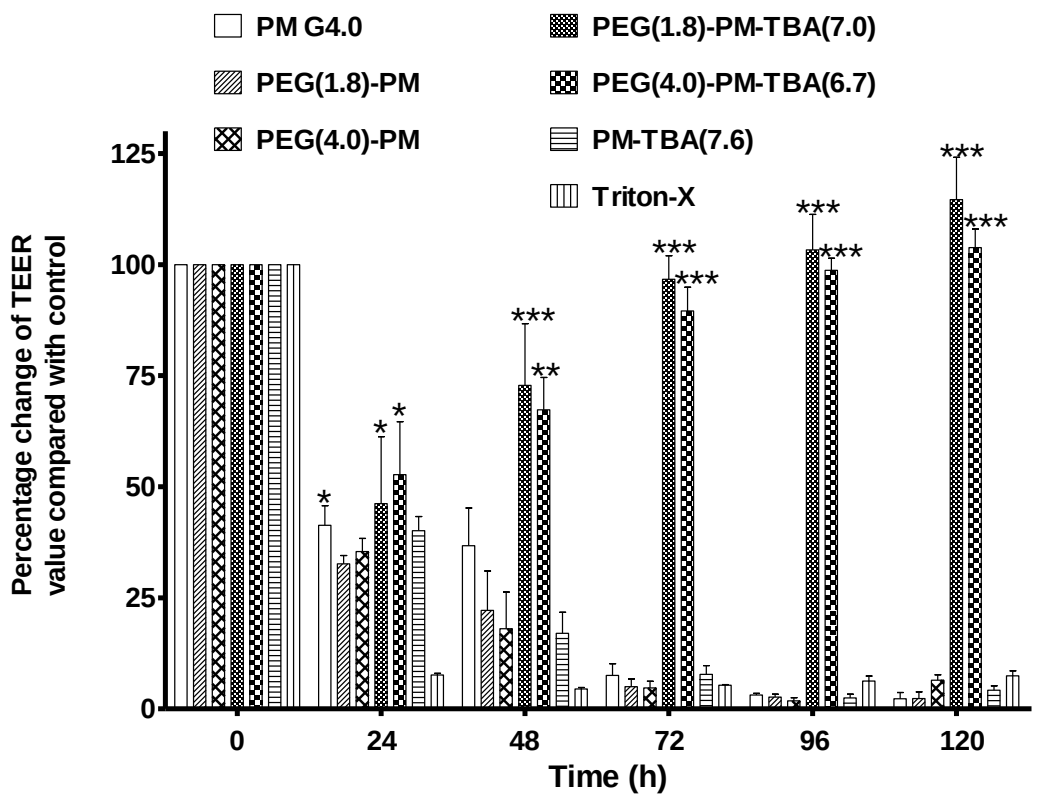

Figure 5.7. Change in TEER upon treatment with dendrimers and Triton-X. The Caco-2 cell monolayer was exposed to dendrimer treatment during first 24 h and subsequent replacement with fresh medium. Data represent mean ± SEM of 3 independent experiments. *$p<0.05$, **$p<0.01$, ***$p<0.001$compared to Triton-X treated group.*

5.3.5 Permeability of FITC-labeled dual-functionalized dendrimers

Since PAMAM is a non-biodegradable polymer, it is important to determine how much of the dual-functionalized dendrimers could pass through the intestinal epithelium. Based on the biological data thus far, PEG(1.8)-PM-TBA(7.0) and PEG(4.0)-PM-TBA(6.7) showed low cytotoxicity to the epithelial cells yet showing P-gp and tight junction modulating effect. As such, these two functionalized dendrimers were selected for evaluation and labeled with FITC to

probe their transport through the Caco-2 monolayer. As shown in Figure 5.8, minimum amount of PEG(1.8)-PM-TBA(7.0) and PEG(4.0)-PM-TBA(6.7) was transported through Caco-2 monolayer after 2 and 4 h of incubation. After 24 h, 5.8% of PEG(1.8)-PM-TBA(7.0) and 17.7% of PEG(4.0)-PM-TBA(6.7) passed through Caco-2 monolayer. Addition of Triton-X increased the amount of dendrimers in the basolateral side, indicating that the low permeability of the two dendrimers was not due to a defect of the Caco-2 monolayer. In addition to basolateral side, the distribution of the FITC-labeled dendrimers was determined for the apical side and within the Caco-2 cellular compartment (Table 5.2). Less than 5% of PEG(1.8)-PM-TBA(7.0) and PEG(4.0)-PM-TBA(6.7) were accumulated in Caco-2 cells. Collectively, the results suggest potentially minimal absorption of PEG(1.8)-PM-TBA(7.0) into systemic circulation.

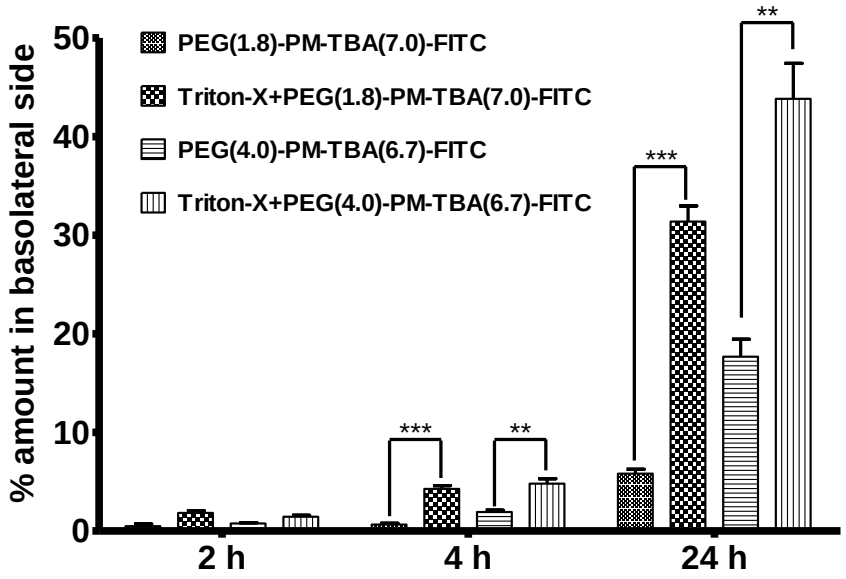

Figure 5.8. Transport of FITC-labeled PEG(1.8)-PM-TBA(7.0) , PEG(4.0)-PM-TBA(6.7) with and without Triton-X through Caco-2 monolayer. Data represent mean ± SEM of 3 independent experiments. ***p<0.01, ***p<0.001*

Table 5.2 Distribution of FITC-labeled dual-functionalized dendrimers after 24 h (n=3).

	Apical side	Basolateral side	Cellular accumulation
PEG(1.8)-PM-TBA(7.0)	90.43 ± 1.59%	5.83 ± 0.44%	3.75 ± 1.51%
PEG(1.8)-PM-TBA(7.0) + Triton-X added at start of incubation	61.14 ± 1.31%	31.38 ± 1.59%	7.48 ± 0.55%
PEG(4.0)-PM-TBA(6.7)	79.68 ± 1.35%	17.69 ± 1.75%	2.63 ± 0.63%
PEG(4.0)-PM-TBA(6.7) + Triton-X added at start of incubation	49.86 ± 2.91%	43.83 ± 3.58%	6.30 ± 1.06%

5.3.6 Pharmacokinetic study of ganciclovir in mice

Plasma pharmacokinetics of GCV free drug and GCV/ PEG(1.8)-PM-TBA(7.0) mixture were conducted in BALB/C mice. The concentration of GCV in plasma samples were determined using LC-MS/MS based method. Figure 5.9 shows representative chromatograms of GCV from extracted plasma samples. ACV was used as the internal standard. The retention time for GCV and ACV were 5.7 min and 7.5 min, respectively. No endogenous interferences co-eluting with GCV or ACV were observed in blank mice plasma as shown in Figure 5.9. Method validation was perfomed by analyzing inter-day precision, bias range, analytical recovery and absolute recovery of the lowest limit of quantification (LLOQ), three quality control (QC) samples against a calibration curve of 9 concentrations. The calibration curve was linear in the range 32.25-1000 ng/ml. The bias range for LLOQ and QC samples were < 20% and 15%, respectively (Table 5.3). The recovery of LLOQ and QC samples were 87.7% and abve 95%, respectively.

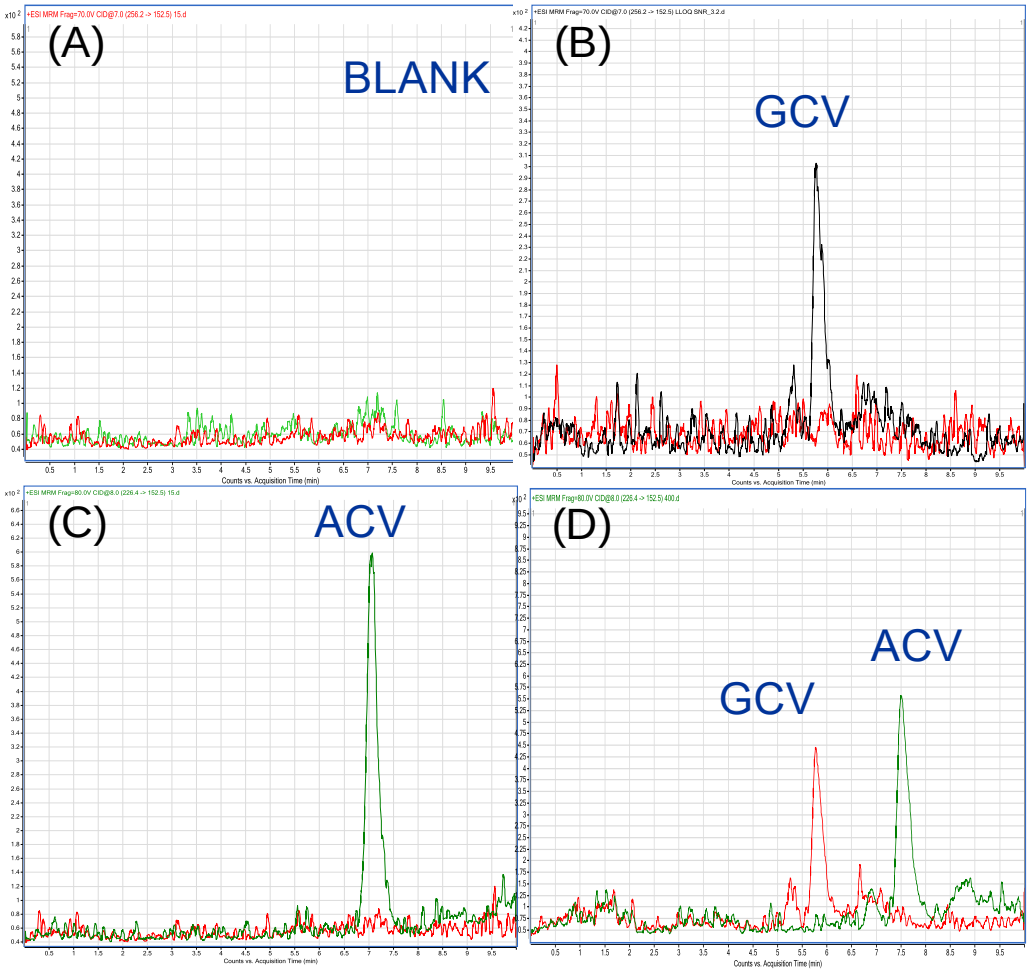

Figure 5.10. Chromatogram of (A) blank plasma extract, (B) GCV alone in plasma sample (C) ACV alone in plasma sample and (D) GCV and ACV in plasma sample.

Table 5.3 Inter-day accuracy, precision and recovery of ganciclovir in plasma sample

Amount spiked (ng/ml)	Amount measured (ng/ml)	Bias range (%)	Precision (RSD, %)	Analytical recovery (%)	Absolute recovery (%)
32.25	29.9 ± 1.6	-18.5 ~ 15.5	13.8	92.1 ± 4.8	87.7 ± 4.6
62.5	59.3 ± 1.8	-9.7 ~ 6.5	8.5	94.9 ± 2.9	96.8 ± 2.9
400	406.9 ±8.5	-6.2 ~ 10.1	5.9	101.7 ± 2.1	103.0 ± 2.3
800	826.0 ±14.7	-2.4 ~ 11.5	5.0	103.2 ± 1.8	101.7 ± 1.8

The plasma GCV concentration-time profiles after oral administration are shown in Figure 5.10. GCV drug concentration quickly reached peaks value within 1 h and decreased rapidly afterwards. Analysis of the concentration-time profiles to derive various pharmacokinetic parameters was performed with WinNonlin 5.0.1 (Pharsight Corporation, CA, USA) by using the non-compartmental analysis. The pharmacokinetic parameters are listed in Table5.3. At 30 min time point (t_{max}), the C_{max} for GCV/ PEG(1.8)-PM-TBA(7.0) group (C_{max} = 1004.1 ng/ml) is 56.8% higher than the C_{max} of GCV group (C_{max} = 640.2 ng/ml) ($p < 0.05$). Area under the plasma concentration time curve (AUC_{last}) for GCV/ PEG(1.8)-PM-TBA(7.0) treated group is increased by 17.2% compared to GCV group, indicating enhanced GCV absorption in the presence of PEG(1.8)-PM-TBA(7.0).

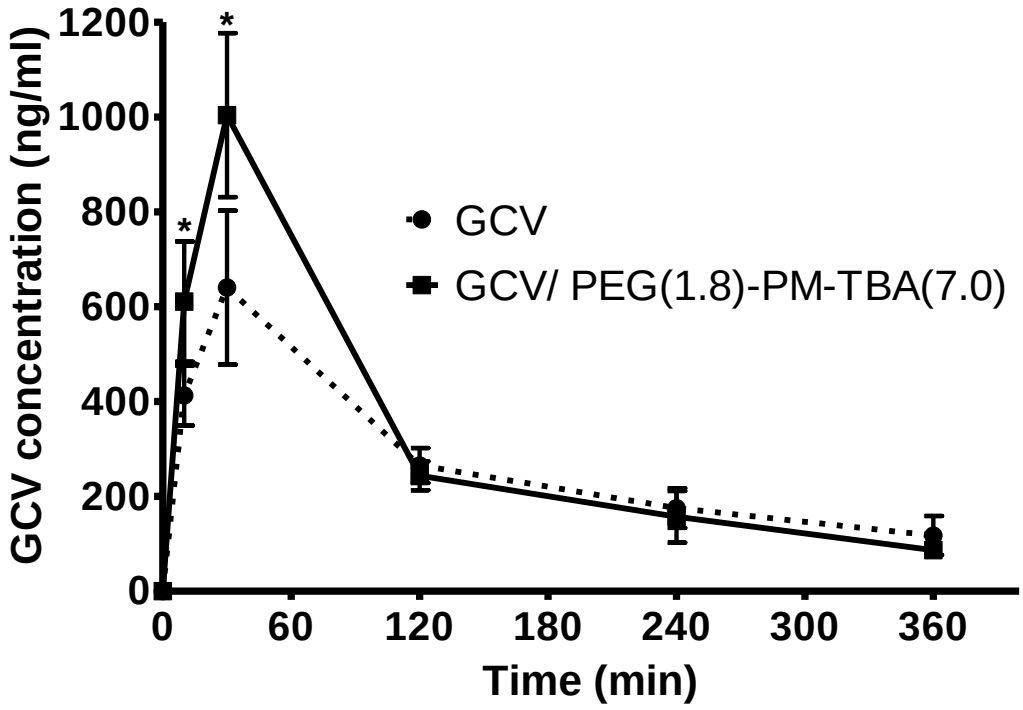

Figure 5.10. Plasma concentration-time curves of GCV after oral administration to mice at dose of 10 mg/kg. Data represent mean ± SEM of 4 independent experiments. * $p < 0.05$

Table 5.4 Plasma pharmacokinetic parameters of GCV after oral administration at dose of 10 mg/kg

Parameters*	GCV	GCV/ PEG(1.8)-PM-TBA(7.0)
AUC_{last} (min*ng/ml)	9.73×10^4	1.14×10^5
AUC_{inf} (min*ng/ml)	1.21×10^5	1.27×10^5
t_{max} (min)	30	30
C_{max} (ng/ml)	640.2	1004.1
$t_{1/2}$ (min)	142.4	100.9
MRT_{inf} (min)	211.5	138.8
$AUMC_{inf}$ (min*min*ng/mL)	2.57×10^7	1.76×10^7
Cl/F (mL/min/kg)	82.4	79.0
Vz/F (mL/kg)	1.69×10^4	1.15×10^4
Relative increase in bioavailability	--	17.2%

*Non-compartmental analysis was used to estimate the various pharmacokinetic parameters. In the calculations, first order elimination was assumed, and uniform weighting was used. Calculation and interpolation formulas are listed below:

$$\int_{t1}^{t2} AUC = (t2 - t1) \times \frac{C2 - C1}{\ln(\frac{C2}{C1})}$$

$$\int_{t1}^{t2} AUMC = (t2 - t1) \times \frac{t2 \times C2 - t1 \times C1}{\ln\left(\frac{C2}{C1}\right)} - (t2 - t1)^2 \times \frac{C2 - C1}{\ln(\frac{C2}{C1})^2}$$

$$AUC_{inf} = AUC_{last} + \frac{C_{last}}{\lambda_z}$$

$$MRT_{inf} = \frac{AUMC_{inf}}{AUC_{inf}}$$

$$t_{1/2} = \frac{\ln(2)}{\lambda_z}$$

$$\frac{Vz}{F} = \frac{Dose}{\lambda_z \times AUC_{inf}}$$

$$\frac{Cl(observed)}{F} = \frac{Dose}{AUC_{inf}}$$

5.4 Discussion

PAMAM dendrimers are originally developed by Tomalia in 1979[222, 223]. Owing to their open internal structures and cavities for forming drug complexes, PAMAM dendrimers have been the most extensively studied among the class of hyperbranched polymers for oral delivery purposes[224]. Previous studies have shown that PAMAM dendrimers could modulate tight junction integrity, as well as increase AUC of drugs via the formation of a drug-dendrimer complex[49, 50, 57, 58]. PAMAM dendrimers could exhibit different surface terminal groups, including amine-terminated, carboxyl-terminated and hydroxyl-terminated, with the amine-terminated PAMAM dendrimers showing the highest tight junction modulating effect[225]. However, these amine-terminated PAMAM dendrimers were relatively more toxic as compared to other terminal groups. Based on such prior findings, the aim of our current work is to surface modify amine-terminated PAMAM dendrimers with the combination of PEGylation and thiolation so as to decrease their toxicities and yet improve their abilities in overcoming the barriers of oral drug delivery, namely, P-gp drug efflux and tight junction. To our knowledge, combination of PEGylation and thiolation to surface modify PAMAM dendrimers is a strategy that has not been reported before. The effect of such surface modifications of PAMAM dendrimers will be discussed in view of PAMAM cytotoxicity, cellular accumulation and permeability across the intestinal epithelium.

5.4.1 Thiol Group Stability Study at various pH conditions

In oral delivery, one of the major challenges is the dramatic change of pH in GI tract. Drug and delivery excipients will experience highly acidic environment in the stomach (pH 1-4) followed by rapid increase to pH 6 in the duodenum. Then the pH will gradually increase in the small intestine from 6 to about 7.4 in the terminal ileum. Since the free thiol groups may be prone to oxidation and reduce the expected P-gp inhibitory effect, it is important to assess the stability of thiol groups under different pH conditions. When we subjected the dual-functionalized PAMAM dendrimers to different pHs using PBS buffered at pH 1.5, 4.0, 6.5 and 7.4, we observed the trend that the PEG might prevent oxidation of the thiol groups, especially when the pH was low (1.5 and 4.0). This might be attributed to the ability of the PEG chains on PAMAM surface to provide steric hindrance to reduce the interaction between the free thiol groups, when the dendrimers are dispersed in the aqueous PBS.

5.4.2 Cytotoxicity of functionalized PAMAM dendrimers

Establishing the cytotoxicity profiles of the dual-functionalized PAMAM dendrimers was the first question addressed in our study. The toxicity of PAMAM G4 has been attributed mainly to the interaction between the positively charged amine groups of PAMAM and the negatively charged cell membrane[50, 186]. As such, functionalizing the surface amines with small molecules or PEG chains has been attempted previously, whereby the toxicity of the PAMAM dendrimers was reduced by a masking effect of the amine terminals[224]. In this

study, increasing the number of PEG chains on the PEGylated PAMAM dendrimers (PEG(1.8)-PM and PEG(4.0)-PM) showed an improvement in PAMAM toxicity profile in Caco-2 and MDCK/MDR1 cells, which is an observation in line with those reported by *Jevprasesphant et al.* that four PEG chains could remarkably decrease the cytotoxicity of PAMAM[226]. In comparison, functionalizing the PAMAM dendrimers with TBA alone gave mixed results, whereby PAMAM toxicity was reduced in MDCK/MDR1 cells but not in Caco-2 cells. In line with the effect of masking the surface amines of PAMAM, dual functionalization of PAMAM with PEG and TBA showed the largest reduction in PAMAM cytotoxicity, as demonstrated in Figure 5.3. Although the dual-functionalized PAMAM dendrimers have significantly lower cytotoxicity, their ability to cross the intestinal epithelium, which suggests their potential to be systemically absorbed, could still pose safety concern since PAMAM is a non-biodegradable polymer. Minimal transport of the dual-functionalized dendrimers through the Caco-2 cell monolayer would be desirable. Results in Table 5.2 showed that the dual-functionalized dendrimers generally exhibited low transepithelial transport and cellular accumulation, suggesting low systemic toxicity potential for the dual-functionalized dendrimers as modulators of oral drug delivery.

5.4.3 Modulation of P-gp efflux by the dual-functionalized PAMAM dendrimers

The next question that we addressed in our study was the ability of dual-functionalized PAMAM dendrimers to overcome the two major barriers to oral

drug delivery, namely, P-gp efflux and tight junction. Previously, thiolation of linear polymers such as polyethyleneimine (PEI)[208], chitosan[179] and poly(acrylic acid) (PAA)[227] has imparted these polymers with enhanced inhibitory effect of P-gp efflux. Thus, thiolation of PAMAM dendrimers might present an approach that could be useful in improving the P-gp inhibitory effect of PAMAM. Indeed, from our results, the ability of thiolated PAMAM dendrimers to enhance cellular accumulation of the P-gp substrate R-123 was significantly increased as compared to unmodified PAMAM. PEGylation alone did not impart significant improvement in the ability of PAMAM to promote R-123 accumulation. Of note, when more PEG chains were functionalized onto the thiolated PAMAM dendrimers, R-123 accumulation and permeation was apparently reduced as we compared the P-gp inhibitory effect of PEG(1.8)-PM-TBA(7.0) and PEG(4.0)-PM-TBA(6.7). Such observation is in line with the steric hindrance effect of PEG chains that may interfere with the formation of covalent disulfide bonds between the thiolated dendrimers with the cysteine residues on P-gp[227].

5.4.4 Tight junction disruption of Caco-2 cell monolayer after exposure to dendrimer derivatives

In terms of tight junction modulating effect, assessment was made based on ZO-1 immunostaining, LY permeation and TEER measurement. Previously, unmodified PM G4.0 has been reported to be able to disrupt the tight junction proteins of Caco-2 monolayer [49]. In this study, surface modification with either PEG or TBA alone or with dual functionalization could improve the ability of PM

G4.0 to increase LY permeation after 24 h of exposure. This observation is in agreement with the studies by *Jevprasesphant et al.* [228] and *Kolhatkar et al.* [159] that surface modification with lauroyl groups and acetyl groups, respectively, could increase the permeation of mannitol in comparison to unmodified dendrimers. This increase in mannitol permeation has been suggested to be a result of the combined effect of paracellular and transepithelial permeation pathways [224]. The collective data from Figures 5.5 – 5.8 and Table 5.2 seem to suggest that the paracellular pathway might be the dominant pathway by which the dual-functionalized dendrimers have acted, as cellular accumulation and basolateral transport of the dual-functionalized dendrimers was low. While tight junction disruption was observed in the surface modified PAMAM dendrimers, such effect was irreversible for PAMAM dendrimers modified with PEG or TBA alone. As intact tight junction is important to cell survival of the intestinal epithelium, irreversible disruption of the epithelial tight junction would be a sign of potential toxicity [229]. Such finding is also in agreement with our cytotoxicity study that dual-functionalized dendrimers showed much lower toxicity to Caco-2 cells as compared to other dendrimer samples.

5.4.5 Effect of dual functionalized dendrimer on pharmacokinetic profile of ganciclovir

With P-gp inhibitory and tight junction modulating effect demonstrated in vitro settings, PEG(1.8)-PM-TBA(7.0) was further selected to test whether this polymer could improve drug absorption in vivo. Ganciclovir (GCV), an acyclic 2'-deoxyguanosin analogue, was selected as the model drug. GCV is indicated in

the treatment of primary and recurrent genital Herpes simplex virus (HSV) [230]. Despite the excellent antiviral activity of GCV against the herpes family of viruses, GCV has low permeability across intestinal epithelial cells [231]. Oral bioavailability of GCV is only about 5% [232] since GCV is a P-gp substrate [233] and it has poor lipophilicity (logP = −1.65). Meanwhile GCV is not metabolized in the intestine and liver by CYP enzymes [234]. Therefore, GCV is selected as a model drug in this study to evaluate the effect of dual functionalized dendrimer on bioavailability of compound with low permeability and suffered from P-gp efflux effect.

The result in this study showed that the C_{max} and AUC_{last} of GCV/ PEG(1.8)-PM-TBA(7.0) group increased by 56.8% and 17.2% compared to GCV group, respectively. Such results indicates that PEG(1.8)-PM-TBA(7.0) improved the absorption of GCV. Figure 5.10 showed the concentration-time curves of GCV after drug administration. The result indicates that PEG(1.8)-PM-TBA(7.0) quickly increased drug absorption in the initial 30 min. The improved drug absorption could be attributed to the P-gp inhibitory effect and tight junction modulation based on the positive findings from the in vitro studies. Previously *Shen et al.* studied the effect of Labrasol (caprylocaproyl macrogol-8 glyceride) on the oral absorption of ganciclovir in rat [233]. The result showed that Labrasol at 0.1% (v/v) significantly enhanced absorption of GCV after oral administration to rats. The C_{max} increased from 3.05 to 5.29 μg/ml and the AUC increased by 1.8-fold. It is proposed by the authors that such improvement was due to

increased intestinal permeability by tight junction opening and P-gp inhibitory effect.

5.5 Conclusion

Based on a balance of acceptable cytotoxicity, cellular accumulation and permeability, the dual-functionalized PAMAM dendrimer, PEG(1.8)-PM-TBA(7.0), seems to be the most promising as a modulator of intestinal epithelial barrier. PEG(1.8)-PM-TBA(7.0) displayed low cytotoxicity in Caco-2 and MDCK/MDR1 cells, while significantly increased cellular accumulation and permeation of the P-gp substrate R-123 as well as reversibly disrupted tight junction integrity shown via TEER measurement over time. This dual functionalized dendrimer also improved oral absorption of GCV as demonstrated by in vivo pharmacokinetic study. Taken together, dual functionalization via PEGylation and thiolation represented a novel and promising approach in altering PAMAM dendrimer surface for potential application as oral delivery modulators.

CHAPTER 6. DENDRIMER-LIPID HYBRID NANOSYSTEM AS A NOVEL DELIVERY VEHICLE FOR PACLITAXEL

6.1 Introduction

In the previous chapter, potential application of surface modified dendrimers in oral drug delivery was explored. Besides surface conjugation, physical complexation is another commonly applied method to modify the physicochemical properties of dendrimers so as to achieve desirable features for applications in drug delivery [235-238].

Since dendrimers, especially cationic ones, can interact with cellular membranes and alter the structure and integrity of the membranes, there are studies to further explore the mechanism of dendrimer and lipid membrane interaction. Atomic force microscopy (AFM) studies of rat1 cell lines and MDCK cells showed that PAMAM G7 dendrimers caused hole formation with diameter of 15-40 nm in cell membranes [239-241]. Liposomes are also employed as tools to investigate the interaction between dendrimer and lipid bilayer. After dendrimer adsorb on the surface of lipid layers and disrupt the bilayer structure, small vesicles were formed [242, 243]. Such vesicles were proposed to be composed of dendrimer surrounded by lipids [243]. These studies indicate that such nano-scale vesicle formed by dendrimer and lipids could be a novel delivery vehicle in pharmaceutical application.

Kwok et al. studied peptide dendrimer/lipid hybrid system as DNA transfection reagents. It was found that addition of lipid components (DOTMA/DOPE) to the

dendrimer-DNA complexes result in a more compact nanoparticle with size between 38 and 50 nm. Moreover, the enhancement of transfection efficiency was increased by 30 to 50-fold compared to dendrimer/DNA complexes alone [244]. There are also a few studies exploring combination of dendrimer and lipids for drug encapsulation and delivery. Generally, the drug encapsulation and release profiles are improved in the formulation containing both dendrimer and liposome. *Khopade et al.* used PAMAM dendrimers with amine surface groups to increase encapsulation of methotrexate (MTX) in liposomes [245]. The drug loading increased as PAMAM generation increased from generation 2 to 4. For the formulation with PAMAM G4, MTX release in 8 h was reduced by ~2.5-fold compared to liposome formulation. In another study, *Papagiannaros et al.* studied encapsulation of doxorubicin-PAMAM dendrimer complex in liposomes [246]. Similarly, Gardikis et al. prepared liposomal locked-in dendrimers (LLDs) nanosystem as carrier of doxorubicin [247]. Both studies demonstrated improved drug loading and slowed drug release profile in the dendrimer-lipid vesicle formulations. In summary, formulation composed of dendrimer and lipids could be a promising formulation to improve drug encapsulation and modified release properties in drug delivery applications.

Paclitaxel (PTX), a mitotic inhibitor, is widely used in cancer chemotherapy. A big challenge to delivery PTX was related to the hydrophobic nature of this compound. Current commercially available i.v. formulation of PTX is composed of Cremophor EL (polyoxyethyleneglycerol triricinoleate 35) in 50% ethanol. Cremophor EL is found to induce hypersensitivity reactions and complement

activation in clinical application [248-250]. It is also known to be responsible for the nonlinear tissue distribution of PTX [251]. Thus, it is still necessary to develop novel formulation system for PTX so as to replace Cremophor EL. There are a few studies to utilize dendrimer as drugdelivery vehicle. Zhou et al. synthesized poly(butylenes oxide) (B)-poly(ethylene oxide) (E)-PAMAM G2 linear-dedritic copolymer (BE-PAMAM) [252]. The solubility of PTX was increased 3700-fold by micellar encapsulation in a 2% (w/v) BE-PAMAM copolymer. A sustained release of 60% PTX from BE-PAMAM copolymeric micelle was observed after 24 h of dialysis. The same research group prepared lauryl chains conjugated PAMAM G3 to delivery PTX. In this study, PTX was covalently conjugated on PAMAM dendrimer [253]. The dendrimer conjugated PTX showed signicantly higher toxicity on Caco-2 and PBECs cells. The permeability of the drug-dendrimer conjugates across both cell monolayers were also improved in both directions, indicating penetration enhance effect of dendrimer on PTX. This chapter will explore the potential application of dendrimer-lipid hybrid nanosystem as a delivery vehicle of PTX and evaluate the therapeutic effect of such system for the treatment of ovarian cancer.

6.2 Materials and Methods

6.2.1 Materials

1,2-dipalmitoyl-s*n*-glycero-3-phosphocholine (DPPC) was purchased from Avanti-Polar-Lipids® (Alabaster, AL, USA). PAMAM G4.0-NH_2 was purchased from Dentritech® Inc (Midland, MI, USA). Paclitaxel (PTX) was purchased from

the Beijing Earlybird Industry Development Co. Ltd. (Beijing, China). 3-(4,5-dimethylthiazolyl-2)-2,5-diphenyltetrazolium bromide (MTT) and dimethyl sulfoxide (DMSO) were purchased from MP Biomedicals Inc (Singapore). All other chemicals were obtained from Sigma-Aldrich (Singapore) unless otherwise stated.

6.2.2 Preparation of the Dendrimer-lipid hybrid nanosystem

20 mg DPPC was dissolved in chloroform. 450 µl PAMAM dendrimer stock solution (50 mg/ml in methanol) and 554 µl Paclitaxel stock solution (5 mg/ml in methanol) were added to DPPC solution (molar ratio of DPPC / PAMAM / PTX is 86:5:9). The solvent was evaporated under a stream of nitrogen gas to obtain a dried thin film. The residual solvent was further removed in vacuum for 4 h. Then, 2.43 ml of pre-warmed (55 ℃) Hank's balanced salt solution (HBSS) was added in the tube to form hybrid system. The hydrated hybrid suspension was stirred for 1 h at 55 ℃ followed by 2 h sonication. The unincorporated paclitaxel and DPPC lipid were removed by centrifugation at 3000 rpm for 3 min. Empty hybrid system was prepared in the same way without PTX.

6.2.3 Size, zeta potential and morphology characterization

The prepared hybrid nanosystem was diluted 50× in HBSS for particle size and zeta potential measurement. The hydrodynamic diameter and zeta potential of the sample were analyzed by Zetasizer Nano-ZS90 (Malvern. Instruments GmbH Herrenberg. Germany). Morphology of hybrid nanosystem was observed via

cryogenic transmission electron microscopy (Cryo-TEM) (JEOL JEM 2010F TEM, JOEL Ltd, Tokyo, Japan).

6.2.4 DPPC Lipid quantification

Lipid concentration was quantified by phophate assay as previously described [254]. 20 µl of diluted hybrid nanosystem or standard solution (0-2 mM Na2HPO4 solution) was added to 700 µl perchloric acid and heated at 190 ℃ for 1 h. After cooling to room temperature, 700 µl Fiske's solution and 7 ml ammonium molybdate solution were added to the sample and heated at 100 ℃ for 20 min. The solutions were cooled to room temperature and measured using UV spectrometry at 830 nm (Tecan Infinite™ 200, Tecan Trading AG, Switzerland). Lipid concentration was calculated from the standard curve of Na_2HPO_4 serial dilutions. Recovery yield% was calculated as follows:

$$Recovery\ yield\% = C_{final} / C_{initial} \times 100\%$$

where C_{final}, $C_{initial}$ represent lipid concentration from hybrid sample or initally added in the formulation.

6.2.5 Paclitaxel quantification

10 µl hybrid stock solution was diluted to 1 ml methanol. Empty hybrid stock solution was used as control for hybrid sample. A standard solution of PTX was prepared at concentration range from 0-25 µg/ml. Absorbance at 230 nm was measured by UV spectrometry (UV-1700, UV-visible spectrophotometer, Shimadzu, Pharmaspec, Kyoto, Japan). PTX concentration was calculated from

the standard curve of PTX serial dilutions. Recovery yield% was calculated as described in section 6.2.4.

6.2.6 PAMAM dendrimer quantification

The concentration of PAMAM dendrimer was quantified based on a previously described method [255].8 µl hybrid sample was diluted in 1000 µl methanol solution. Standard solution of PAMAM was prepared at concentration range from 0-0.2 mg/ml. The following solutions were added to the samples sequentially, (a) 800 µl of 200 mM sodium tetraborate buffer, pH 10, (b) 40 µl of 30 mg/ml phthaldiadehyde (OPA) in ethanol, (c) 40 µl of 30 mg/ml N-acetyl-d-penicillamine in methanol. The mixture was incubated at 50℃ for 3 hours to complete analyte derivatization. Absorbance was measured by UV spectrometry at 330 nm. Since PTX and DPPC lipid do not have primary amine groups in the structure, the presence of both compounds does not interfere with the reaction and analysis. PAMAM concentration was calculated from the standard curve of PAMAM serial dilutions. Recovery yield% was calculated as described in section 6.2.4.

6.2.7 In vitro PTX release study

The PTX hybrid nanosystem was diluted with HBSS to a PTX concentration of 140 µg/ml. 8 ml of the sample was transferred to a Slide-A-Lyzer 3.5K dialysis cassette. The cassette was placed in 1000 ml PBS at 37℃ with stirring. 200 µl of sample was withdrawn at specific time intervals from top side of the dialysis cassette. During the experiment, no obvious precipitation of paclitaxel was

observed in the dialysis cassette. If paclitaxel were released and aggregated in aqueous solution, it is likely to be released out to the container or precipitated in the bottom of the cassette. Since samples were withdrawn from top of the cassette, the measured concentration of paclitaxel should indicate the amount of paclitaxel remained stable inside the hybrid nanosystem. PTX concentration was determined as described in previous section. The cumulative percentage of drug released was calculated as follows:

$$PTX\ release\% = (C_{initial} - C_t) / Cinitial \times 100\%$$

where $C_{initial}$, C_t represent the concentration of PTX at time 0 and at time t.

Then the PTX release data were fitted into various mathematical models for drug release kinetics, including 0 order model, 1st order model, 2nd order model, Higuchi model, Peppas-Sahlin model, and Alfrey model. The equations of these models are listed as follows:

$C_t / C_{initial} = k \times t$	zero order
$ln\ [C_{initial}] = -k \times t + ln\ [C_t]$	1st order model
$1 / C_{initial} = 1 / C_t + k \times t$	2nd order model
$C_t / C_{initial} = k \times t^{1/2}$	Higuchi model [256]
$C_t / C_{initial} = k_1 \times t^m + k_2 \times t^{2m}$	Peppas-Sahlin model [257]
$C_t / C_{initial} = k_1 \times t + k_2 \times t^{1/2}$	Alfrey model [258]

where $C_{initial}$, C_t represent the concentration of PTX at time 0 and at time t.

$C_t = Plateau + SpanFast \times e^{(-KFast \times t)} + SpanSlow \times e^{(-KSlow \times t)}$ two exponential decay model

where $SpanFast=(C_0 - Plateau) \times PercentFast \times 0.01$

$SpanSlow=(C_0 - Plateau) \times (100-PercentFast) \times 0.01$

6.2.8 Cell Culture

IGROV-1 cell line was a generous gift from Professor Larry H. Matherly (Wayne State University, School of Medicine, USA), and was maintained in RPMI-1640 media supplemented with 10% FBS, 100 units/ml penicillin and 100 μg/ml streptomycin. Cells were grown in T-75 cm^2 flasks in a humidified atmosphere containing 5% CO_2 at 37 ℃.

6.2.9 Cell viability assay

Briefly, IGROV-1 cells were seeded in 96-well plates at 5000 cells/well overnight before exposure to treatment. Then, the cells were exposed to various fixed concentrations of samples for either 24 h at 37 ℃ in the CO_2 incubator. After the treatment, MTT was added to the cells at a final concentration of 0.2 mg/ml for 4 h at 37 ℃. Then the culture medium was removed from each well and 150 μL DMSO was added to solubilize the purple formazan precipitate for 10 min in dark. Measurement of absorbance was performed at 570 nm. Cell viability was determined as follows:

$Cell\ viability\% = (abs_{test} - abs_{blank}) / (abs_{vehicle} - abs_{blank}) \times 100\%$

where abs_{test}, abs_{blank} and $abs_{vehicle}$ represent the absorbance reading of tested cells, blank control and vehicle control, respectively.

Data obtained from the MTT assay were subject to median effect analysis using the CalcuSyn® software (version 2, Biosoft, Cambridge, UK). The Combination Index (C.I.) was computed by the following equation:

$$C.I. = [(D)_1 / (Dx)_1] + [(D)_2 / (Dx)_2]$$

where D_1 and D_2 represent doses of drug 1 and drug 2, respectively, used in the combination to induce a defined effect (e.g. 50% cell death). $(Dx)_1$ and $(Dx)_2$ represent the doses of drug 1 and drug 2, respectively, required to have the same effect when the two drugs were administered as single agents. C.I. < 1, ~ 1 and > 1 represent synergistic, additive and antagonistic effects for a drug combination, respectively [259].

6.2.10 Cellular uptake study

IGROV-1 cells were seeded in 4-well Lab-tek chamber glass slides from Nalge Nunc Inc (Naperville, IL) at density of 2×10^4 cells/well and cultured for 5 days before experiment. Cells were exposed to hybrid nanosystem with 10% FITC labelled PAMAM and 5% Di-I for 4 h or 24 h at 37 ℃. Then, cells were washed with HBSS for three times and viewed under a Carl Zeiss fluorescence confocal microscope using 40 × objective (Carl Zeiss Jena, Germany).

6.2.11 In vivo therapeutic efficacy study

All animal studies were completed using protocols approved by the Institutional Animal Care and Use Committee (IACUC) of National University of Singapore. CB17/Icr-Prkdc^{scid}/IcrCrl (SCID) mice were purchased from Invivos Pte Ltd (Singapore). Mice were acclimatized for 7 days before intraperitoneal inoculation of 5×10^6 IGROV-1 ovarian cancer cells. After 14 days of tumor cell inoculation, mice were randomly divided into 4 groups, and were injected intravenously with (1) 0.9% saline (1/week×3 times), (2) free PTX at 2 mg/ml (20mg/kg × 1/week × 3 times), (3) PTX loaded hybrid nanosystem at 0.2 mg/ml (2mg/kg × 1/week × 2 times), (4) empty hybrid nanosystem (equivalent dilution as PTX loaded hybrid nanosystem × 1/week×2 times). Drug regimens were given on day 14, day 21 and day 28. General condition, body weight, and survival of the mice were monitored daily. Mice were euthanized if they developed any of the following symptoms: weight loss > 20%, scruffy coat, hunched appearance, and moribund state, and death was defined as the day following euthanization. The endpoint of the study was stipulated at 60 days post tumor cell inoculation according to the approved animal protocol. Mice surviving until the end of the efficacy experiment were termed as long term survivors (LTS) and euthanized accordingly. After euthanization, the tumor tissues in abdomen were collected and weighed.

6.2.12 Statistical analysis

All data were reported as mean ± standard error of the mean (SEM). Statistical differences were determined using the Student t-test or one-way ANOVA with

Newman-Keuls test for post-hoc multiple comparisons. Survival curves were plotted according to the Kaplan–Meier method, and the log-rank test was used to determine significant differences among groups. P values of < 0.05 were considered to be statistically significant.

6.3 Results

6.3.1 Physicochemical characterization of dendrimer-lipid hybrid nanosystem

The dendrimer-lipid hybrid nanosystem was prepared by a 5-step procedure: physical mixing, organic solvent evaporation, hydration, sonication and centrifugation (Figure 6.1). Size and zeta potential data are shown in Table 6.1. For PTX-PM and PTX-DPPC system, the particle size was 863 ± 121 nm and 626 ± 64 nm, much larger than the hybrid nanosystem. PDI was also increased for PM only or DPPC only preparations, indicating large and non-uniform size distribution. Moreover, obvious precipitations were observed for PTX-PM and PTX-DPPC samples, indicating instability of such preparation with dendrimer or lipid only. However, if the dendrimer and lipids were put together to form the hybrid nanosystem, the particle size of hybrid nanosystem was much smaller (30-40 nm). Encapsulation of PTX did not change the particle size of the hybrid system. The zeta potentials of all these preparations were near neutral values. The morphology of hybrid nanosystem was further observed under Cryo-TEM as shown in Figure 6.2. The hybrid nanosystem exhibited spherical, vesicular morphology with denser signal in the external areas than internal cavity. In line

with the size data, the particle size was <50 nm as observed from the cryo-TEM images.

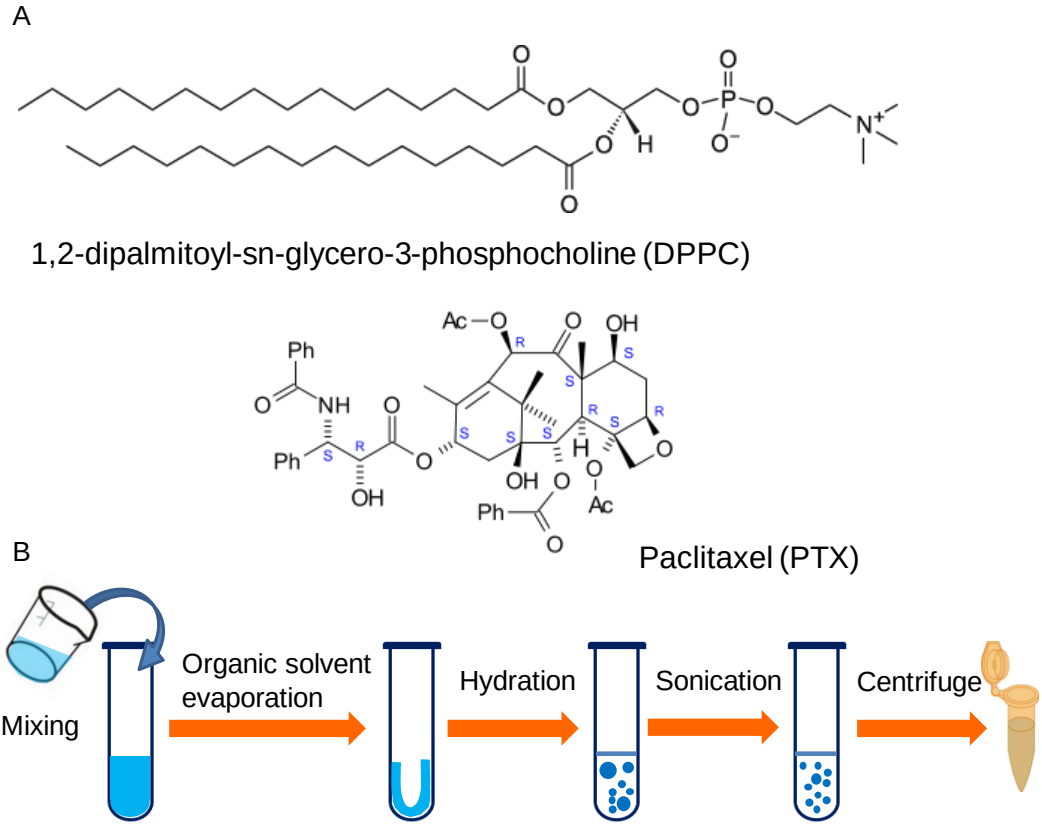

Figure 6.1. (A) Chemical structure of DPPC and PTX. (B) Preparation process of dendrimer-lipid hybrid nanosystem.

Table 6.1. Size and zeta potential characterization

	Size (nm)	Zeta potential (+mV)	PDI
PTX-Hybrid[a]	37.6 ± 6.9	2.5 ± 0.1	0.58 ± 0.03
Empty-Hybrid[b]	36.8 ± 3.0	2.9 ± 0.2	0.55 ± 0.08
PTX-PM[c]	863 ± 121	1.3 ± 0.1	0.77 ± 0.14
PTX-DPPC[d]	626 ± 64	5.1 ± 0.9	0.84 ± 0.16
PM (no PTX)[e]	4.3 ± 0.4	30.1 ± 0.9	0.40 ± 0.08

[a] PTX encapsulated hybrid nanosystem
[b] Empty hybrid nanosystem prepared without PTX encapsulation
[c] Formulation of PTX and PAMAM dendrimer with the same preparation process as hybrid nanosystem
[d] Formulation of PTX and DPPC lipid with the same preparation process as hybrid nanosystem
[e] PAMAM dendrimer without loading PTX

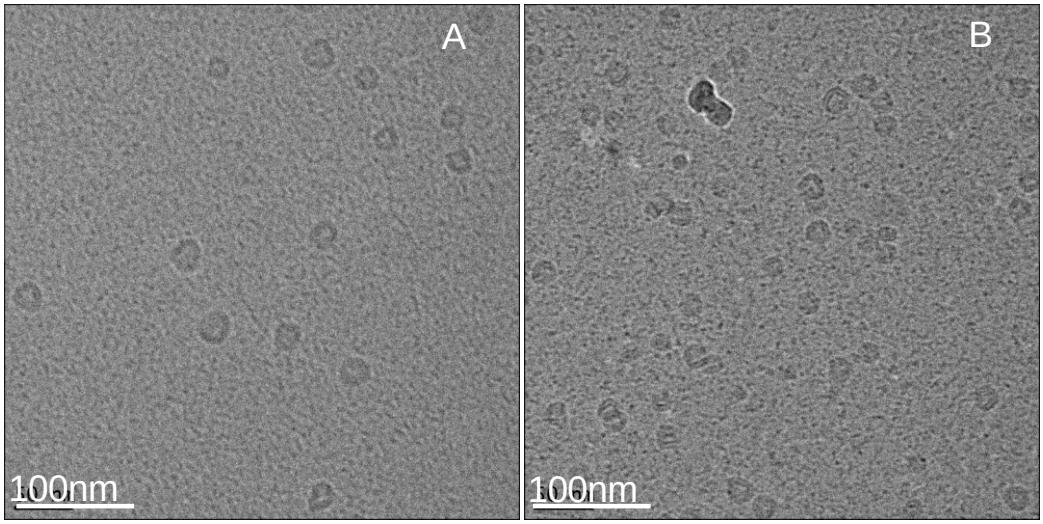

Figure 6.2. Representative Cryo-TEM images of (A) PTX loaded hybrid system, (B) Drug free hybrid system. The experiments were repeated twice, each time with a minimum of three views of the same sample was captured.

The recovery of PM dendrimer, DPPC lipid and PTX in each system was quantified and presented in Figure 6.3. Both DPPC and PM had >80% of recovery in hybrid nanosystem (Figure 6.3 (A) and (B)). In comparison, for

DPPC only or PM only preparation, the recovery of DPPC or PM was relatively lower than in hybrid nanosystem. Importantly, PTX recovery in hybrid nanosystem was about 80%, significantly higher than the PTX recovery in PM only or DPPC only formulation. Thus, the precipitation observed in the centrifuge step was mainly composed of PTX. This result also indicated that combination of PM and DPPC could significantly increase encapsulation of PTX in the hybrid nanosystem than the preparation with a single excipient.

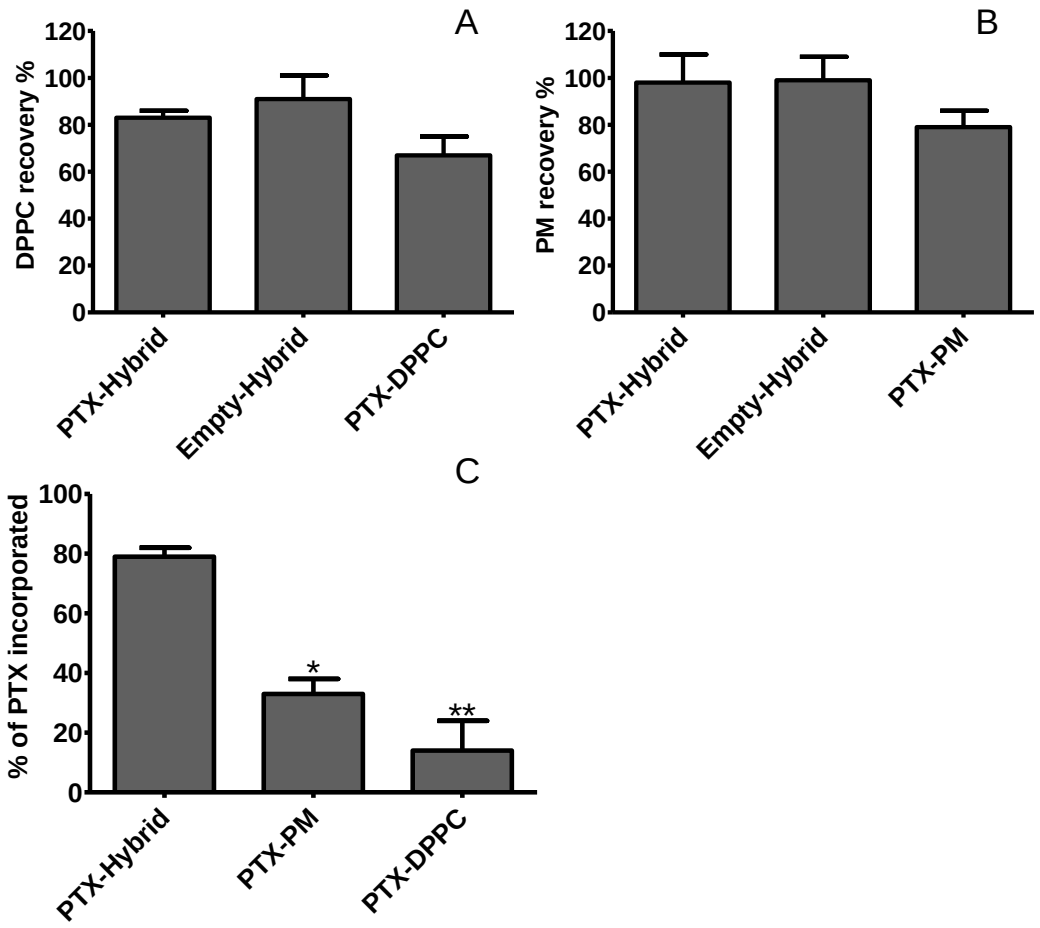

Figure 6.3. Recovery yield (%) of (A) DPPC lipid, (B) PM dendrimer and (C) Percentage of PTX incorporated in hybrid nanosystem, PM only, or DPPC only formulation, respectively. Data are expressed as mean ± SEM of 3 independent experiments. * $p < 0.05$, ** $p < 0.01$

6.3.2 In vitro PTX release study

The in vitro PTX release profile was studied over a 24 h period at 37 ℃ in PBS (Figure 6.4). Majority of PTX (>95%) was released from hybrid nanosystem within 24 h. The release data was fitted to several commonly used drug release kinetic models as shown in figure 6.4. PTX release from hybrid nanosystem fitted best in second order model with R^2 = 0.9968. An important property of second order release is that half-life is related to the initial concentration:

$$t_{1/2} = 1 / (k \times C_0)$$

where the $t_{1/2}$, k, C_0 represents half-life, slope of the regression curve, and initial concentration, respectively.

According to the half life equation, the drug will release faster in the initial stage, when the drug concentration is relatively higher in the carrier. As the drug concentration decreases, the half life becomes slower accordingly.

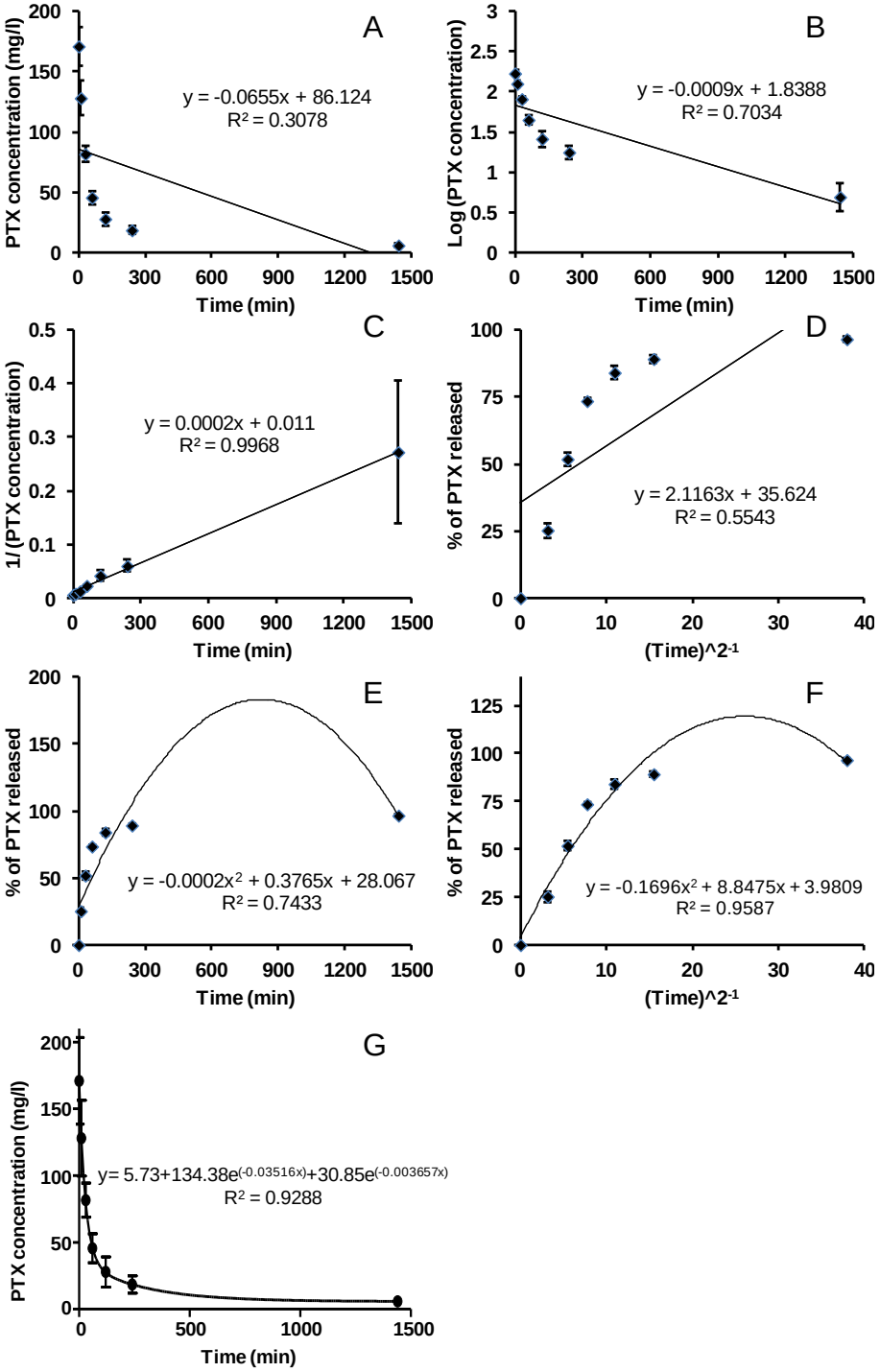

Figure 6.4. PTX release profile in different release models. (A) 0 order model, (B) 1st order model, (C) 2nd order model, (D) Higuchi model, (E) Peppas-Sahlin model, (F) Alfrey model (G) two exponential decay model.

6.3.3 Cytotoxicity of PTX loaded hybrid nanosystem on IGROV-1 cells

Next, the inhibitory effect of PTX on human ovarian cancer cell line IGROV-1 cells was evaluated in vitro. The purpose of this study was to evaluate whether the hybrid nanosystem would have any influence on the biological activity of PTX. Cell viability after 24 h treatment with either PTX or PTX in hybrid nanosystem was shown in Figure 6.5. The PTX in hybrid nanosystem showed improved inhibitory effect against IGROV-1 cells. The IC_{50} of PTX-Hybrid was 2.43 ± 1.23 μg/ml, significantly lower than the IC_{50} of free drug PTX (88.51 ± 15.11 μg/ml), indicating improved therapeutic effect of PTX in the hybrid system. The IC_{50} of empty hybrid nanosystem was more than 280 fold higher than the PTX-Hybrid nanosystem. In comparison, PTX was conjugated to PAMAM G4 with hydroxyl terminal groups. The cytotoxictiy of PTX was enhanced by 10-fold on A2780 human ovarian cancinoma cells. Additionally, aqueous solubility of PTX was improved to 3.2 mg/ml [260].

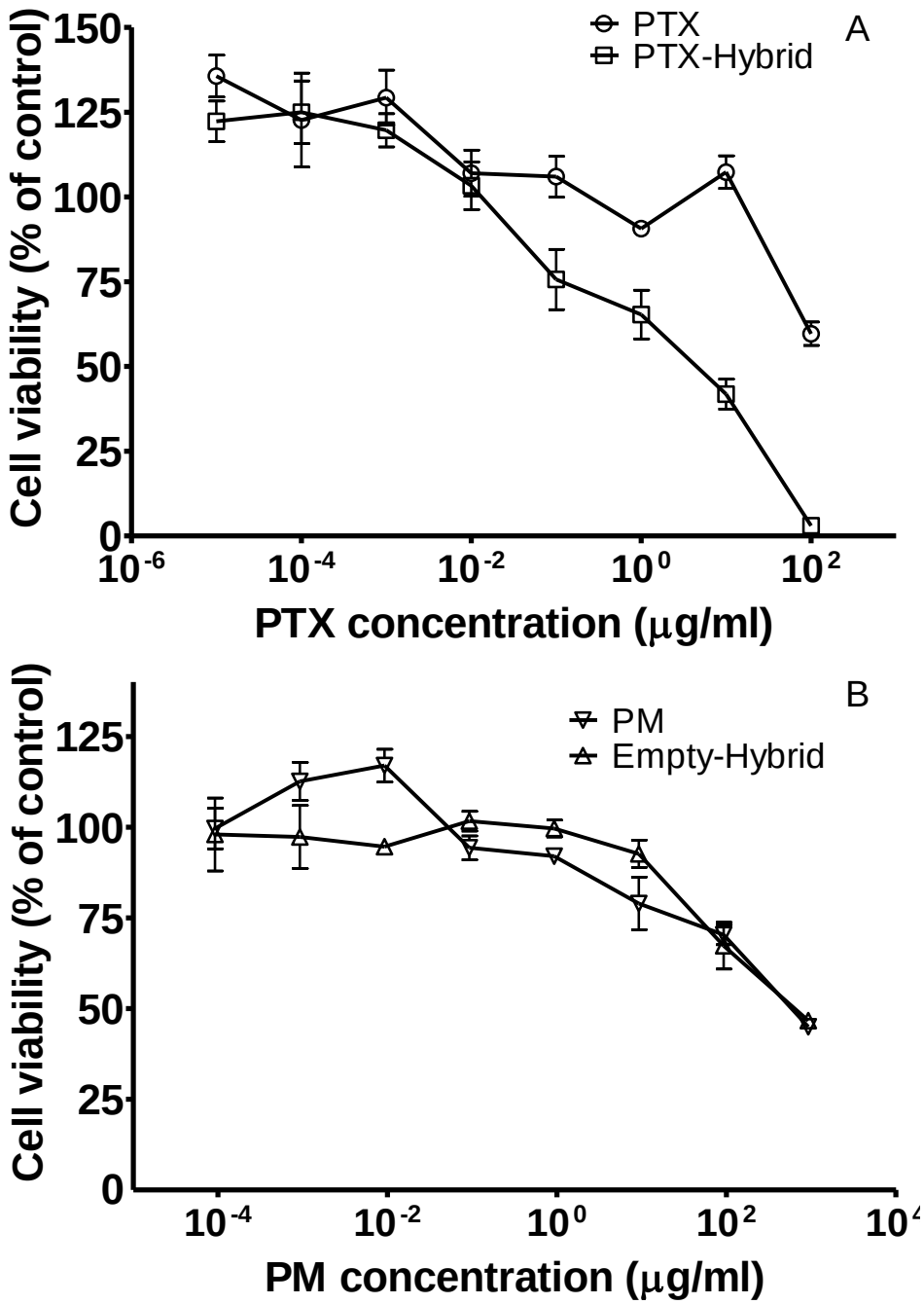

Figure 6.5. IGROV-1 cell viability after 24 h treatment with (A) PTX and PTX-Hybrid, (B) PM and Empty-Hybrid nanosystem. Data are expressed as mean ± SEM of at least 3 independent experiments.

Since the PTX-Hybrid nanosystem release majority of PTX within 24 h, according to the in vitro PTX release study shown in section 6.3.2, this might be a

reason for the improved cellular inhibitory effect on IGROV-1 cells. Next, the possible synergistic effect of PTX and PM in the hybrid nanosystem was assessed based on the 24 h IC_{50} data. The combination index was calculated and presented in Table 6.2. Interestingly, the combination index of PTX-Hybrid versus Empty-Hybrid alone was 0.05, indicating that PTX and PM have synergistic effect in the hybrid nanosystem.

Table 6.2. IC_{50} and combination index (CI) of 24 h cytotoxicity study on IGROV-1

	IC_{50} (μg/ml)
PTX-Hybrid	2.43 ± 1.23
PTX	88.51 ± 15.11
PM	697.27 ± 189.32
Empty-Hybrid	1059.33 ± 335.42
	CI at ED_{50}*
PTX-Hybrid vs Empty-Hybrid alone or PTX alone	0.05

*ED_{50}: median effective dose

6.3.4 Cellular uptake study of hybrid nanosystem

In order to further understand the distribution of such hybrid nanosystem in cellular environment, cellular uptake study of hybrid nanosystem was examined in IGROV-1 cells. FITC labeled PM dendrimers emitted green fluorescent signal and Di-I emitted red fluorescent signal under confocal fluorescent microscope. The imaging result after 4 h and 24 h incubation with the dye labeled hybrid nanosystem was shown in Figure 6.6. The FITC-PM was mainly accumulated inside the cells while Di-I was mainly localized in peripheral areas. As incubation

time increased from 4 h to 24 h, the increased signal indicates time dependent accumulation in cells. Such observation is in line with previous reports that PM dendrimer was able to disrupt the cell membrane and internalize inside the cells [240]. Such result might explain the improved inhibitory effect of PTX-Hybrid system. When the hybrid nanosystem gets contact with cell membranes, positively charged PM dendrimer disrupts cellular membrane and promotes hole formation, which makes it easier for PTX to be localized inside the cells. Meanwhile, dendrimer itself also internalizes inside the cells and damage the cells as described previously [145-147]. Thus, the PTX-Hybrid nanosystem has synergistic inhibitory effect.

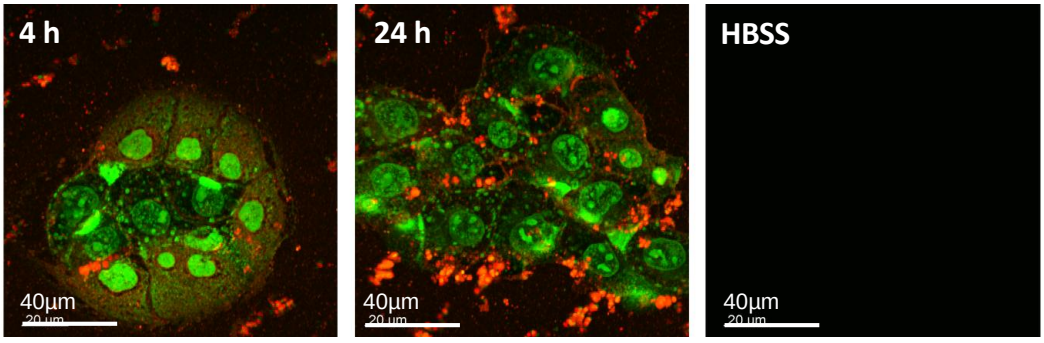

Figure 6.6. Cellular uptake of hybrid nanosystem with 10% FITC labeled PM and 5% Di-I for 4h or 24h. The experiments were repeated twice, each time with a minimum of three views of the same sample was captured.

6.3.5 In vivo therapeutic efficacy study on IGROV-1 ovarian tumor inoculated SCID mice

The therapeutic efficacy of PTX or PTX in hybrid nanosystem was evaluated in the intraperitoneally grown, human IGROV-1 ovarian tumor xenograft model as reported previously [261]. All mice were inoculated with 5×10^6 IGROV-1

ovarian cancer cells intraperitoneally and kept for 14 days before the treatment. The inoculated mice were then randomized into four study groups: saline control, free PTX, empty hybrid and PTX in hybrid nanosystem. The dose of free PTX was 20 mg/kg, which was the maximum tolerated dose (MTD). PTX-Hybrid was given at 2 mg/kg which was the max tolerated dose. Kaplan-Meier Survival analysis result was summarized in Figure 6.7 (A). Both PTX and PTX Hybrid group significantly improved mice survival compared to saline control group ($p<0.05$). Although no significant difference was observed in Kaplan-Meier survival curves for PTX and PTX Hybrid group ($p = 0.059$), it is worth to note that PTX Hybrid was given at 10-fold lower dose than free PTX. Moreover, PTX Hybrid treatment significantly prolonged both median survival time (42 d) and mean survival time (46.3 d) compared to all the other three groups as shown in Table 6.3.

Animal body weight was monitored over the study period as an indicator of the general well-being of the animals during treatment. The percentage body weight change was shown in Figure 6.7 (B). The animals showed more than 10% body weight loss upon treatment. Such body weight loss might be due to treatment related toxicity as well as tumor deterioration. Taken together, PTX in hybrid nanosystem was effective in prolonging the survival of the animals at dose 10-fold lower than the free PTX.

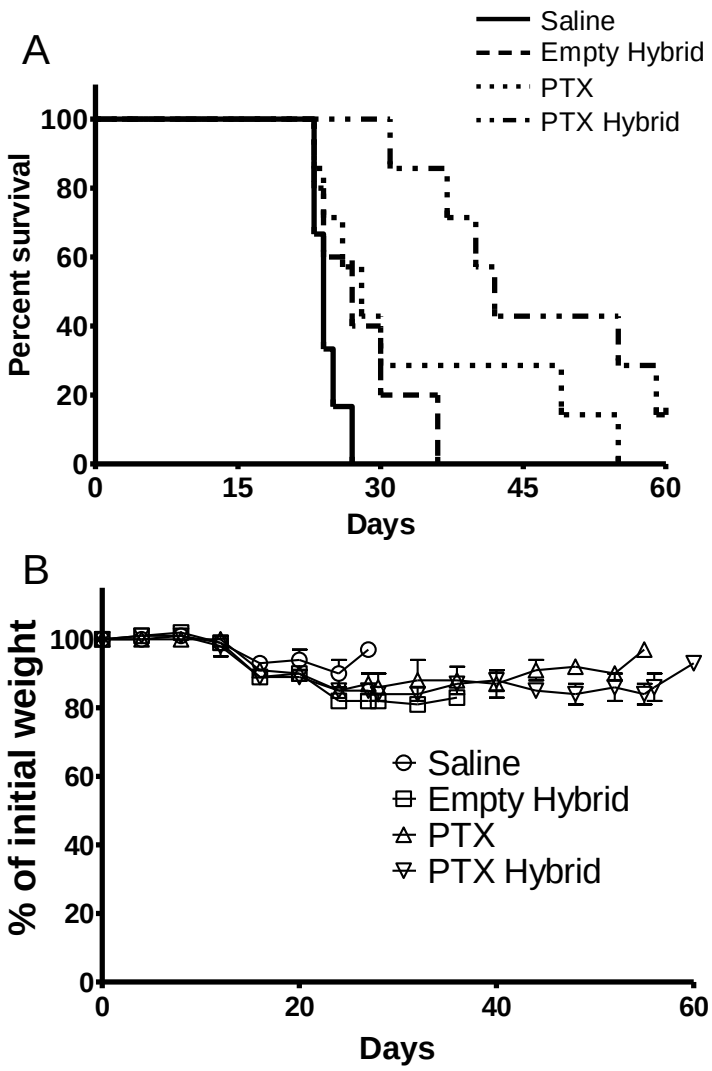

Figure 6.7 In vivo efficacy of PTX as free drug or in hybrid nanosystem in human IGROV-1 intraperitoneal ovarian tumor xenograft model. (A) Kaplan-Meier survival curves for saline, empty hybrid, free PTX and PTX-Hybrid. Drug treatment started 14 days post tumor cell inoculation. (B) Animal body weight change for different treatment groups.

Table 6.3. Comparison of mean and median survival

	Mean survival time (Days)	Median survival time (Days)	Survivors at day 60
Saline	$24.3 \pm 0.6^{**}$	$24 \pm 0.6^{***}$	0/6
Empty-Hybrid	$28 \pm 2.3^{**}$	$27 \pm 3.3^{**}$	0/5
PTX	$33.6 \pm 4.9^{*}$	$28 \pm 2.6^{***}$	0/7
PTX Hybrid	46.3 ± 4.0	42 ± 2.6	1/7

* $P < 0.05$, ** $P < 0.01$, *** $P < 0.001$ compared to PTX Hybrid

6.4 Discussion

6.4.1 Formation of dendrimer-lipid hybrid nanosystem

Dendrimers are known to interact with cell membrane lipids and disrupt the membrane structure on a size and charge dependent basis. Previous studies have investigated the interaction between dendrimer and lipid bilayers and their results showed that cationic dendrimers could form holes on the bilayer surface and may remove lipids from it [262-266]. These studies formed the basis to form such dendrimer-lipid hybrid nanosystem.

Gardikis et al. examined the incorporation of PAMAM G4 and G3.5 in DPPC bilayers by DSC and Raman spectroscopy method. The result showed that the maximum 5 mol% PAMAM G4 and 3.5 mol% G3.5 can be incorporated into the multilamellar liposomes [267]. Thus, 5 mol% of PAMAM dendrimer was used to prepare hybrid nanosystem in this study. The molar percentage of PTX was tested from 1.5 mol% to 9 mol%. As PTX percentage increase from 1.5 mol% to 9 mol%, the recovery of PTX was also increased. So 5 mol% PAMAM, 9 mol%

PTX and 86 mol% DPPC were chosen as the composition of the hybrid nanosystem. In the future study, it is interesting to evaluate the effect of different dendrimer generations, concentrations and surface groups on the formation of hybrid nanosystem.

When the PTX was encapsulated in the hybrid formulation at 9 mol%, it has recovery of about 80%. However, for the same preparation procedure with PTX-DPPC only or PTX-PM only, the recovery yield was significantly lower than PTX-Hybrid as shown in Figure 6.3. PTX-PM showed relatively higher recovery yield than PTX-DPPC. This might be due to the hydrophobic internal space of PM that can retain more PTX when they form a complex in the solution. However, the recovery yield was <50% because PTX could freely diffuse out of the PM cavity and precipitate. In comparison, if PM and DPPC were combined together to form a hybrid system, the PTX could be retained in the vesicle structure formed by PM and DPPC. Thus, the recovery yield was significantly improved. In previous study, PTX was conjugated with polyglycerol dendrimers (PGDs) generation 4 and 5. The PTX solubilities in 10 wt% of PGDs were improved to 80 to 128 μg/ml [268]. In comparison, the concentration of PTX in the hybrid nanosystem was 794.7 $\pm$ 44.7μg/ml, 6 to 10 fold higher than the PTX-PGDs conjugates. This is a great advantage of combining PM dendrimer together with DPPC lipids to encapsulate hydrophobic compounds PTX.

The morphology of the hybrid nanosystems was observed from Cryo-TEM as shown in Figure 6.2. The hybrid nanosystem were spherical, vesicular shape with diameter less than 50 nm, agrees with the size data measured by Zetasizer Nano-

ZS90 (Malvern. Instruments GmbH Herrenberg. Germany). The zeta potential of the hybrid system was nearly neutral while PAMAM G4 had positive charge of +30.1 mV. This result indicates that dendrimer was likely embedded inside the hybrid nanosystem. There are a few studies to investigate the structural interaction between dendrimer and lipid. *Wrobel et al.* studied the influence of cationic phosphorus-containing dendrimers generation 3 and 4 on model DMPC or DPPC lipid membranes. The measurement result of fluorescence anisotropy and DSC showed that dendrimers can interact both with the hydrophobic part and the polar head-group region of the phospholipid bilayer [269].

Berenyi et al. studied the effect of PAMAM G5 on multilamellar DPPC vesicles. It was found that the terminal amino groups of dendrimers strongly interacted with phophate headgroups as the initial step. Then the dendrimer disrupted the regular multilamellar structure of DPPC and form small vesicles [242].

Pieter et al. used solid-state NMR method to study the interaction between PAMAM G5, G7 with lipid bilayer. It was found that dendrimers had stronger interaction with alkyl chain regions than the headgroups and restricted the motion of bilayer lipid tails [270].

Taken together, the formation of hybrid nanosystem is likely initiated from the interaction between the terminal amino groups of dendrimer and phophate headgroups of lipids. Then, the internal hydrophobic cavity of dendrimer interacts strongly with alkyl chain of the lipids to form small vesicles, which helps to encapsulate hydrophobic compound.

6.4.2 Cytotoxicity of PTX-Hybrid nanosystem on IGROV-1 cells

In the cytotoxicity study on IGROV-1 cells, PTX-Hybrid nanosystem showed significantly improved efficacy compared to PTX free drug after 24 h treatment. The drug release profile in Figure 6.4 explained that such effect reached maximum at 24 h as majority of PTX was released within 24 h, which also explained the similar cell viability curve of PTX-Hybrid and PTX after 72 h treatment. Based on 24 h cell viability result, the combination index of PTX-Hybrid versus both PTX/PM and PTX/Empty-Hybrid were < 1, indicating synergistic effect of PTX and PM in hybrid nanosystem. As Figure 6.6 showed that PM accumulated intracellularly after 24 h of incubation, this observation indicated that PM might help increase cellular accumulation of PTX so as to improve the therapeutic effect of PTX. At the same time, PM also induced cytotoxicity effect as shown in Figure 6.5.

6.4.3 PTX-Hybrid nanosystem for the treatment of IGROV-1 ovarian tumor inoculated SCID mice

Ovarian cancer ranks the most mortal of all gynecologic malignancies and the 5th leading cause of cancer related death [271]. Intravenous administration of taxane-based chemotherapy is the most active and extensively used treatment for ovarian carcinoma. Although these approaches improved survival over the past years and have been considered as current standard treatment, relapses and undesirable side effects represent the major problems for patients with advanced disease [272, 273]. One possible solution to decrease adverse effect as well as to improve therapeutic

effect is to deliver the drugs via local route of administration rather than i.v. injection. Theoretically, intraperitoneal injection directly delivers the drug within the peritoneum to achieve increased exposure of tumor to the antineoplastic agents [274]. In this study, the dose of PTX-Hybrid nanosystem was given at 2 mg/kg, 10-fold lower than the MTD. No obvious behavior change or significant weight loss was found for the treatment. Meanwhile, the survival of mice bearing IGVOR-1 ovarian tumor significantly improved. Also, the mean survival time and median survival time were significantly improved compared to the treatment of commercial standard drug Taxol at MTD (20 mg/kg). Such result indicates that PTX-Hybrid nanosystem achieved better therapeutic effect than Taxol, meanwhile the PTX induced side effects might be diminished due to a reduced administration dose.

6.5 Conclusion

In this chapter, PM dendrimer was successfully surface modified with DPPC lipids by complexation to form hybrid nanosystem to encapsulate PTX. This hybrid nanosystem was observed as spherical and uniform vesicles with diameters of 30-40 nm. One major advantage of PTX-hybrid nanosystem is that the encapsulation of PTX at 9 mol% is nearly 80%, significantly higher than the PTX formulated with either DPPC or PM alone. Moreover, the potency of PTX could be significantly improved by 37-fold when presented in the hybrid nanosystem, as reflected by the reduction in IC50 values. PTX in the hybrid nanosystem could significantly improve the survival of tumor-bearing animals, with 50% increase in the median survival time, despite a 10-fold dose reduction. Taken together, this

dendrimer-hybrid nanosystem demonstrated advantages to deliver PTX for ovarian cancer treatment. It could also be further explore as a novel drug delivery vehicle in biomedical applications.

CHAPTER 7. CONCLUSION AND FUTURE PERSPECTIVES

The unique structural properties of dendrimers have brought a lot of interests to study their potential applications in the biomedical field. Dendrimer toxicity is always a hurdle to be overcome so that safety aspect is warranted. Thus, seeking a balance between applications and toxicities of dendrimers for drug delivery is the main focus of current research. There are two common approaches to modify dendrimer surface to achieve desirable effects: chemical conjugation and physical complexation. In this thesis, both approaches are explored to modify dendrimer surface to achieve improved properties in drug delivery applications.

In the chemical conjugation approach to modify dendrimer surface, PAMAM G4 dendrimer were successfully surface modified by PEGylation and thiolation. Subsequently, the compatibility of various dendrimer derivatives with major blood components was studied. In general, the unmodified amine-terminated dendrimer displayed generation- and concentration-dependent toxic effects on blood components and functions. PEGylation was an effective method to decrease toxicity of cationic dendrimers to blood components. Further modifying PEGylated dendrimers with thiolation reduced their effect on haemolysis, complement activation, PT and aPTT. These findings suggested that dual functionalization with PEGylation and thiolation could reduce the toxicity of cationic PAMAM dendrimer to certain blood components.

With improved toxicity profile of such surface modified PAMAM dendrimers, these materials were further studied for their potential application in oral drug

delivery. The effect of dendrimer derivatives on two major biological barriers in oral delivery, P-gp drug efflux pump and tight junction, were evaluated. With acceptable cytotoxicity to Caco-2 cell monolayer, dual functionalized PAMAM dendrimers increased cellular accumulation and permeation of the P-gp substrate R-123 in both Caco-2 and MDCK/MDR1 cells, indicating the P-gp inhibitory effect of the dual functionalized dendrimers. Meanwhile, dual functionalized dendrimer derivatives could reversibly disrupt the tight junction integrity over time. Based on these in vitro results, the PEG(1.8)-PM-TBA(7.0) was further evaluated in vivo for its potential to increase the oral bioavailability of GCV, a BCS class III drug. The results showed that PEG(1.8)-PM-TBA(7.0) could improve oral bioavailability of GCV. To the best of our knowledge, this is the first study to evaluate such surface modification approaches of dendrimer for oral drug delivery application. Taken together, dual functionalization via PEGylation and thiolation represented a novel and promising approach in altering PAMAM dendrimer surface for potential application such as oral drug delivery modulators.

In the complexation approach to modify dendrimer surface, PAMAM G4 dendrimer was modified with the lipid DPPC via the formation of a physical complex. Such dendrimer-lipid hybrid nanosystem was studied as a carrier of PTX to treat ovarian cancer via i.p. route of administration. PTX is not easily formulated due to the very hydrophobic nature of this compound. The prepared dendrimer-lipid hybrid nanosystem incorporated nearly 80% of PTX, significantly higher than that prepared in either DPPC or PM alone formulation. The potency of PTX could be significantly improved by 37-fold when presented in the hybrid

nanosystem, as reflected by the reduction in IC_{50} values. In the survival study of tumor-bearing animals, PTX in the hybrid nanosystem could significantly improve the survival of IGROV-1 ovarian tumor inoculated SCID mice, with 50% increase in the median survival time, despite a 10-fold dose reduction. Taken together, this dendrimer-hybrid nanosystem demonstrated great advantages to deliver PTX for ovarian cancer treatment.

PAMAM dendrimer generation 4.0 with amine surface group is selected as the model dendrimer in this study for a few reasons. This dendrimer shows promising biological effects at concentration with acceptable cytotoxic effects. If the generation increases further, the cytotoxicity will be too pronounced that the dendrimer could only be applied at very low concentration. Another reason for choosing this dendrimer is due to its popularity in the field of dendrimer research, which will provide more information for comparison with other studies. However, PAMAM dendrimers are not biodegradable. Thus, this class of dendrimers faces the challenge of long term safety concerns for clinical applications. A potential solution to overcome this challenge is to explore biodegradable dendrimers in future studies. Some recent examples of biodegradable dendrimers reported in the literature include polyester bis(methylol)propionic acid (bis-MPA) dendrimers [275], poly-l-lysine (PLL) dendrimers [276], or poly(glycerol succinic acid) (PGLSA) dendrimers [277].

In a broader perspective, there are a few directions to explore in the future.

(1) To evaluate the absorption enhancing effect of dual functionalized dendrimer on a broader spectrum of drugs. BCS class III drug GCV showed increased oral absorption in the presence of dual functionalized dendrimer in this study. This is mainly due to the P-gp inhibition and tight junction modulation effect of the dual functionalized dendrimer. The penetration enhancing effect of dual functionalized dendrimer might also be applicable to other drugs that suffer from P-gp efflux or low permeability through paracellular pathway. Both BCS class II and class IV drugs have challenge of low solubility, meanwhile some drugs in these two classes also suffer from P-gp efflux, for example, loperamide (BCS class II) [278] and digoxin (BCS class IV) [279]. In additional to the P-gp inhibitory and tight junction modulating benefits of dual functionalized dendrimer derivatives, the internal hydrophobic cavity of dendrimer might help encapsulate the drug so as to improve the stability of the hydrophobic drug in solution. Thus, the dendrimer derivatives might be applicable to a wide range of drugs for the improvement of their oral bioavailability.

(2) To explore other surface conjugation ligands for biomedical applications. In the current study, dendrimer and lipids were complexed to form a hybrid nanosystem. It is also possible to conjugate the lipid groups on dendrimer surface. Dendrimers possess high density of hydrophilic surface groups. After surface conjugation with lipid groups, the whole structure will become more hydrophobic in nature, which might help promote interaction with lipophilic components in biological environment. One of the potential targets could be the hydrophobic lipopolysaccharides in bacterial cell wall and the phospholipids in bacterial

membranes. Since cationic PAMAM and PPI dendrimers have been reported to possess antimicrobial properties [280-282], surface modification with lipid chains may help further improve anti-microbial activities of dendrimers. Thus, further exploration of the dendrimer-lipid conjugates as anti-bacterial reagent could be a potentially interesting direction in the future.

(3) To explore drug-dendrimer conjugates for improved drug delivery application. By careful design of the linking chemistry, the drug-dendrimer conjugates could achieve desirable release under certain environment, such as change of pH, presence of enzyme or other intracellular component [283]. Additionally, drug-dendrimer conjugates may also enhance stability, solubility or absorption of various types of therapeutic reagents [284]. The prodrug conjugates could be further modified with lipid ligands as discussed in point (2) so that the dendrimer could enhance its interaction with cellular membrane. This might help to increase intracellular delivery of the drug. Thus, it is important to explore drug-dendrimer conjugates for improved drug release and delivery profile in the future.

(4) To explore in vivo pharmacokinetic profile and toxicity of PAMAM dendrimer as well as the dendrimer derivatives in this study. Although PAMAM dendrimer is the first developed dendrimer type and also the most extensively studies dendrimer so far, a major concern for this class of dendrimer is biodegradability and toxicity issue. Since PAMAM dendrimers are not biodegradable in nature, it is important for us to stress PK profile as well as in vivo toxicity of PAMAM dendrimers in the future study. In chapter 4 of this thesis, the effect of dendrimer on major blood components were evaluated in vitro

models. However, in the future, it is necessary to address chronic toxic effect of dendrimers in animal models. In chapter 6, the lipid-dendrimer hybrid nanosystem was administrated via intraperitoneal injection. Thus, the biodistribution and toxic effect on major organs should be evaluated in the fture study.

(5) To evaluate the stability of dendrimer derivatives as penetration enhancer and the lipid-dendrimer hybrid nanosystem. In chapter 5, the pH stability of the dendrimer derivatives were evaluated up to 6 h. Since the thiol groups are prone to oxidation process, the stability of thiol groups over long period of storage should be evaluated in the future. For the PTX loaded hybrid nanosystem, short-term and long-term stability test will be carried out in the future study.

In conclusion, the findings in this thesis demonstrate that surface modification with multiple groups or complexation could improve dendrimer functionality in drug delivery applications as well as reducing its toxicity. In the future, it is of great interest and potential to explore other dendrimer surface modification strategies to achieve enhanced drug delivery applications.

REFERENCES

[1] S.C. Zimmerman, Dendritic Macromolecules: Concepts, Syntheses, Perspectives (Newkome, G. R.; Moorefield, C. N.; Vögtle, F.), Journal of Chemical Education, 76 (1999) 31.
[2] D.A. Tomalia, H. Baker, J. Dewald, M. Hall, G. Kallos, S. Martin, J. Roeck, J. Ryder, P. Smith, A New Class of Polymers: Starburst-Dendritic Macromolecules, Polym J, 17 (1985) 117-132.
[3] R. Kolhatkar, D. Sweet, H. Ghandehari, Functionalized Dendrimers as Nanoscale Drug Carriers, in: V. Torchilin (Ed.) Multifunctional Pharmaceutical Nanocarriers, Springer New York, 2008, pp. 201-232.
[4] X. Huang, Z. Wu, W. Gao, Q. Chen, B. Yu, Polyamidoamine dendrimers as potential drug carriers for enhanced aqueous solubility and oral bioavailability of silybin, Drug development and industrial pharmacy, 37 (2011) 419-427.
[5] Y. Wang, R. Guo, X. Cao, M. Shen, X. Shi, Encapsulation of 2-methoxyestradiol within multifunctional poly(amidoamine) dendrimers for targeted cancer therapy, Biomaterials, 32 (2011) 3322-3329.
[6] C. Dufes, I.F. Uchegbu, A.G. Schatzlein, Dendrimers in gene delivery, Advanced drug delivery reviews, 57 (2005) 2177-2202.
[7] S. Langereis, A. Dirksen, T.M. Hackeng, M.H.P. van Genderen, E.W. Meijer, Dendrimers and magnetic resonance imaging, New Journal of Chemistry, 31 (2007) 1152-1160.
[8] D. Astruc, E. Boisselier, C. Ornelas, Dendrimers Designed for Functions: From Physical, Photophysical, and Supramolecular Properties to Applications in Sensing, Catalysis, Molecular Electronics, Photonics, and Nanomedicine, Chemical Reviews, 110 (2010) 1857-1959.
[9] D.A. Tomalia, Birth of a new macromolecular architecture: Dendrimers as quantized building blocks for nanoscale synthetic organic chemistry, Aldrichim Acta, 37 (2004) 39-57.
[10] E. Buhleier, W. Wehner, F. Vogtle, Cascade-Chain-Like and Nonskid-Chain-Like Syntheses of Molecular Cavity Topologies, Synthesis-Stuttgart, (1978) 155-158.
[11] D.A. Tomalia, A.M. Naylor, W.A. Goddard, Starburst Dendrimers: Molecular-Level Control of Size, Shape, Surface Chemistry, Topology, and Flexibility from Atoms to Macroscopic Matter, Angewandte Chemie International Edition in English, 29 (1990) 138-175.
[12] B. Klajnert, M. Bryszewska, Dendrimers: properties and applications, Acta biochimica Polonica, 48 (2001) 199-208.
[13] C.J. Hawker, J.M.J. Frechet, Preparation of Polymers with Controlled Molecular Architechture - A New Convergent Approach to Dendritic Macromolecules, Journal of the American Chemical Society, 112 (1990) 7638-7647.
[14] S. Svenson, D.A. Tomalia, Dendrimers in biomedical applications--reflections on the field, Advanced drug delivery reviews, 57 (2005) 2106-2129.

[15] R. Esfand, D.A. Tomalia, Laboratory Synthesis of Poly(amidoamine)(PAMAM) Dendrimers, in: Dendrimers and Other Dendritic Polymers, John Wiley & Sons, Ltd, 2002, pp. 587-604.
[16] M.A. Mintzer, M.W. Grinstaff, Biomedical applications of dendrimers: a tutorial, Chemical Society Reviews, 40 (2011) 173.
[17] G. Caminati, N.J. Turro, D.A. Tomalia, Photophysical investigation of starburst dendrimers and their interactions with anionic and cationic surfactants, Journal of the American Chemical Society, 112 (1990) 8515-8522.
[18] M. Fischer, F. Vögtle, Dendrimers: From Design to Application—A Progress Report, Angewandte Chemie International Edition, 38 (1999) 884-905.
[19] S. Svenson, D.A. Tomalia, Dendrimers in biomedical applications--reflections on the field, Adv Drug Deliv Rev, 57 (2005) 2106-2129.
[20] K. Jain, P. Kesharwani, U. Gupta, N.K. Jain, Dendrimer toxicity: Let's meet the challenge, International journal of pharmaceutics, 394 (2010) 122-142.
[21] J.M. Frechet, Functional polymers and dendrimers: reactivity, molecular architecture, and interfacial energy, Science (New York, N.Y.), 263 (1994) 1710-1715.
[22] T.H. Mourey, S.R. Turner, M. Rubinstein, J.M.J. Frechet, C.J. Hawker, K.L. Wooley, Unique behavior of dendritic macromolecules: intrinsic viscosity of polyether dendrimers, Macromolecules, 25 (1992) 2401-2406.
[23] M.A. Quadir, R. Haag, Biofunctional nanosystems based on dendritic polymers, Journal of controlled release : official journal of the Controlled Release Society, 161 (2012) 484-495.
[24] I. Gössl, L. Shu, A.D. Schlüter, J.P. Rabe, Molecular Structure of Single DNA Complexes with Positively Charged Dendronized Polymers, Journal of the American Chemical Society, 124 (2002) 6860-6865.
[25] R. Haag, F. Kratz, Polymer therapeutics: concepts and applications, Angewandte Chemie (International ed. in English), 45 (2006) 1198-1215.
[26] J. Haensler, F.C. Szoka, Jr., Polyamidoamine cascade polymers mediate efficient transfection of cells in culture, Bioconjugate chemistry, 4 (1993) 372-379.
[27] J.F. Kukowska-Latallo, A.U. Bielinska, J. Johnson, R. Spindler, D.A. Tomalia, J.R. Baker, Efficient transfer of genetic material into mammalian cells using Starburst polyamidoamine dendrimers, Proceedings of the National Academy of Sciences, 93 (1996) 4897-4902.
[28] M.X. Tang, C.T. Redemann, F.C. Szoka, Jr., In vitro gene delivery by degraded polyamidoamine dendrimers, Bioconjugate chemistry, 7 (1996) 703-714.
[29] C.L. Gebhart, A.V. Kabanov, Evaluation of polyplexes as gene transfer agents, Journal of controlled release : official journal of the Controlled Release Society, 73 (2001) 401-416.
[30] J.F. Kukowska-Latallo, E. Raczka, A. Quintana, C. Chen, M. Rymaszewski, J.R. Baker, Jr., Intravascular and endobronchial DNA delivery to murine lung tissue using a novel, nonviral vector, Human gene therapy, 11 (2000) 1385-1395.
[31] F. Kihara, H. Arima, T. Tsutsumi, F. Hirayama, K. Uekama, In vitro and in vivo gene transfer by an optimized alpha-cyclodextrin conjugate with polyamidoamine dendrimer, Bioconjugate chemistry, 14 (2003) 342-350.

[32] K. Wada, H. Arima, T. Tsutsumi, Y. Chihara, K. Hattori, F. Hirayama, K. Uekama, Improvement of gene delivery mediated by mannosylated dendrimer/alpha-cyclodextrin conjugates, Journal of controlled release : official journal of the Controlled Release Society, 104 (2005) 397-413.
[33] D. Shcharbin, A. Shakhbazau, M. Bryszewska, Poly(amidoamine) dendrimer complexes as a platform for gene delivery, Expert opinion on drug delivery, 10 (2013) 1687-1698.
[34] C. Dufès, W.N. Keith, A. Bilsland, I. Proutski, I.F. Uchegbu, A.G. Schätzlein, Synthetic Anticancer Gene Medicine Exploits Intrinsic Antitumor Activity of Cationic Vector to Cure Established Tumors, Cancer Research, 65 (2005) 8079-8084.
[35] H. Nakanishi, O. Mazda, E. Satoh, H. Asada, H. Morioka, T. Kishida, M. Nakao, Y. Mizutani, A. Kawauchi, M. Kita, J. Imanishi, T. Miki, Nonviral genetic transfer of Fas ligand induced significant growth suppression and apoptotic tumor cell death in prostate cancer in vivo, Gene therapy, 10 (2003) 434-442.
[36] H. Maruyama-Tabata, Y. Harada, T. Matsumura, E. Satoh, F. Cui, M. Iwai, M. Kita, S. Hibi, J. Imanishi, T. Sawada, O. Mazda, Effective suicide gene therapy in vivo by EBV-based plasmid vector coupled with polyamidoamine dendrimer, Gene therapy, 7 (2000) 53-60.
[37] L. Vincent, J. Varet, J.Y. Pille, H. Bompais, P. Opolon, A. Maksimenko, C. Malvy, M. Mirshahi, H. Lu, J.P. Vannier, C. Soria, H. Li, Efficacy of dendrimer-mediated angiostatin and TIMP-2 gene delivery on inhibition of tumor growth and angiogenesis: in vitro and in vivo studies, International journal of cancer. Journal international du cancer, 105 (2003) 419-429.
[38] A.V. Shakhbazau, D.G. Shcharbin, N.V. Goncharova, I.N. Seviaryn, S.M. Kosmacheva, N.A. Kartel, M. Bryszewska, J.P. Majoral, M.P. Potapnev, Neurons and stromal stem cells as targets for polycation-mediated transfection, Bulletin of experimental biology and medicine, 151 (2011) 126-129.
[39] A. Shakhbazau, D. Shcharbin, I. Seviaryn, N. Goncharova, S. Kosmacheva, M. Potapnev, M. Bryszewska, R. Kumar, J. Biernaskie, R. Midha, Dendrimer-driven neurotrophin expression differs in temporal patterns between rodent and human stem cells, Molecular pharmaceutics, 9 (2012) 1521-1528.
[40] H. Zhao, J. Li, F. Xi, L. Jiang, Polyamidoamine dendrimers inhibit binding of Tat peptide to TAR RNA, FEBS letters, 563 (2004) 241-245.
[41] W. Wang, Z. Guo, Y. Chen, T. Liu, L. Jiang, Influence of generation 2-5 of PAMAM dendrimer on the inhibition of Tat peptide/ TAR RNA binding in HIV-1 transcription, Chemical biology & drug design, 68 (2006) 314-318.
[42] H. Liu, H. Wang, W. Yang, Y. Cheng, Disulfide Cross-Linked Low Generation Dendrimers with High Gene Transfection Efficacy, Low Cytotoxicity, and Low Cost, Journal of the American Chemical Society, 134 (2012) 17680-17687.
[43] H.A. Kim, B.W. Lee, D. Kang, J.H. Kim, S.H. Ihm, M. Lee, Delivery of hypoxia-inducible VEGF gene to rat islets using polyethylenimine, Journal of drug targeting, 17 (2009) 1-9.

[44] D. Bhadra, S. Bhadra, S. Jain, N.K. Jain, A PEGylated dendritic nanoparticulate carrier of fluorouracil, International journal of pharmaceutics, 257 (2003) 111-124.
[45] N. Malik, E.G. Evagorou, R. Duncan, Dendrimer-platinate: a novel approach to cancer chemotherapy, Anti-cancer drugs, 10 (1999) 767-776.
[46] J.F. Kukowska-Latallo, K.A. Candido, Z. Cao, S.S. Nigavekar, I.J. Majoros, T.P. Thomas, L.P. Balogh, M.K. Khan, J.R. Baker, Jr., Nanoparticle targeting of anticancer drug improves therapeutic response in animal model of human epithelial cancer, Cancer Res, 65 (2005) 5317-5324.
[47] L. Gonz âlez-Mariscal, A. Betanzos, P. Nava, B.E. Jaramillo, Tight junction proteins, Progress in Biophysics and Molecular Biology, 81 (2003) 1-44.
[48] T. Sakthivel, I. Toth, A.T. Florence, Distribution of a lipidic 2.5 nm diameter dendrimer carrier after oral administration, International journal of pharmaceutics, 183 (1999) 51-55.
[49] M. El-Sayed, M. Ginski, C. Rhodes, H. Ghandehari, Transepithelial transport of poly(amidoamine) dendrimers across Caco-2 cell monolayers., Journal of Controlled Release, 81 (2002) 355-365.
[50] R. Wiwattanapatapee, B. Carreno-Gomez, N. Malik, R. Duncan, Anionic PAMAM dendrimers rapidly cross adult rat intestine in vitro: a potential oral delivery system?, Pharmaceutical research, 17 (2000) 991-998.
[51] S. Sadekar, H. Ghandehari, Transepithelial transport and toxicity of PAMAM dendrimers: implications for oral drug delivery, Advanced drug delivery reviews, 64 (2012) 571-588.
[52] M. El-Sayed, M. Ginski, C. Rhodes, H. Ghandehari, Transepithelial transport of poly(amidoamine) dendrimers across Caco-2 cell monolayers, Journal of controlled release : official journal of the Controlled Release Society, 81 (2002) 355-365.
[53] M. El-Sayed, M. Ginski, C.A. Rhodes, H. Ghandehari, Influence of surface chemistry of poly(amidoamine) dendrimers on Caco-2 cell monolayers, J Bioact Compat Pol, 18 (2003) 7-22.
[54] K.M. Kitchens, R.B. Kolhatkar, P.W. Swaan, N.D. Eddington, H. Ghandehari, Transport of poly(amidoamine) dendrimers across Caco-2 cell monolayers: Influence of size, charge and fluorescent labeling, Pharmaceutical research, 23 (2006) 2818-2826.
[55] K.M. Kitchens, R.B. Kolhatkar, P.W. Swaan, H. Ghandehari, Endocytosis inhibitors prevent poly(amidoamine) dendrimer internalization and permeability across Caco-2 cells, Molecular pharmaceutics, 5 (2008) 364-369.
[56] D.S. Goldberg, H. Ghandehari, P.W. Swaan, Cellular Entry of G3.5 Poly (amido amine) Dendrimers by Clathrin- and Dynamin-Dependent Endocytosis Promotes Tight Junctional Opening in Intestinal Epithelia, Pharmaceutical research, 27 (2010) 1547-1557.
[57] X. Huang, Z. Wu, W. Gao, Q. Chen, B. Yu, Polyamidoamine dendrimers as potential drug carriers for enhanced aqueous solubility and oral bioavailability of silybin, Drug development and industrial pharmacy, (2010) 1-10.

[58] W. Ke, Y. Zhao, R. Huang, C. Jiang, Y. Pei, Enhanced oral bioavailability of doxorubicin in a dendrimer drug delivery system, J Pharm Sci, 97 (2008) 2208-2216.
[59] A. D'Emanuele, R. Jevprasesphant, J. Penny, D. Attwood, The use of a dendrimer-propranolol prodrug to bypass efflux transporters and enhance oral bioavailability, Journal of controlled release : official journal of the Controlled Release Society, 95 (2004) 447-453.
[60] D.S. Goldberg, N. Vijayalakshmi, P.W. Swaan, H. Ghandehari, G3.5 PAMAM dendrimers enhance transepithelial transport of SN38 while minimizing gastrointestinal toxicity, Journal of controlled release : official journal of the Controlled Release Society, 150 (2011) 318-325.
[61] M. Najlah, S. Freeman, D. Attwood, A. D'Emanuele, In vitro evaluation of dendrimer prodrugs for oral drug delivery, International journal of pharmaceutics, 336 (2007) 183-190.
[62] Z. Wang, Y. Itoh, Y. Hosaka, I. Kobayashi, Y. Nakano, I. Maeda, F. Umeda, J. Yamakawa, M. Kawase, K. Yag, Novel transdermal drug delivery system with polyhydroxyalkanoate and starburst polyamidoamine dendrimer, Journal of bioscience and bioengineering, 95 (2003) 541-543.
[63] A. Filipowicz, S. Wolowiec, Solubility and in vitro transdermal diffusion of riboflavin assisted by PAMAM dendrimers, International journal of pharmaceutics, 408 (2011) 152-156.
[64] K. Borowska, B. Laskowska, A. Magon, B. Mysliwiec, M. Pyda, S. Wolowiec, PAMAM dendrimers as solubilizers and hosts for 8-methoxypsoralene enabling transdermal diffusion of the guest, International journal of pharmaceutics, 398 (2010) 185-189.
[65] A.S. Chauhan, S. Sridevi, K.B. Chalasani, A.K. Jain, S.K. Jain, N.K. Jain, P.V. Diwan, Dendrimer-mediated transdermal delivery: enhanced bioavailability of indomethacin, Journal of controlled release : official journal of the Controlled Release Society, 90 (2003) 335-343.
[66] Y. Cheng, N. Man, T. Xu, R. Fu, X. Wang, X. Wang, L. Wen, Transdermal delivery of nonsteroidal anti-inflammatory drugs mediated by polyamidoamine (PAMAM) dendrimers, J Pharm Sci, 96 (2007) 595-602.
[67] V.H. Lee, J.R. Robinson, Topical ocular drug delivery: recent developments and future challenges, Journal of ocular pharmacology, 2 (1986) 67-108.
[68] D. Miller, J.D. Peczon, C.G. Whitworth, CORTICOSTEROIDS AND FUNCTIONS IN THE ANTERIOR SEGMENT OF THE EYE, American journal of ophthalmology, 59 (1965) 31-34.
[69] B. Manzouri, G.C. Vafidis, R.K. Wyse, Pharmacotherapy of fungal eye infections, Expert opinion on pharmacotherapy, 2 (2001) 1849-1857.
[70] D.S. Hull, J.E. Hine, J.F. Edelhauser, R.A. Hyndiuk, Permeability of the isolated rabbit cornea to corticosteroids, Investigative ophthalmology, 13 (1974) 457-459.
[71] T. Loftsson, H. Sigurdsson, D. Hreinsdóttir, F. Konráðsdóttir, E. Stefánsson, Dexamethasone delivery to posterior segment of the eye, J Incl Phenom Macrocycl Chem, 57 (2007) 585-589.

[72] T.F. Vandamme, L. Brobeck, Poly(amidoamine) dendrimers as ophthalmic vehicles for ocular delivery of pilocarpine nitrate and tropicamide, Journal of controlled release : official journal of the Controlled Release Society, 102 (2005) 23-38.
[73] W. Yao, K. Sun, H. Mu, N. Liang, Y. Liu, C. Yao, R. Liang, A. Wang, Preparation and characterization of puerarin-dendrimer complexes as an ocular drug delivery system, Drug development and industrial pharmacy, 36 (2010) 1027-1035.
[74] W.J. Yao, K.X. Sun, Y. Liu, N. Liang, H.J. Mu, C. Yao, R.C. Liang, A.P. Wang, Effect of poly(amidoamine) dendrimers on corneal penetration of puerarin, Biological & pharmaceutical bulletin, 33 (2010) 1371-1377.
[75] C. Yao, W. Wang, X. Zhou, T. Qu, H. Mu, R. Liang, A. Wang, K. Sun, Effects of poly(amidoamine) dendrimers on ocular absorption of puerarin using microdialysis, Journal of ocular pharmacology and therapeutics : the official journal of the Association for Ocular Pharmacology and Therapeutics, 27 (2011) 565-569.
[76] J.C. Sung, B.L. Pulliam, D.A. Edwards, Nanoparticles for drug delivery to the lungs, Trends in biotechnology, 25 (2007) 563-570.
[77] S. Chono, T. Tanino, T. Seki, K. Morimoto, Influence of particle size on drug delivery to rat alveolar macrophages following pulmonary administration of ciprofloxacin incorporated into liposomes, Journal of drug targeting, 14 (2006) 557-566.
[78] O.R. Justo, A.M. Moraes, Incorporation of antibiotics in liposomes designed for tuberculosis therapy by inhalation, Drug delivery, 10 (2003) 201-207.
[79] S. Kimura, K. Egashira, L. Chen, K. Nakano, E. Iwata, M. Miyagawa, H. Tsujimoto, K. Hara, R. Morishita, K. Sueishi, R. Tominaga, K. Sunagawa, Nanoparticle-mediated delivery of nuclear factor kappaB decoy into lungs ameliorates monocrotaline-induced pulmonary arterial hypertension, Hypertension, 53 (2009) 877-883.
[80] H.M. Mansour, Y.S. Rhee, X. Wu, Nanomedicine in pulmonary delivery, International journal of nanomedicine, 4 (2009) 299-319.
[81] S. Bai, C. Thomas, F. Ahsan, Dendrimers as a carrier for pulmonary delivery of enoxaparin, a low-molecular weight heparin, J Pharm Sci, 96 (2007) 2090-2106.
[82] S. Bai, F. Ahsan, Synthesis and evaluation of pegylated dendrimeric nanocarrier for pulmonary delivery of low molecular weight heparin, Pharmaceutical research, 26 (2009) 539-548.
[83] T.P. Thomas, A.K. Patri, A. Myc, M.T. Myaing, J.Y. Ye, T.B. Norris, J.R. Baker, Jr., In vitro targeting of synthesized antibody-conjugated dendrimer nanoparticles, Biomacromolecules, 5 (2004) 2269-2274.
[84] R. Shukla, T.P. Thomas, J.L. Peters, A.M. Desai, J. Kukowska-Latallo, A.K. Patri, A. Kotlyar, J.R. Baker, Jr., HER2 specific tumor targeting with dendrimer conjugated anti-HER2 mAb, Bioconjugate chemistry, 17 (2006) 1109-1115.
[85] A. Quintana, E. Raczka, L. Piehler, I. Lee, A. Myc, I. Majoros, A.K. Patri, T. Thomas, J. Mule, J.R. Baker, Jr., Design and function of a dendrimer-based

therapeutic nanodevice targeted to tumor cells through the folate receptor, Pharmaceutical research, 19 (2002) 1310-1316.
[86] R. Guo, H. Wang, C. Peng, M. Shen, L. Zheng, G. Zhang, X. Shi, Enhanced X-ray attenuation property of dendrimer-entrapped gold nanoparticles complexed with diatrizoic acid, Journal of Materials Chemistry, 21 (2011) 5120-5127.
[87] P. Kesharwani, K. Jain, N.K. Jain, Dendrimer as nanocarrier for drug delivery, Progress in Polymer Science, 39 (2014) 268-307.
[88] E.C. Wiener, M.W. Brechbiel, H. Brothers, R.L. Magin, O.A. Gansow, D.A. Tomalia, P.C. Lauterbur, Dendrimer-based metal chelates: a new class of magnetic resonance imaging contrast agents, Magnetic resonance in medicine : official journal of the Society of Magnetic Resonance in Medicine / Society of Magnetic Resonance in Medicine, 31 (1994) 1-8.
[89] H. Kobayashi, K. Reijnders, S. English, A.T. Yordanov, D.E. Milenic, A.L. Sowers, D. Citrin, M.C. Krishna, T.A. Waldmann, J.B. Mitchell, M.W. Brechbiel, Application of a macromolecular contrast agent for detection of alterations of tumor vessel permeability induced by radiation, Clinical cancer research : an official journal of the American Association for Cancer Research, 10 (2004) 7712-7720.
[90] E.C. Wiener, S. Konda, A. Shadron, M. Brechbiel, O. Gansow, Targeting dendrimer-chelates to tumors and tumor cells expressing the high-affinity folate receptor, Investigative radiology, 32 (1997) 748-754.
[91] Y. Fu, D.E. Nitecki, D. Maltby, G.H. Simon, K. Berejnoi, H.J. Raatschen, B.M. Yeh, D.M. Shames, R.C. Brasch, Dendritic iodinated contrast agents with PEG-cores for CT imaging: synthesis and preliminary characterization, Bioconjugate chemistry, 17 (2006) 1043-1056.
[92] T.P. Thomas, M.T. Myaing, J.Y. Ye, K. Candido, A. Kotlyar, J. Beals, P. Cao, B. Keszler, A.K. Patri, T.B. Norris, J.R. Baker, Jr., Detection and analysis of tumor fluorescence using a two-photon optical fiber probe, Biophysical journal, 86 (2004) 3959-3965.
[93] O. Finikova, A. Galkin, V. Rozhkov, M. Cordero, C. Hagerhall, S. Vinogradov, Porphyrin and tetrabenzoporphyrin dendrimers: tunable membrane-impermeable fluorescent pH nanosensors, J Am Chem Soc, 125 (2003) 4882-4893.
[94] M.S. Shchepinov, I.A. Udalova, A.J. Bridgman, E.M. Southern, Oligonucleotide dendrimers: synthesis and use as polylabelled DNA probes, Nucleic acids research, 25 (1997) 4447-4454.
[95] J. Wang, M. Jiang, T.W. Nilsen, R.C. Getts, Dendritic Nucleic Acid Probes for DNA Biosensors, Journal of the American Chemical Society, 120 (1998) 8281-8282.
[96] H.C. Yoon, M.-Y. Hong, H.-S. Kim, Affinity Biosensor for Avidin Using a Double Functionalized Dendrimer Monolayer on a Gold Electrode, Analytical Biochemistry, 282 (2000) 121-128.
[97] V.J. Pugh, Q.S. Hu, X. Zuo, F.D. Lewis, L. Pu, Optically active BINOL core-based phenyleneethynylene dendrimers for the enantioselective fluorescent recognition of amino alcohols, The Journal of organic chemistry, 66 (2001) 6136-6140.

[98] J. Khandare, A. Mohr, M. Calderon, P. Welker, K. Licha, R. Haag, Structure-biocompatibility relationship of dendritic polyglycerol derivatives, Biomaterials, 31 (2010) 4268-4277.
[99] C.F. Jones, R.A. Campbell, A.E. Brooks, S. Assemi, S. Tadjiki, G. Thiagarajan, C. Mulcock, A.S. Weyrich, B.D. Brooks, H. Ghandehari, D.W. Grainger, Cationic PAMAM Dendrimers Aggressively Initiate Blood Clot Formation, ACS Nano, 6 (2012) 9900-9910.
[100] N. Malik, R. Wiwattanapatapee, R. Klopsch, K. Lorenz, H. Frey, J.W. Weener, E.W. Meijer, W. Paulus, R. Duncan, Dendrimers: relationship between structure and biocompatibility in vitro, and preliminary studies on the biodistribution of 125I-labelled polyamidoamine dendrimers in vivo, Journal of controlled release : official journal of the Controlled Release Society, 65 (2000) 133-148.
[101] Z.Y. Zhang, B.D. Smith, High-generation polycationic dendrimers are unusually effective at disrupting anionic vesicles: membrane bending model, Bioconjugate chemistry, 11 (2000) 805-814.
[102] R. Jevprasesphant, J. Penny, R. Jalal, D. Attwood, N.B. McKeown, A. D'Emanuele, The influence of surface modification on the cytotoxicity of PAMAM dendrimers, International journal of pharmaceutics, 252 (2003) 263-266.
[103] H.B. Agashe, T. Dutta, M. Garg, N.K. Jain, Investigations on the toxicological profile of functionalized fifth-generation poly (propylene imine) dendrimer, The Journal of pharmacy and pharmacology, 58 (2006) 1491-1498.
[104] N.A. Stasko, C.B. Johnson, M.H. Schoenfisch, T.A. Johnson, E.L. Holmuhamedov, Cytotoxicity of polypropylenimine dendrimer conjugates on cultured endothelial cells, Biomacromolecules, 8 (2007) 3853-3859.
[105] M. Bessis, Red cell shapes. An illustrated classification and its rationale, Nouvelle revue francaise d'hematologie, 12 (1972) 721-745.
[106] J.S. Owen, D.J. Brown, D.S. Harry, N. McIntyre, G.H. Beaven, H. Isenberg, W.B. Gratzer, Erythrocyte echinocytosis in liver disease. Role of abnormal plasma high density lipoproteins, The Journal of clinical investigation, 76 (1985) 2275-2285.
[107] D.M. Domanski, B. Klajnert, M. Bryszewska, Influence of PAMAM dendrimers on human red blood cells, Bioelectrochemistry, 63 (2004) 189-191.
[108] M.P. Sheetz, S.J. Singer, Biological membranes as bilayer couples. A molecular mechanism of drug-erythrocyte interactions, Proceedings of the National Academy of Sciences of the United States of America, 71 (1974) 4457-4461.
[109] B. Ziemba, I. Halets, D. Shcharbin, D. Appelhans, B. Voit, I. Pieszynski, M. Bryszewska, B. Klajnert, Influence of fourth generation poly(propyleneimine) dendrimers on blood cells, Journal of biomedical materials research. Part A, 100 (2012) 2870-2880.
[110] R.K. Kainthan, J. Janzen, E. Levin, D.V. Devine, D.E. Brooks, Biocompatibility testing of branched and linear polyglycidol, Biomacromolecules, 7 (2006) 703-709.

[111] T.L. Zhang, Y.X. Gao, J.F. Lu, K. Wang, Arsenite, arsenate and vanadate affect human erythrocyte membrane, Journal of inorganic biochemistry, 79 (2000) 195-203.
[112] B. Klajnert, S. Pikala, M. Bryszewska, Haemolytic activity of polyamidoamine dendrimers and the protective role of human serum albumin, Proceedings of the Royal Society A: Mathematical, Physical and Engineering Science, 466 (2010) 1527-1534.
[113] M.S. Highley, E.A. De Bruijn, Erythrocytes and the transport of drugs and endogenous compounds, Pharmaceutical research, 13 (1996) 186-195.
[114] U. Kragh-Hansen, Structure and ligand binding properties of human serum albumin, Danish medical bulletin, 37 (1990) 57-84.
[115] J.S. Mandeville, H.A. Tajmir-Riahi, Complexes of dendrimers with bovine serum albumin, Biomacromolecules, 11 (2010) 465-472.
[116] H. M, E. Azzazy, R.H. Christenson, All About Albumin: Biochemistry, Genetics, and Medical Applications. Theodore Peters, Jr. San Diego, CA: Academic Press, 1996, 432 pp, $85.00. ISBN 0-12-552110-3, Clinical Chemistry, 43 (1997) 2014a-2015.
[117] B. Klajnert, M. Bryszewska, Fluorescence studies on PAMAM dendrimers interactions with bovine serum albumin, Bioelectrochemistry, 55 (2002) 33-35.
[118] H.M. Suresh Kumar, R.S. Kunabenchi, J.S. Biradar, N.N. Math, J.S. Kadadevarmath, S.R. Inamdar, Analysis of fluorescence quenching of new indole derivative by aniline using Stern–Volmer plots, Journal of Luminescence, 116 (2006) 35-42.
[119] J. Giri, M.S. Diallo, A.J. Simpson, Y. Liu, W.A. Goddard, R. Kumar, G.C. Woods, Interactions of poly(amidoamine) dendrimers with human serum albumin: binding constants and mechanisms, ACS Nano, 5 (2011) 3456-3468.
[120] F. Chiba, T. Chou, L.J. Twyman, M. Wagstaff, Dendrimers as size selective inhibitors to protein-protein binding, Chemical Communications, (2008) 4351-4353.
[121] X.M. He, D.C. Carter, Atomic structure and chemistry of human serum albumin, Nature, 358 (1992) 209-215.
[122] B. Mitev.
[123] B. Klajnert, L. Stanislawska, M. Bryszewska, B. Palecz, Interactions between PAMAM dendrimers and bovine serum albumin, Biochimica et biophysica acta, 1648 (2003) 115-126.
[124] E. Froehlich, J.S. Mandeville, C.J. Jennings, R. Sedaghat-Herati, H.A. Tajmir-Riahi, Dendrimers bind human serum albumin, The journal of physical chemistry. B, 113 (2009) 6986-6993.
[125] S. Sekowski, A. Kazmierczak, J. Mazur, M. Przybyszewska, M. Zaborski, D. Shcharbin, T. Gabryelak, The interaction between PAMAM G3.5 dendrimer, Cd2+, dendrimer–Cd2+ complexes and human serum albumin, Colloids and Surfaces B: Biointerfaces, 69 (2009) 95-98.
[126] M. Ciolkowski, J.F. Petersen, M. Ficker, A. Janaszewska, J.B. Christensen, B. Klajnert, M. Bryszewska, Surface modification of PAMAM dendrimer improves its biocompatibility, Nanomedicine : nanotechnology, biology, and medicine, 8 (2012) 815-817.

[127] S. Curry, H. Mandelkow, P. Brick, N. Franks, Crystal structure of human serum albumin complexed with fatty acid reveals an asymmetric distribution of binding sites, Nature structural biology, 5 (1998) 827-835.
[128] J. Reyes-Reveles, R. Sedaghat-Herati, D.R. Gilley, A.M. Schaeffer, K.C. Ghosh, T.D. Greene, H.E. Gann, W.A. Dowler, S. Kramer, J.M. Dean, R.K. Delong, mPEG-PAMAM-G4 nucleic acid nanocomplexes: enhanced stability, rnase protection, and activity of splice switching oligomer and poly I:C RNA, Biomacromolecules, 14 (2013) 4108-4115.
[129] S. Sekowski, A. Buczkowski, B. Palecz, T. Gabryelak, Interaction of polyamidoamine (PAMAM) succinamic acid dendrimers generation 4 with human serum albumin, Spectrochimica acta. Part A, Molecular and biomolecular spectroscopy, 81 (2011) 706-710.
[130] M.B. Gorbet, M.V. Sefton, Biomaterial-associated thrombosis: roles of coagulation factors, complement, platelets and leukocytes, Biomaterials, 25 (2004) 5681-5703.
[131] M. Toda, T. Kitazawa, I. Hirata, Y. Hirano, H. Iwata, Complement activation on surfaces carrying amino groups, Biomaterials, 29 (2008) 407-417.
[132] N.M. Lamba, J.M. Courtney, J.D. Gaylor, G.D. Lowe, In vitro investigation of the blood response to medical grade PVC and the effect of heparin on the blood response, Biomaterials, 21 (2000) 89-96.
[133] M.S. Payne, T.A. Horbett, Complement activation by hydroxyethylmethacrylate-ethylmethacrylate copolymers, Journal of biomedical materials research, 21 (1987) 843-859.
[134] J. Janatova, Activation and control of complement, inflammation, and infection associated with the use of biomedical polymers, ASAIO journal (American Society for Artificial Internal Organs : 1992), 46 (2000) S53-62.
[135] S. Meri, M.K. Pangburn, Regulation of alternative pathway complement activation by glycosaminoglycans: specificity of the polyanion binding site on factor H, Biochemical and biophysical research communications, 198 (1994) 52-59.
[136] P.E. Stenberg, J. Levin, Mechanisms of platelet production, Blood cells, 15 (1989) 23-47.
[137] J.M. Paulus, Platelet size in man, Blood, 46 (1975) 321-336.
[138] J. Simak, Nanotoxicity in Blood: Effects of Engineered Nanomaterials on Platelets, in: Nanotoxicity, John Wiley & Sons, Ltd, 2009, pp. 191-225.
[139] M.A. Dobrovolskaia, A.K. Patri, J. Simak, J.B. Hall, J. Semberova, S.H. De Paoli Lacerda, S.E. McNeil, Nanoparticle size and surface charge determine effects of PAMAM dendrimers on human platelets in vitro, Molecular pharmaceutics, 9 (2012) 382-393.
[140] C.F. Jones, R.A. Campbell, Z. Franks, C.C. Gibson, G. Thiagarajan, A. Vieira-de-Abreu, S. Sukavaneshvar, S.F. Mohammad, D.Y. Li, H. Ghandehari, A.S. Weyrich, B.D. Brooks, D.W. Grainger, Cationic PAMAM dendrimers disrupt key platelet functions, Molecular pharmaceutics, 9 (2012) 1599-1611.
[141] C.F. Jones, R.A. Campbell, A.E. Brooks, S. Assemi, S. Tadjiki, G. Thiagarajan, C. Mulcock, A.S. Weyrich, B.D. Brooks, H. Ghandehari, D.W.

Grainger, Cationic PAMAM dendrimers aggressively initiate blood clot formation, ACS Nano, 6 (2012) 9900-9910.
[142] K. Greish, G. Thiagarajan, H. Herd, R. Price, H. Bauer, D. Hubbard, A. Burckle, S. Sadekar, T. Yu, A. Anwar, A. Ray, H. Ghandehari, Size and surface charge significantly influence the toxicity of silica and dendritic nanoparticles, Nanotoxicology, 6 (2012) 713-723.
[143] J.C. Roberts, M.K. Bhalgat, R.T. Zera, Preliminary biological evaluation of polyamidoamine (PAMAM) Starburst dendrimers, Journal of biomedical materials research, 30 (1996) 53-65.
[144] P. Rajananthanan, G.S. Attard, N.A. Sheikh, W.J. Morrow, Evaluation of novel aggregate structures as adjuvants: composition, toxicity studies and humoral responses, Vaccine, 17 (1999) 715-730.
[145] P.C. Naha, M. Davoren, F.M. Lyng, H.J. Byrne, Reactive oxygen species (ROS) induced cytokine production and cytotoxicity of PAMAM dendrimers in J774A.1 cells, Toxicology and applied pharmacology, 246 (2010) 91-99.
[146] S.P. Mukherjee, H.J. Byrne, Polyamidoamine dendrimer nanoparticle cytotoxicity, oxidative stress, caspase activation and inflammatory response: experimental observation and numerical simulation, Nanomedicine : nanotechnology, biology, and medicine, 9 (2013) 202-211.
[147] S.P. Mukherjee, F.M. Lyng, A. Garcia, M. Davoren, H.J. Byrne, Mechanistic studies of in vitro cytotoxicity of poly(amidoamine) dendrimers in mammalian cells, Toxicology and applied pharmacology, 248 (2010) 259-268.
[148] A.S. Chauhan, N.K. Jain, P.V. Diwan, Pre-clinical and behavioural toxicity profile of PAMAM dendrimers in mice, Proceedings of the Royal Society A: Mathematical, Physical and Engineering Science, (2009).
[149] J.B. Pryor, B.J. Harper, S.L. Harper, Comparative toxicological assessment of PAMAM and thiophosphoryl dendrimers using embryonic zebrafish, International journal of nanomedicine, 9 (2014) 1947-1956.
[150] S. Sadekar, A. Ray, M. Janat-Amsbury, C.M. Peterson, H. Ghandehari, Comparative biodistribution of PAMAM dendrimers and HPMA copolymers in ovarian-tumor-bearing mice, Biomacromolecules, 12 (2011) 88-96.
[151] V. Gajbhiye, P.V. Kumar, R.K. Tekade, N.K. Jain, Pharmaceutical and Biomedical Potential of PEGylated Dendrimers, Current Pharmaceutical Design, 13 (2007) 415-429.
[152] R. Qi, Y. Gao, Y. Tang, R.R. He, T.L. Liu, Y. He, S. Sun, B.Y. Li, Y.B. Li, G. Liu, PEG-conjugated PAMAM dendrimers mediate efficient intramuscular gene expression, The AAPS journal, 11 (2009) 395-405.
[153] D. Luo, K. Haverstick, N. Belcheva, E. Han, W.M. Saltzman, Poly(ethylene glycol)-Conjugated PAMAM Dendrimer for Biocompatible, High-Efficiency DNA Delivery, Macromolecules, 35 (2002) 3456-3462.
[154] S. Zhu, M. Hong, G. Tang, L. Qian, J. Lin, Y. Jiang, Y. Pei, Partly PEGylated polyamidoamine dendrimer for tumor-selective targeting of doxorubicin: the effects of PEGylation degree and drug conjugation style, Biomaterials, 31 (2010) 1360-1371.

[155] T.I. Kim, H.J. Seo, J.S. Choi, H.S. Jang, J.U. Baek, K. Kim, J.S. Park, PAMAM-PEG-PAMAM: novel triblock copolymer as a biocompatible and efficient gene delivery carrier, Biomacromolecules, 5 (2004) 2487-2492.
[156] H.T. Chen, M.F. Neerman, A.R. Parrish, E.E. Simanek, Cytotoxicity, hemolysis, and acute in vivo toxicity of dendrimers based on melamine, candidate vehicles for drug delivery, J Am Chem Soc, 126 (2004) 10044-10048.
[157] P. Agrawal, U. Gupta, N.K. Jain, Glycoconjugated peptide dendrimers-based nanoparticulate system for the delivery of chloroquine phosphate, Biomaterials, 28 (2007) 3349-3359.
[158] D. Bhadra, A.K. Yadav, S. Bhadra, N.K. Jain, Glycodendrimeric nanoparticulate carriers of primaquine phosphate for liver targeting, International journal of pharmaceutics, 295 (2005) 221-233.
[159] R.B. Kolhatkar, K.M. Kitchens, P.W. Swaan, H. Ghandehari, Surface acetylation of polyamidoamine (PAMAM) dendrimers decreases cytotoxicity while maintaining membrane permeability, Bioconjugate chemistry, 18 (2007) 2054-2060.
[160] C.L. Waite, S.M. Sparks, K.E. Uhrich, C.M. Roth, Acetylation of PAMAM dendrimers for cellular delivery of siRNA, BMC biotechnology, 9 (2009) 38.
[161] R.X. Zhuo, B. Du, Z.R. Lu, In vitro release of 5-fluorouracil with cyclic core dendritic polymer, Journal of controlled release : official journal of the Controlled Release Society, 57 (1999) 249-257.
[162] V. Chechik, R.M. Crooks, Monolayers of Thiol-Terminated Dendrimers on the Surface of Planar and Colloidal Gold, Langmuir, 15 (1999) 6364-6369.
[163] M. Algarra, B.B. Campos, B. Alonso, M.S. Miranda, Á.M. Mart ńez, C.M. Casado, J.C.G. Esteves da Silva, Thiolated DAB dendrimers and CdSe quantum dots nanocomposites for Cd(II) or Pb(II) sensing, Talanta, 88 (2012) 403-407.
[164] R.S. Navath, Y.E. Kurtoglu, B. Wang, S. Kannan, R. Romero, R.M. Kannan, Dendrimer-drug conjugates for tailored intracellular drug release based on glutathione levels, Bioconjugate chemistry, 19 (2008) 2446-2455.
[165] Y.E. Kurtoglu, R.S. Navath, B. Wang, S. Kannan, R. Romero, R.M. Kannan, Poly(amidoamine) dendrimer-drug conjugates with disulfide linkages for intracellular drug delivery, Biomaterials, 30 (2009) 2112-2121.
[166] S.K. Yandrapu, P. Kanujia, K.B. Chalasani, L. Mangamoori, R.V. Kolapalli, A. Chauhan, Development and optimization of thiolated dendrimer as a viable mucoadhesive excipient for the controlled drug delivery: an acyclovir model formulation, Nanomedicine : nanotechnology, biology, and medicine, 9 (2013) 514-522.
[167] C. Wangler, G. Moldenhauer, M. Eisenhut, U. Haberkorn, W. Mier, Antibody-dendrimer conjugates: the number, not the size of the dendrimers, determines the immunoreactivity, Bioconjugate chemistry, 19 (2008) 813-820.
[168] R. Shukla, T.P. Thomas, A.M. Desai, A. Kotlyar, S.J. Park, J.R. Baker, HER2 specific delivery of methotrexate by dendrimer conjugated anti-HER2 mAb, Nanotechnology, 19 (2008) 295102.
[169] A.K. Patri, A. Myc, J. Beals, T.P. Thomas, N.H. Bander, J.R. Baker, Jr., Synthesis and in vitro testing of J591 antibody-dendrimer conjugates for targeted prostate cancer therapy, Bioconjugate chemistry, 15 (2004) 1174-1181.

[170] H. Kobayashi, N. Sato, T. Saga, Y. Nakamoto, T. Ishimori, S. Toyama, K. Togashi, J. Konishi, M.W. Brechbiel, Monoclonal antibody-dendrimer conjugates enable radiolabeling of antibody with markedly high specific activity with minimal loss of immunoreactivity, European journal of nuclear medicine, 27 (2000) 1334-1339.
[171] K. Kono, H. Akiyama, T. Takahashi, T. Takagishi, A. Harada, Transfection activity of polyamidoamine dendrimers having hydrophobic amino acid residues in the periphery, Bioconjugate chemistry, 16 (2005) 208-214.
[172] J.S. Choi, K. Nam, J.Y. Park, J.B. Kim, J.K. Lee, J.S. Park, Enhanced transfection efficiency of PAMAM dendrimer by surface modification with L-arginine, Journal of controlled release : official journal of the Controlled Release Society, 99 (2004) 445-456.
[173] T.P. Thomas, R. Shukla, A. Kotlyar, B. Liang, J.Y. Ye, T.B. Norris, J.R. Baker, Jr., Dendrimer-epidermal growth factor conjugate displays superagonist activity, Biomacromolecules, 9 (2008) 603-609.
[174] T.A. Larson, P.P. Joshi, K. Sokolov, Preventing protein adsorption and macrophage uptake of gold nanoparticles via a hydrophobic shield, ACS Nano, 6 (2012) 9182-9190.
[175] M. Ogris, S. Brunner, S. Schuller, R. Kircheis, E. Wagner, PEGylated DNA/transferrin-PEI complexes: reduced interaction with blood components, extended circulation in blood and potential for systemic gene delivery, Gene therapy, 6 (1999) 595-605.
[176] Y.M. Thasneem, S. Sajeesh, C.P. Sharma, Effect of thiol functionalization on the hemo-compatibility of PLGA nanoparticles, Journal of biomedical materials research. Part A, 99 (2011) 607-617.
[177] H. Gappa-Fahlenkamp, R.S. Lewis, Improved hemocompatibility of poly(ethylene terephthalate) modified with various thiol-containing groups, Biomaterials, 26 (2005) 3479-3485.
[178] S. Zhu, M. Hong, L. Zhang, G. Tang, Y. Jiang, Y. Pei, PEGylated PAMAM Dendrimer-Doxorubicin Conjugates: In Vitro Evaluation and In Vivo Tumor Accumulation, Pharmaceutical research, 27 (2009) 161-174.
[179] M. Werle, M. Hoffer, Glutathione and thiolated chitosan inhibit multidrug resistance P-glycoprotein activity in excised small intestine, Journal of Controlled Release, 111 (2006) 41-46.
[180] T. Schmitz, J. Hombach, A. Bernkop-Schnürch, Chitosan-N-Acetyl Cysteine Conjugates:In VitroEvaluation of Permeation Enhancing and P-Glycoprotein Inhibiting Properties, Drug delivery, 15 (2008) 245-252.
[181] M. Roldo, M. Hornof, P. Caliceti, A. Bernkopschnurch, Mucoadhesive thiolated chitosans as platforms for oral controlled drug delivery: synthesis and in vitro evaluation, European Journal of Pharmaceutics and Biopharmaceutics, 57 (2004) 115-121.
[182] K. Maculotti, I. Genta, P. Perugini, M. Imam, A. Bernkop-Schnürch, F. Pavanetto, Preparation andin vitroevaluation of thiolated chitosan microparticles, Journal of Microencapsulation, 22 (2005) 459-470.
[183] X. Shi, W. Lesniak, M.T. Islam, M.C. MuÑiz, L.P. Balogh, J.R. Baker Jr, Comprehensive characterization of surface-functionalized poly(amidoamine)

dendrimers with acetamide, hydroxyl, and carboxyl groups, Colloids and Surfaces A: Physicochemical and Engineering Aspects, 272 (2006) 139-150.
[184] M.A. Dobrovolskaia, S.E. McNeil, Understanding the correlation between in vitro and in vivo immunotoxicity tests for nanomedicines, Journal of controlled release : official journal of the Controlled Release Society, 172 (2013) 456-466.
[185] D.C. Cardinal, R.J. Flower, The electronic aggregometer: a novel device for assessing platelet behavior in blood, Journal of pharmacological methods, 3 (1980) 135-158.
[186] N. Malik, R. Wiwattanapatapee, R. Klopsch, K. Lorenz, H. Frey, J.W. Weener, E.W. Meijer, W. Paulus, R. Duncan, Dendrimers:: Relationship between structure and biocompatibility in vitro, and preliminary studies on the biodistribution of 125I-labelled polyamidoamine dendrimers in vivo, Journal of Controlled Release, 65 (2000) 133-148.
[187] M. Eftink, Fluorescence Quenching Reactions, in: T.G. Dewey (Ed.) Biophysical and Biochemical Aspects of Fluorescence Spectroscopy, Springer US, 1991, pp. 1-41.
[188] D.A. Tomalia, Dendritic effects: dependency of dendritic nano-periodic property patterns on critical nanoscale design parameters (CNDPs), New Journal of Chemistry, 36 (2012) 264-281.
[189] B. Ziemba, G. Matuszko, M. Bryszewska, B. Klajnert, Influence of dendrimers on red blood cells, Cellular & molecular biology letters, 17 (2012) 21-35.
[190] R.I. Weed, M. Bessis, The discocyte-stomatocyte equilibrium of normal and pathologic red cells, Blood, 41 (1973) 471-475.
[191] P. Matarrese, E. Straface, D. Pietraforte, L. Gambardella, R. Vona, A. Maccaglia, M. Minetti, W. Malorni, Peroxynitrite induces senescence and apoptosis of red blood cells through the activation of aspartyl and cysteinyl proteases, The FASEB Journal, 19 (2005) 416-418.
[192] Z. Liu, J. Janzen, D.E. Brooks, Adsorption of amphiphilic hyperbranched polyglycerol derivatives onto human red blood cells, Biomaterials, 31 (2010) 3364-3373.
[193] W. Wang, W. Xiong, Y. Zhu, H. Xu, X. Yang, Protective effect of PEGylation against poly(amidoamine) dendrimer-induced hemolysis of human red blood cells, Journal of Biomedical Materials Research Part B: Applied Biomaterials, 93B (2010) 59-64.
[194] R. Duncan, L. Izzo, Dendrimer biocompatibility and toxicity, Advanced drug delivery reviews, 57 (2005) 2215-2237.
[195] T. Peters, All About Albumin: Biochemistry, Genetics, and Medical Applications, Elsevier Science, 1995.
[196] T. Peters, Jr., Serum albumin, Advances in protein chemistry, 37 (1985) 161-245.
[197] O.M. Merkel, R. Urbanics, P. Bedőcs, Z. Rozsnyay, L. Rosivall, M. Toth, T. Kissel, J. Szebeni, In vitro and in vivo complement activation and related anaphylactic effects associated with polyethylenimine and polyethylenimine-graft-poly(ethylene glycol) block copolymers, Biomaterials, 32 (2011) 4936-4942.

[198] J. Szebeni, C.R. Alving, L. Rosivall, R. Bünger, L. Baranyi, P. Bedöcs, M. Tóth, Y. Barenholz, Animal Models of Complement-Mediated Hypersensitivity Reactions to Liposomes and Other Lipid-Based Nanoparticles, Journal of Liposome Research, 17 (2007) 107-117.
[199] M.A. Dobrovolskaia, P. Aggarwal, J.B. Hall, S.E. McNeil, Preclinical studies to understand nanoparticle interaction with the immune system and its potential effects on nanoparticle biodistribution, Molecular pharmaceutics, 5 (2008) 487-495.
[200] C. Plank, K. Mechtler, F.C. Szoka, Jr., E. Wagner, Activation of the complement system by synthetic DNA complexes: a potential barrier for intravenous gene delivery, Human gene therapy, 7 (1996) 1437-1446.
[201] H. Gappa-Fahlenkamp, R.S. Lewis, Improved hemocompatibility of poly(ethylene terephthalate) modified with various thiol-containing groups, Biomaterials, 26 (2005) 3479-3485.
[202] F. Thiebaut, T. Tsuruo, H. Hamada, M.M. Gottesman, I. Pastan, M.C. Willingham, Cellular localization of the multidrug-resistance gene product P-glycoprotein in normal human tissues, Proceedings of the National Academy of Sciences of the United States of America, 84 (1987) 7735-7738.
[203] C. Cordon-Cardo, J.P. O'Brien, J. Boccia, D. Casals, J.R. Bertino, M.R. Melamed, Expression of the multidrug resistance gene product (P-glycoprotein) in human normal and tumor tissues, J Histochem Cytochem, 38 (1990) 1277-1287.
[204] K. Yusa, T. Tsuruo, Reversal mechanism of multidrug resistance by verapamil: direct binding of verapamil to P-glycoprotein on specific sites and transport of verapamil outward across the plasma membrane of K562/ADM cells, Cancer research, 49 (1989) 5002-5006.
[205] C.P. Yang, S.G. DePinho, L.M. Greenberger, R.J. Arceci, S.B. Horwitz, Progesterone interacts with P-glycoprotein in multidrug-resistant cells and in the endometrium of gravid uterus, J Biol Chem, 264 (1989) 782-788.
[206] A. Tsuji, P-glycoprotein-mediated efflux transport of anticancer drugs at the blood-brain barrier, Ther Drug Monit, 20 (1998) 588-590.
[207] H. Goldberg, V. Ling, P.Y. Wong, K. Skorecki, Reduced cyclosporin accumulation in multidrug-resistant cells, Biochemical and biophysical research communications, 152 (1988) 552-558.
[208] J. Iqbal, J. Hombach, B. Matuszczak, A. Bernkop-Schnürch, Design and in vitro evaluation of a novel polymeric P-glycoprotein (P-gp) inhibitor, Journal of Controlled Release, 147 (2010) 62-69.
[209] F. Foger, T. Schmitz, A. Bernkop-Schnurch, In vivo evaluation of an oral delivery system for P-gp substrates based on thiolated chitosan, Biomaterials, 27 (2006) 4250-4255.
[210] A. Bernkop-Schnurch, Thiomers: a new generation of mucoadhesive polymers, Advanced drug delivery reviews, 57 (2005) 1569-1582.
[211] M. El-Sayed, M. Ginski, C. Rhodes, H. Ghandehari, Transepithelial transport of poly(amidoamine) dendrimers across Caco-2 cell monolayers, Journal of Controlled Release, 81 (2002) 355-365.

[212] R. Wiwattanapatapee, B. Carreno-Gomez, N. Malik, R. Duncan, Anionic PAMAM dendrimers rapidly cross adult rat intestine in vitro: a potential oral delivery system?, Pharmaceutical Research, 17 (2000) 991-998.
[213] S. Sadekar, H. Ghandehari, Transepithelial transport and toxicity of PAMAM dendrimers: Implications for oral drug delivery, Advanced drug delivery reviews, (2011).
[214] I. Hubatsch, E.G.E. Ragnarsson, P. Artursson, Determination of drug permeability and prediction of drug absorption in Caco-2 monolayers, Nat. Protocols, 2 (2007) 2111-2119.
[215] Y. Wang, R. Guo, X. Cao, M. Shen, X. Shi, Encapsulation of 2-methoxyestradiol within multifunctional poly(amidoamine) dendrimers for targeted cancer therapy, Biomaterials, 32 (2011) 3322-3329.
[216] D.F. Evans, G. Pye, R. Bramley, A.G. Clark, T.J. Dyson, J.D. Hardcastle, Measurement of gastrointestinal pH profiles in normal ambulant human subjects, Gut, 29 (1988) 1035-1041.
[217] E.V. Batrakova, H.Y. Han, D.W. Miller, A.V. Kabanov, Effects of pluronic P85 unimers and micelles on drug permeability in polarized BBMEC and Caco-2 cells, Pharmaceutical research, 15 (1998) 1525-1532.
[218] E.V. Batrakova, S. Li, D.W. Miller, A.V. Kabanov, Pluronic P85 increases permeability of a broad spectrum of drugs in polarized BBMEC and Caco-2 cell monolayers, Pharmaceutical research, 16 (1999) 1366-1372.
[219] N.N. Salama, N.D. Eddington, A. Fasano, Tight junction modulation and its relationship to drug delivery, Advanced drug delivery reviews, 58 (2006) 15-28.
[220] I.J. Hidalgo, T.J. Raub, R.T. Borchardt, Characterization of the human colon carcinoma cell line (Caco-2) as a model system for intestinal epithelial permeability, Gastroenterology, 96 (1989) 736-749.
[221] R. Konsoula, F.A. Barile, Correlation of in vitro cytotoxicity with paracellular permeability in Caco-2 cells, Toxicology in vitro : an international journal published in association with BIBRA, 19 (2005) 675-684.
[222] D.A. Tomalia, Dendrimer molecules, Sci. Am., 272 (1995) 62-66.
[223] D.A. Tomalia, H. Baker, J. Dewald, M. Hall, G. Kallos, S. Martin, J. Roeck, J. Ryder, P. Smith, A new class of polymers: starburst dendritic macromolecules, Polymer Journal, 17 (1985) 117-132.
[224] S. Sadekar, H. Ghandehari, Transepithelial transport and toxicity of PAMAM dendrimers: Implications for oral drug delivery, Advanced Drug Delivery Reviews, 64 (2012) 571-588.
[225] K. Kitchens, M. Elsayed, H. Ghandehari, Transepithelial and endothelial transport of poly (amidoamine) dendrimers, Advanced drug delivery reviews, 57 (2005) 2163-2176.
[226] R. Jevprasesphant, J. Penny, R. Jalal, D. Attwood, N.B. McKeown, A. D'Emanuele, The influence of surface modification on the cytotoxicity of PAMAM dendrimers, International journal of pharmaceutics, 252 (2003) 263-266.
[227] M. Greindl, F. Foger, J. Hombach, A. Bernkop-Schnurch, In vivo evaluation of thiolated poly(acrylic acid) as a drug absorption modulator for MRP2 efflux pump substrates, European journal of pharmaceutics and

biopharmaceutics : official journal of Arbeitsgemeinschaft fur Pharmazeutische Verfahrenstechnik e.V, 72 (2009) 561-566.
[228] R. Jevprasesphant, J. Penny, D. Attwood, N.B. McKeown, A. D'Emanuele, Engineering of dendrimer surfaces to enhance transepithelial transport and reduce cytotoxicity, Pharmaceutical research, 20 (2003) 1543-1550.
[229] K.G. Dickman, S.J. Hempson, J. Anderson, S. Lippe, L. Zhao, R. Burakoff, R.D. Shaw, Rotavirus alters paracellular permeability and energy metabolism in Caco-2 cells, Am J Physiol Gastrointest Liver Physiol., 279 (2000) G757-766.
[230] J.C. Martin, C.A. Dvorak, D.F. Smee, T.R. Matthews, J.P. Verheyden, 9-[(1,3-Dihydroxy-2-propoxy)methyl]guanine: a new potent and selective antiherpes agent, Journal of medicinal chemistry, 26 (1983) 759-761.
[231] S. Gunda, R. Earla, K. Cholkar, A.K. Mitra, Pharmacokinetic studies and LC-MS/MS method development of ganciclovir and dipeptide monoester prodrugs in Sprague Dawley rats, European journal of drug metabolism and pharmacokinetics, (2014).
[232] W.G. Nichols, M. Boeckh, Recent advances in the therapy and prevention of CMV infections, Journal of clinical virology : the official publication of the Pan American Society for Clinical Virology, 16 (2000) 25-40.
[233] Y. Shen, Y. Lu, M. Jv, J. Hu, Q. Li, J. Tu, Enhancing effect of Labrasol on the intestinal absorption of ganciclovir in rats, Drug development and industrial pharmacy, 37 (2011) 1415-1421.
[234] A. Loregian, R. Gatti, G. Palu, E.F. De Palo, Separation methods for acyclovir and related antiviral compounds, Journal of chromatography. B, Biomedical sciences and applications, 764 (2001) 289-311.
[235] K. Yamamoto, M. Higuchi, S. Shiki, M. Tsuruta, H. Chiba, Stepwise radial complexation of imine groups in phenylazomethine dendrimers, Nature, 415 (2002) 509-511.
[236] A.U. Bielinska, J.F. Kukowska-Latallo, J.R. Baker, Jr., The interaction of plasmid DNA with polyamidoamine dendrimers: mechanism of complex formation and analysis of alterations induced in nuclease sensitivity and transcriptional activity of the complexed DNA, Biochimica et biophysica acta, 1353 (1997) 180-190.
[237] Y. Omidi, A.J. Hollins, R.M. Drayton, S. Akhtar, Polypropylenimine dendrimer-induced gene expression changes: the effect of complexation with DNA, dendrimer generation and cell type, Journal of drug targeting, 13 (2005) 431-443.
[238] P.K. Maiti, B. Bagchi, Structure and dynamics of DNA-dendrimer complexation: role of counterions, water, and base pair sequence, Nano letters, 6 (2006) 2478-2485.
[239] A. Mecke, S. Uppuluri, T.M. Sassanella, D.K. Lee, A. Ramamoorthy, J.R. Baker, Jr., B.G. Orr, M.M. Banaszak Holl, Direct observation of lipid bilayer disruption by poly(amidoamine) dendrimers, Chemistry and physics of lipids, 132 (2004) 3-14.
[240] S. Hong, A.U. Bielinska, A. Mecke, B. Keszler, J.L. Beals, X. Shi, L. Balogh, B.G. Orr, J.R. Baker, Jr., M.M. Banaszak Holl, Interaction of poly(amidoamine) dendrimers with supported lipid bilayers and cells: hole

formation and the relation to transport, Bioconjugate chemistry, 15 (2004) 774-782.
[241] S. Hong, P.R. Leroueil, E.K. Janus, J.L. Peters, M.M. Kober, M.T. Islam, B.G. Orr, J.R. Baker, Jr., M.M. Banaszak Holl, Interaction of polycationic polymers with supported lipid bilayers and cells: nanoscale hole formation and enhanced membrane permeability, Bioconjugate chemistry, 17 (2006) 728-734.
[242] S. Berenyi, J. Mihaly, A. Wacha, O. Toke, A. Bota, A mechanistic view of lipid membrane disrupting effect of PAMAM dendrimers, Colloids and surfaces. B, Biointerfaces, 118 (2014) 164-171.
[243] S. Parimi, T.J. Barnes, C.A. Prestidge, PAMAM dendrimer interactions with supported lipid bilayers: a kinetic and mechanistic investigation, Langmuir, 24 (2008) 13532-13539.
[244] A. Kwok, G.A. Eggimann, J.L. Reymond, T. Darbre, F. Hollfelder, Peptide dendrimer/lipid hybrid systems are efficient DNA transfection reagents: structure--activity relationships highlight the role of charge distribution across dendrimer generations, ACS Nano, 7 (2013) 4668-4682.
[245] A.J. Khopade, F. Caruso, P. Tripathi, S. Nagaich, N.K. Jain, Effect of dendrimer on entrapment and release of bioactive from liposomes, International journal of pharmaceutics, 232 (2002) 157-162.
[246] A. Papagiannaros, K. Dimas, G.T. Papaioannou, C. Demetzos, Doxorubicin-PAMAM dendrimer complex attached to liposomes: cytotoxic studies against human cancer cell lines, International journal of pharmaceutics, 302 (2005) 29-38.
[247] K. Gardikis, S. Hatziantoniou, M. Bucos, D. Fessas, M. Signorelli, T. Felekis, M. Zervou, C.G. Screttas, B.R. Steele, M. Ionov, M. Micha-Screttas, B. Klajnert, M. Bryszewska, C. Demetzos, New drug delivery nanosystem combining liposomal and dendrimeric technology (liposomal locked-in dendrimers) for cancer therapy, J Pharm Sci, 99 (2010) 3561-3571.
[248] W. Lorenz, H.J. Reimann, A. Schmal, P. Dormann, B. Schwarz, E. Neugebauer, A. Doenicke, Histamine release in dogs by Cremophor El® and its derivatives: Oxethylated oleic acid is the most effective constituent, Agents and Actions, 7 (1977) 63-67.
[249] R.T. Dorr, Pharmacology and toxicology of Cremophor EL diluent, The Annals of pharmacotherapy, 28 (1994) S11-14.
[250] J. Szebeni, F.M. Muggia, C.R. Alving, Complement activation by Cremophor EL as a possible contributor to hypersensitivity to paclitaxel: an in vitro study, Journal of the National Cancer Institute, 90 (1998) 300-306.
[251] A. Sparreboom, O. van Tellingen, W.J. Nooijen, J.H. Beijnen, Nonlinear pharmacokinetics of paclitaxel in mice results from the pharmaceutical vehicle Cremophor EL, Cancer Res, 56 (1996) 2112-2115.
[252] Z. Zhou, A. D'Emanuele, D. Attwood, Solubility enhancement of paclitaxel using a linear-dendritic block copolymer, International journal of pharmaceutics, 452 (2013) 173-179.
[253] H.M. Teow, Z. Zhou, M. Najlah, S.R. Yusof, N.J. Abbott, A. D'Emanuele, Delivery of paclitaxel across cellular barriers using a dendrimer-based nanocarrier, International journal of pharmaceutics, 441 (2013) 701-711.

[254] C.H. Fiske, Y. Subbarow, THE COLORIMETRIC DETERMINATION OF PHOSPHORUS, Journal of Biological Chemistry, 66 (1925) 375-400.
[255] R.A. Rajewski, D.G. Kosednar, T.A. Matches, O.S. Wong, K. Burchett, K. Thakker, Stereo-specific analysis of a novel protein kinase C inhibitor, Journal of pharmaceutical and biomedical analysis, 13 (1995) 247-253.
[256] T. Higuchi, MECHANISM OF SUSTAINED-ACTION MEDICATION. THEORETICAL ANALYSIS OF RATE OF RELEASE OF SOLID DRUGS DISPERSED IN SOLID MATRICES, J Pharm Sci, 52 (1963) 1145-1149.
[257] N.A. Peppas, J.J. Sahlin, A simple equation for the description of solute release. III. Coupling of diffusion and relaxation, International journal of pharmaceutics, 57 (1989) 169-172.
[258] T. Alfrey, E.F. Gurnee, W.G. Lloyd, Diffusion in glassy polymers, Journal of Polymer Science Part C: Polymer Symposia, 12 (1966) 249-261.
[259] T.C. Chou, Theoretical basis, experimental design, and computerized simulation of synergism and antagonism in drug combination studies, Pharmacological reviews, 58 (2006) 621-681.
[260] J.J. Khandare, S. Jayant, A. Singh, P. Chandna, Y. Wang, N. Vorsa, T. Minko, Dendrimer versus linear conjugate: Influence of polymeric architecture on the delivery and anticancer effect of paclitaxel, Bioconjugate chemistry, 17 (2006) 1464-1472.
[261] I.M. Shaikh, K.-B. Tan, A. Chaudhury, Y. Liu, B.-J. Tan, B.M.J. Tan, G.N.C. Chiu, Liposome co-encapsulation of synergistic combination of irinotecan and doxorubicin for the treatment of intraperitoneally grown ovarian tumor xenograft, Journal of Controlled Release, 172 (2013) 852-861.
[262] A. Mecke, I.J. Majoros, A.K. Patri, J.R. Baker, Jr., M.M. Holl, B.G. Orr, Lipid bilayer disruption by polycationic polymers: the roles of size and chemical functional group, Langmuir, 21 (2005) 10348-10354.
[263] C.V. Kelly, M.G. Liroff, L.D. Triplett, P.R. Leroueil, D.G. Mullen, J.M. Wallace, S. Meshinchi, J.R. Baker, B.G. Orr, M.M. Banaszak Holl, Stoichiometry and Structure of Poly(amidoamine) Dendrimer-Lipid Complexes, ACS Nano, 3 (2009) 1886-1896.
[264] H. Lee, R.G. Larson, Molecular dynamics simulations of PAMAM dendrimer-induced pore formation in DPPC bilayers with a coarse-grained model, The journal of physical chemistry. B, 110 (2006) 18204-18211.
[265] C.V. Kelly, P.R. Leroueil, E.K. Nett, J.M. Wereszczynski, J.R. Baker, B.G. Orr, M.M. Banaszak Holl, I. Andricioaei, Poly(amidoamine) Dendrimers on Lipid Bilayers I: Free Energy and Conformation of Binding, The Journal of Physical Chemistry B, 112 (2008) 9337-9345.
[266] C.V. Kelly, P.R. Leroueil, B.G. Orr, M.M. Banaszak Holl, I. Andricioaei, Poly(amidoamine) Dendrimers on Lipid Bilayers II: Effects of Bilayer Phase and Dendrimer Termination, The Journal of Physical Chemistry B, 112 (2008) 9346-9353.
[267] K. Gardikis, S. Hatziantoniou, K. Viras, M. Wagner, C. Demetzos, A DSC and Raman spectroscopy study on the effect of PAMAM dendrimer on DPPC model lipid membranes, International journal of pharmaceutics, 318 (2006) 118-123.

[268] T. Ooya, J. Lee, K. Park, Hydrotropic dendrimers of generations 4 and 5: synthesis, characterization, and hydrotropic solubilization of paclitaxel, Bioconjugate chemistry, 15 (2004) 1221-1229.
[269] D. Wrobel, M. Ionov, K. Gardikis, C. Demetzos, J.P. Majoral, B. Palecz, B. Klajnert, M. Bryszewska, Interactions of phosphorus-containing dendrimers with liposomes, Biochimica et biophysica acta, 1811 (2011) 221-226.
[270] P.E. Smith, J.R. Brender, U.H. Durr, J. Xu, D.G. Mullen, M.M. Banaszak Holl, A. Ramamoorthy, Solid-state NMR reveals the hydrophobic-core location of poly(amidoamine) dendrimers in biomembranes, J Am Chem Soc, 132 (2010) 8087-8097.
[271] M.N. Barnes, W.E. Grizzle, C.J. Grubbs, E.E. Partridge, Paradigms for primary prevention of ovarian carcinoma, CA: a cancer journal for clinicians, 52 (2002) 216-225.
[272] M.J. Piccart, K. Bertelsen, K. James, J. Cassidy, C. Mangioni, E. Simonsen, G. Stuart, S. Kaye, I. Vergote, R. Blom, R. Grimshaw, R.J. Atkinson, K.D. Swenerton, C. Trope, M. Nardi, J. Kaern, S. Tumolo, P. Timmers, J.A. Roy, F. Lhoas, B. Lindvall, M. Bacon, A. Birt, J.E. Andersen, B. Zee, J. Paul, B. Baron, S. Pecorelli, Randomized intergroup trial of cisplatin-paclitaxel versus cisplatin-cyclophosphamide in women with advanced epithelial ovarian cancer: three-year results, Journal of the National Cancer Institute, 92 (2000) 699-708.
[273] S.A. Cannistra, Cancer of the ovary, The New England journal of medicine, 351 (2004) 2519-2529.
[274] A. Banzato, S. Bobisse, M. Rondina, D. Renier, F. Bettella, G. Esposito, L. Quintieri, L. Melendez-Alafort, U. Mazzi, P. Zanovello, A. Rosato, A paclitaxel-hyaluronan bioconjugate targeting ovarian cancer affords a potent in vivo therapeutic activity, Clinical cancer research : an official journal of the American Association for Cancer Research, 14 (2008) 3598-3606.
[275] N. Feliu, M.V. Walter, M.I. Montanez, A. Kunzmann, A. Hult, A. Nystrom, M. Malkoch, B. Fadeel, Stability and biocompatibility of a library of polyester dendrimers in comparison to polyamidoamine dendrimers, Biomaterials, 33 (2012) 1970-1981.
[276] J.S. Choi, E.J. Lee, Y.H. Choi, Y.J. Jeong, J.S. Park, Poly(ethylene glycol)-block-poly(L-lysine) dendrimer: novel linear polymer/dendrimer block copolymer forming a spherical water-soluble polyionic complex with DNA, Bioconjugate chemistry, 10 (1999) 62-65.
[277] M.A. Carnahan, M.W. Grinstaff, Synthesis and Characterization of Poly(glycerol−succinic acid) Dendrimers, Macromolecules, 34 (2001) 7648-7655.
[278] C. Wandel, R. Kim, M. Wood, A. Wood, Interaction of morphine, fentanyl, sufentanil, alfentanil, and loperamide with the efflux drug transporter P-glycoprotein, Anesthesiology, 96 (2002) 913-920.
[279] J. Hughes, A. Crowe, Inhibition of P-glycoprotein-mediated efflux of digoxin and its metabolites by macrolide antibiotics, Journal of pharmacological sciences, 113 (2010) 315-324.
[280] A.I. Lopez, R.Y. Reins, A.M. McDermott, B.W. Trautner, C. Cai, Antibacterial activity and cytotoxicity of PEGylated poly(amidoamine) dendrimers, Molecular bioSystems, 5 (2009) 1148-1156.

[281] M.K. Calabretta, A. Kumar, A.M. McDermott, C. Cai, Antibacterial activities of poly(amidoamine) dendrimers terminated with amino and poly(ethylene glycol) groups, Biomacromolecules, 8 (2007) 1807-1811.
[282] A. Felczak, N. Wronska, A. Janaszewska, B. Klajnert, M. Bryszewska, D. Appelhans, B. Voit, S. Rozalska, K. Lisowska, Antimicrobial activity of poly(propylene imine) dendrimers, New Journal of Chemistry, 36 (2012) 2215-2222.
[283] Y.E. Kurtoglu, M.K. Mishra, S. Kannan, R.M. Kannan, Drug release characteristics of PAMAM dendrimer-drug conjugates with different linkers, International journal of pharmaceutics, 384 (2010) 189-194.
[284] J. Liu, W.D. Gray, M.E. Davis, Y. Luo, Peptide- and saccharide-conjugated dendrimers for targeted drug delivery: a concise review, Interface focus, 2 (2012) 307-324.